# Developing an Alternative Method to Determine the Heat Transfer Coefficients of Dwellings in Warmer Climates

Elizabeth Karen Chard

MPhil Built Environment

University of Salford
School of Science, Engineering and Environment

2022

## Table of Contents

## List of Figures

## List of Tables

## List of Equations

## Acknowledgments

I appreciate everyone who has helped and encouraged me whilst I undertook my MPhil.

Firstly, I would like to thank my supervisor and co-supervisor, Richard Fitton and David Farmer for sharing with me your knowledge and expertise as I undertook this research and for your honest feedback. Richard, thank you also for your guidance and encouragement over the last year and for bringing me back to the present when I got too far ahead of myself. Dave, thank you for keeping me optimistic and for helping me break things down when I struggled to see the bigger picture.

Grant Henshaw, thank you, not only for your help in the organisation and setting up of equipment for this research or for always being happy to take time out of your day to give your opinion on results and guidance on how to carry out analysis, but also for being a brilliant friend and supporting me every step of the way. It has really meant a lot.

To the rest of the Energy House Labs team, thank you all for making me feel so welcome and a member of the team. I have thoroughly enjoyed working alongside all of you.

A big thank you to Barratt Developments Ltd., for allowing me the use of the Zed House whilst I undertook this research.

To Richard Pilkington, thank you for always having the time to sit down with me and talk through whatever may have been on my mind. Your time, support and wisdom have meant a great deal to me.

Finally, but by no means least, I would like to extend my sincere thanks to all of my amazing family and friends who have always been a constant unwavering source of love and support. Most of all: to my wonderful parents, Karen and Simon, who have always encouraged me to do my best. Your support this past year, as always, has grounded me, especially when I've struggled; thank you for being people I can always lean on and look to for guidance or go to for a listening ear. To my brilliant sister Sarah, thank you for always reminding me to take a break and take some time for myself. To my lovely grandparents, Pat and Godfrey, thank you for always

checking in to see how I’m doing and for our many much-enjoyed chats over coffee. To my best friends, Emma, Becca and Ethan, thank you: Emma for always knowing what to say at any given time and being someone I know I can always count on, Becca for being able to keep my spirits up, and Ethan, for many much-needed enjoyable evenings playing D&D. Thank you all for everything, I wouldn’t be where I am today without every single one of you.

# Abstract

Whole house heat loss test methods are used to determine the heat transfer coefficient (HTC) of dwellings. Having reliable methods of measuring as-built performance makes it possible to improve the energy efficiency of dwellings, aiding in the global endeavour to reach net zero-carbon. However, there is a gap in current research, as prevailing methods can only be carried out when external climatic conditions are colder, making them ineffective in warmer climates, including outside of the winter months in temperate climates.

Therefore, the aim of the research presented in this thesis is to determine whether it is possible to develop a heat loss test method capable of determining the HTCs of domestic buildings in warmer climates. Using DesignBuilder, a building energy performance simulator, the alternative method was developed and performed on a simple model of the Barratt Zed House, a modern dwelling located on the University of Salford’s Peel Park Campus. For comparison purposes, the well-established co-heating method was also performed; firstly, in real conditions on the Zed House itself to determine an as-built baseline HTC (137.2 ± 12.2 $W \cdot K^{-1}$), and then on the simplified model of the Zed House in DesignBuilder to determine a simulated baseline HTC (93.6 ± 5.3 $W \cdot K^{-1}$).

Through development and analysis of the alternative method, the research explored cooling systems, testing periods, aggregation intervals and temperature conditions. By considering protocols such as statistical validity and collinearity, the most appropriate HTC from the resulting fifteen data sets was determined as 96.8 ± 12.7 $W \cdot K^{-1}$. Additional analysis was then carried out by simulating the alternative method on the Zed House model in three Australian climates: Darwin, Brisbane and Perth. Perth provided the only statistically valid HTC (81.8 ± 19.1 $W \cdot K^{-1}$).

Overall, the alternative method opens new doors for measuring the performance gap in warmer climates. However, the alternative method still had some difficulty performing well in the UK summertime climate, and high levels of solar irradiance also seemed to impact the alternative method’s performance.

## Chapter 1

# Introduction

### Chapter Overview

This chapter introduces the research presented in this thesis and consists of the following sections:

- **1.1 Why the Research is Relevant and Necessary**: explains why the research presented in this thesis is relevant and necessary by giving a brief outline of previous research and literature.
- **1.2 Aim and Objectives**: presents the research questions that form the foundation of the research presented in this thesis.
- **1.3 Research Questions**: establishes the objectives that would need to be considered and met in to order answer the research questions.
- **1.4 Scope**: outlines the key boundaries that were considered for the research to be undertaken.
- **1.5 Thesis Overview**: gives an overview of the remaining chapters in this thesis.

## 1.1 Why the Research is Relevant and Necessary

Heat loss test methods are often used by researchers and commercial companies and are an integral way of determining the as-built performance of a dwelling’s building fabric. Understanding the as-built performance of a dwelling’s building fabric means that the performance gap of that dwelling can be determined. Reducing the performance gap of dwellings is an issue recognised across the globe (Fitton, 2021). Currently used heat loss test methods, such as the more commonly used and well established co-heating method (Johnston et al., 2013), cannot cope with seasonality; they must be performed during the ‘heating season’, i.e., the coldest months of the year when it is possible to have an internal-external temperature difference of at least 10 K (Kelvin). This temperature difference is much harder to achieve through heating techniques in cooling dominated climates. A recent international piece of research (Annex 71: Subtasks 1 and 4 (Fitton, 2021)) determined that there is a need for a new heat loss test method to be developed that can be performed in warmer climates. Therefore, it is the ambition of this research to propose and develop a method that begins to address this need so as to be performed in warmer climates, including warmer months in temperate climates, such as summertime in the UK. Having reliable methods of measuring the as-built performance of domestic buildings means it is possible to improve the energy efficiency of dwellings and thus help towards reducing the issue of performance gap whilst also reducing the carbon emissions and energy consumption in the buildings sector. More needs to be done in the UK and around the rest of the world in order to reach net zero-carbon, as has become apparent from the recent 2021 COP26 international conference (United Nations, 2021a).

## 1.2 Aim and Objectives

The aim of the research presented in this thesis is to determine whether it is possible to develop a heat loss test method capable of determining the HTC of a domestic building in warmer climates. In order to achieve this aim a number of objectives were established. These objectives are listed below:

- Understand relevant literature and previous research to determine whether or not there is a need for a new heat loss test method that is capable of determining the HTC of a domestic building in warmer climates, and if so, why.
- Establish a known, reliable method to be directly compared against and use this known method to determine a ‘baseline’ HTC.
- Select a suitable facility (domestic dwelling) for the research to be carried out in.
- Attempt to develop a new heat loss test method that fits the requirements and needs found in the relevant literature and previous research.
- Form an analysis method that can be used to analyse data acquired from the new heat loss test method.
- Compare the HTC derived from the new heat loss test method to the established baseline.
- Discuss the results obtained from the research and formulate conclusions and recommendations.

## 1.3 Research Questions

The research questions that form the main foundation of this research are written below:

1. Is there a need for a new heat loss test method to determine the HTC of a domestic building in warmer climates?
2. Is it possible to develop a heat loss test method that can determine the HTC of a domestic building in warmer climates?
3. What needs to be considered for a heat loss test method, which could be used to determine the HTC of domestic buildings in warmer climates, to be developed?
4. Is the developed heat loss test method capable of determining the HTC of a domestic building in warmer climates?

The research presented in this thesis could be deemed successful if, regardless of the outcome, these research questions have been explored and have, to some extent, been answered.

## 1.4 Scope

This section covers the scope, or boundaries, of the research.

Several fabric performance measurements have been discussed in this thesis to provide a more rounded picture of the test dwelling's design and as-built performance as well as for use in model simulations, however the HTC is the primary measurement that has been focused on. In addition, a selection of whole house heat loss test methods have been explored and one selected to use as a 'baseline' to compare against.

The main focus of this thesis is developing an alternative method that can be performed in warmer climates, including warmer months in temperate climates, starting with testing in the UK summertime. Some additional thought was also put into how the alternative method may perform in an Australian climate given that (Law & Wong, 2020) have shown that the co-heating method is often not an effective method of determining fabric performance in selected areas around Australia.

Along with determining the as-built HTC of the test dwelling from a co-heating test, the HTC determined from running a co-heating method simulation, using the same conditions, on a simplified model of the test dwelling was also found. The simplified model of the test dwelling was built in an energy modelling software using the as-built air change rate ($ac{\cdot}h^{-1}$) and design U-values of the dwelling (this was due to a lack of as-built U-value measurements as a result of time and equipment constraints). Unfortunately, thermal bridging heat loss could not be included in the model. This was because the test dwelling SAP document did not provide the individual psi values for each element required by the energy modelling software, whilst the energy modelling software did not have an option to account for total thermal bridging heat loss, as there was nowhere within the model data tabs to input a y-value. Simulations of the alternative method were then run on the same model of the test dwelling so that different time periods and climatic conditions could more easily be explored within the research time frame.

Gaining an understanding of how air conditioning systems work was necessary in order to determine which type of air conditioning unit would be most suitable for simulating the alternative method.

## 1.5 Thesis Overview

The structure of the rest of this thesis is outlined below.

Chapter 2 consists of the literature review, firstly looking at the bigger picture and the need for government policies to reach net zero-carbon. The literature review then focuses on the buildings sector, in particular performance gap, including contributions to a dwelling's performance gap and ways of measuring the performance gap. From this the key measurements that can be made to determine a dwelling's fabric performance are explored, followed by different whole house heat loss test methods that can be used to determine the HTC of a dwelling, in particular the co-heating method. The chapter is concluded by a section which highlights the gap in current research regarding the difficulty current whole house heat loss test methods have in coping with seasonality, followed by the thought process around developing an alternative method.

Chapter 3 looks at the research methodology and begins by outlining the aim and research questions which lead to the considerations of how the research would be undertaken, including the need for a baseline HTC to be determined and later compared against. From these considerations, the selected research methodology is explained, including the dwelling to be tested, the chosen whole house heat loss test method to determine the baseline HTC (the co-heating method), and thoughts regarding how the alternative method would be developed and tested, i.e., using simulation software. The methodologies used to determine the as-built performance of the test dwelling are then explained along with the relevant analysis techniques. Following this, an overview of the energy modelling software is given including how the test dwelling was modelled and how the co-heating method was simulated. Finally, the alternative method simulation is detailed, including the model data and weather data used, and the data analysis method presented.

The as-built and simulated results are presented and discussed in Chapter 4. The as-built results from the co-heating method and other fabric performance tests are displayed and the as-built HTC is compared to the design and building regulations HTCs. The performance of the test dwelling during the simulated co-heating test is then examined and the results from the simulation are compared to the as-built and design/target HTCs. Finally in this chapter, the findings from simulating the alternative method on the test dwelling model are analysed, explaining the particular protocols which were taken into consideration in order to determine the most appropriate HTC from the alternative method to be compared against the simulated baseline and design/target HTCs.

Chapter 5 considers the implications of the research, looking first at the alternative method's performance overall. Similarities between the co-heating method and the alternative method regarding their limitations caused by external elements is then discussed. This leads into the practical barriers that were identified, and which would need to be considered before applying the alternative method in a real-world environment, followed by the implications of these barriers.

The thesis is concluded in Chapter 6, which reflects on what the alternative method was able to achieve during the research period, as well as considering the key limitations and further research which may address these limitations. Finally, the chapter is summarised by linking back to the research questions and evaluating how the initial proposal of the alternative method performed overall.

# Chapter 2

# Literature Review

## Chapter Overview

This chapter provides a detailed review of the relevant literature and contains the following sections:

- **2.1 Striving Towards Zero-Carbon**: an in-depth look into the current polices tackling climate change and global energy consumption as well as targets for a net zero-carbon future.
- **2.2 Performance Gap**: a discussion on what the performance gap is and previous research that has investigated what impacts the performance gap and ways of reducing the performance gap of a dwelling.
- **2.3 Fabric Performance**: explores the key measurements that can be made to determine a dwelling's fabric performance, including the HTC.
- **2.4 Whole House Heat Loss Test Methods**: reviews whole house heat loss test methods used in determining the HTC of a dwelling.
- **2.5 The Issue of Seasonality**: highlights the gap in the current research regarding how whole house heat loss test methods struggle with coping with seasonality.
- **2.6 Developing the Alternative Method**: acknowledges considerations taken into account when developing the alternative method as well as presenting an initial proposal as to how the alternative method might work.

## 2.1 Striving Towards Zero-Carbon

### 2.1.1 Global Policies and Initiatives

A legally binding commitment, known as The Paris Agreement (United Nations, 2015), was signed by 191 countries and the European Union (EU) in 2015. By signing the Agreement, all the countries involved committed to reducing their greenhouse gas emissions as well as working together to tackle climate change. In addition to this, each party must put forward an up to date Nationally Determined Contribution (NDC) every five years, i.e., an action plan to address climate change and reduce greenhouse gas emissions. The long-term aim of the Paris Agreement is to limit the increase in global temperature to 1.5°C and also to significantly decrease greenhouse gas emissions on a worldwide scale.

The year 2021 saw the meeting of Government officials from around the world for the 26th Climate Change Conference (COP26) in the UK. Prior to the conference, a document about COP26, released by the United Nations (United Nations, 2021a), explained that the world appeared to not be on track to keep global warming within the 1.5°C target set out in The Paris Agreement (United Nations, 2015). Anything above 1.5°C and control of the climate could be lost. There were two key outcomes that resulted from COP26: the signing of Glasgow Climate Pact and the Paris Rulebook along with the statement that the goal of keeping the global temperatures from rising more than 1.5°C is currently being sustained (Carver, 2022).

The Glasgow Climate Pact is not legally binding and does not dictate what countries must do, however it does set out various resolutions and agreements that expand on the Paris Agreement (Carver, 2022). The Pact focuses on four main areas: mitigation, adaptation, finance and collaboration. At the moment more than 90% of the global Gross Domestic Product (GDP) is covered by net zero commitments (United Nations, 2021b). In addition, NDCs have been put forward by 153 countries with new 2030 emissions targets. Commitments have also been made to stop and reverse deforestation, make the switch to electric vehicles faster, reduce methane emissions and use alternatives to coal power so that we can move away from that as a source of energy. More is being done to be prepared for climate impacts and risks, for example 80 countries around the world are now protected by National

Adaptation Plans or Adaptation Communications. There is a commitment, by 2025, to double the 2019 levels of adaptation finance. The $100 billion climate finance goal will be reached by 2023 at the latest due to the progress made by developed countries, and the steps necessary for the post-2025 climate finance goal have been agreed. Collaboration, in order to achieve the established climate goals, between governments, businesses and civil society will have been increased as a result of COP26 and, during the conference, the Paris Rulebook was finalised (United Nations, 2021b). The Paris Rulebook outlines guidelines and agreements for how the Paris Agreement can be achieved including the reporting of emissions and support, known as the enhanced transparency framework, new standards and mechanisms for international carbon markets and common timeframes for reaching emissions reductions targets (Carver, 2022).

### 2.1.2 Policies and Initiatives in Individual Countries

2.1.2.1 United States of America

Following the appointment of President Biden in 2020, the United States (US) set a target to reduce its net greenhouse gas emissions by at least 50%, compared to its 2005 levels, by 2030. Additionally, the US re-joined the Paris Agreement, having left in 2017, and is also striving to reach net zero emissions by 2050, at the latest (USGPO, 2021).

2.1.2.2 Australia

Australia has put forward its National Climate Resilience and Adaptation Strategy 2021-2025 (NCRAS, 2021). The document outlines three key objectives in order to become resilient towards, as well as adapt to, climate change between 2021 and 2025 (and beyond). The first of these objectives is for them to adapt to climate change through the Australian governments, communities and businesses collaborating and sharing skills, knowledge, and their different points of view. Secondly, they aim to provide improved information regarding the climate as well as services, in order to allow for more rounded and informed decisions to be made when considering the climate. Finally, they plan to regularly assess the progress made towards adapting to climate change so that it can constantly evolve and improve with time.

#### 2.1.2.3 Denmark and Belgium

The ECO-Life project (Hummelshøj et al., 2016) began in Europe in December 2009 and finished in June 2017. The project aimed to demonstrate in two communities, located in Denmark and Belgium, 'ECO Buildings', as well as introducing sources of renewable energy to energy supplies on a large scale. Planning for the project was also undertaken in communities in Lithuania. The project resulted in a yearly reduction of 2,100 tonnes of carbon dioxide (CO2) from the use of renewable energy sources alone, along with the 'ECO Buildings' causing a CO2 reduction of 1,131 tonnes.

#### 2.1.2.4 United Kingdom

The UK has been making efforts to reduce its greenhouse gas emissions and energy consumption since before The Paris Agreement was signed in 2015. The UK Government enacted a law, known as the Climate Change Act, in 2008 (The National Archives, 2008), stating that the UK must cut its net carbon emission by at least 80% by 2050. As of 2019, this legislation was revised and now requires that by the year 2050, the UK net carbon emission must be at least 100% lower than the 1990 baseline, i.e., the UK must reach zero net carbon emission by 2050 (The National Archives, 2008).

In 2009, according to The Carbon Plan (The National Archives, 2011), the heating and powering of buildings, including domestic buildings, was responsible for 37% of emissions. The UK Government at the time initiated The Carbon Plan, which aimed, within the decade and where possible, to insulate all cavity walls and lofts, as well as provide support for other energy efficient measures, in order to try and reduce the heating demand. Also, within the decade, it was expected that over

130,000 low carbon heat installations would be carried out through the Renewable Heat Incentive and the Renewable Heat Premium Payment.

As of 2021, the UK Government enacted the Net Zero Strategy (The National Archives, 2021) which listed a set of key policies to ‘Build Back Greener’. They set out the aim for no new gas boilers to be sold by 2035, and for grants to be offered to households for the installation of low-carbon heating systems courtesy of a new three-year Boiler Upgrade Scheme costing £450 million. Additionally, funding would be provided for leading-edge heat pump technologies from a new £60 million Heat Pump Ready Programme which would look to support the 600,000 installations a year target set by the government by 2028. Funding of £1.75 billion would also be available for Home Upgrade Grants and the Social Housing Decarbonisation Scheme, and policy costs from electricity bills to gas bills would be rebalanced in order to deliver cheaper energy. Finally, a Hydrogen Village trial was scheduled to be launched in order to make an informed decision regarding the role of hydrogen heating systems in the future.

### 2.1.3 Energy Consumption and Emissions in the Building Sector

The reason for the policies and plans described above was, and still is, to reduce the net carbon emissions and the energy consumption in the UK and across the world. One would think that having such measures and strategies put in place would mean that the world is well on its way to tackling climate change. However, recent information and data would seem to show this is not entirely the case, and that, when it comes to combatting climate change, we still fall short and more needs to be done.

For example, over 18th and 19th July 2022, the UK experienced new highest daily maximum temperatures, achieving, in one location, its first ever recorded daily maximum temperature above 40°C (Press Office, 2022). Coningsby, in Lincolnshire, England, reached 40.3°C, whilst Hawarden, in Flintshire, Wales, reached 37.1°C and Charterhall, on the Scottish Borders, achieved 34.8°C, the highest daily maximum temperatures recorded for each of those countries (Press Office, 2022). The previous hottest UK daily maximum temperature was achieved in 2019 when a temperature of 38.7°C was recorded. Looking at the Met Office statistics for the top ten hottest UK days on record (Press Office, 2022), the hottest days on record appear to have become more common and increasing in temperature since 1990, with nine of the top ten hottest recorded UK days falling between 1990 and 2022. Of these, four of the top five have occurred since 2019 (inclusive). Heatwaves are becoming more frequent and extreme. This data demonstrates, as one example, how much and how quickly climate change is taking effect on the world around us. According to the Press Office, the UK reaching temperatures above 40°C would be impossible if not for the human induced climate change the planet is currently experiencing (Press Office, 2022).

#### 2.1.3.1 Global Energy Consumption and Emissions

According to the United Nations Environment Programme (UNEP) (UNEP, 2021), on a global scale, the world's building sector was accountable for 36% of the final global energy consumption in 2020, 22% of which residential buildings were responsible for. The building sector also contributed to 37% of the global energy-related carbon emissions in the same year, with residential buildings responsible for 17% of that.

Due to impacts resulting from the COVID-19 pandemic, global energy demand in 2020 actually dropped by 4%, compared to 2019, whilst global carbon emissions decreased by nearly 6%, as shown in the International Energy Agency's (IEA) Global Energy Review 2021 (IEA, 2021). It was outlined, in the same report that, in 2021, both these figures had risen sharply again, with energy demand slightly higher than 2019 levels, and global carbon emissions nearly 5% higher than 2020.

#### 2.1.3.2 UK Energy Consumption and Emissions

The domestic sector was responsible for approximately 32% of the UK energy consumption in 2020, according to National Statistics (National Statistics, 2021). Due to the COVID-19 pandemic and the consequential need for people to remain at home, the resulting domestic sector consumption increased by 2.3% compared to 2019. This increase seems surprisingly low given that during the COVID-19 lockdowns, many people were urged to stay at home by the UK Government for considerable periods of time, thus leading to the plausible assumption that the energy consumption from the domestic sector would be much higher than it actually turned out to be. This may be the visible result of the policies and plans, laid out by the UK Government over the years, working. Meanwhile, that year, energy consumption in other sectors decreased, in particular the transport sector, though this sector was still the largest consumer overall (National Statistics, 2021). In 2021, the domestic sector was responsible for a 5.8% increase in energy consumption from 2020 levels (National Statistics, 2022a). This was attributed to people continuing to work from home, following the COVID-19 pandemic. On a more positive note however, whilst total energy consumption between 2020 and 2021 increased by 4.6%, it still remained below pre-COVID-19 levels (National Statistics, 2022a).

National Statistics' document on Energy Consumption in UK 1970-2021 (National Statistics, 2020) provides a more representative outlook of the UK energy consumption and progress made in recent years. Over the last few years, the domestic sector has been responsible for about 28-29% of the UK energy consumption, the second largest contributor after the transport sector. CO2 caused 80% of the UK's greenhouse gas emissions in 2019, as shown in the 2019 UK Greenhouse Gas Emissions report (The National Archives, 2019). The report also noted that the residential/domestic sector was responsible for 15% of greenhouse gas emissions in 2019. This was 1% lower than 2018 and 14% lower than data collected in 1990. Again this could possibly point to the conclusion that the UK Government initiatives seem to be having a positive impact, although, according to 2021 provisional statistics (National Statistics, 2022b), UK territorial greenhouse gas emissions were 4.7% higher than 2020 but still 5.2% lower than 2019. All sectors drove the increase in CO2 emissions in 2021, with transport increasing the most (10%). The domestic/residential sector increased by 5.8% (National Statistics, 2022b) and a further document released by National Statistics (National Statistics, 2022c) stated this increase came about as a result of colder weather in 2021 compared to 2020. Hopefully the rise in emissions seen in 2021 will not continue to increase over the coming years.

One possible contributing factor to energy consumption in the building/domestic sector could be the presence of a performance gap in dwellings, where the building does not perform as well as it was designed to. In 2014, the Zero Carbon Hub (Zero Carbon Hub, 2014) were commissioned to examine evidence for the significance of the performance gap in domestic buildings and investigate reasons for this as well as suggest ways these could be addressed. One suggestion was that new methods for assessing building performance should be developed. They also put forward their ‘2020 Ambition’, involving the support of over 160 industrial experts from 90 different companies. The initiative aimed to show, from 2020, that the performance of a minimum of 90% of all new domestic buildings in the UK would at least meet their designed energy/carbon performance, in order to continue the national decrease in energy consumption and carbon emission. Given how much the buildings sector contributes to carbon emissions, this was a promising initiative in tackling carbon emissions from domestic buildings. Unfortunately, in 2016, the Zero Carbon Hub ceased operations due to Government funding cuts (Zero Carbon Hub, 2016). Given the lengths the UK has gone to in order to tackle climate change, this seems surprising and a step backwards. This said, the Government released the Net Zero Strategy in 2021 (The National Archives, 2021), which hopefully will continue to move progress in the right direction. It must be considered, however, how much more progress could have been made in recent years if the Zero Carbon Hub had continued with their ‘2020 Ambition’.

Reducing the performance gap of dwellings is an issue recognised across the globe (Fitton, 2021) and in reducing performance gap, energy consumption may also be reduced. In order to reduce performance gap, it must first be measured, and this is explored, along with current limitations, in the rest of this literature review.

## 2.2 Performance Gap

The domestic sector in the UK, as well as other industrialised countries, is a large contributor to $CO_2$ emissions and national energy usage. According to field evidence, (Doran, 2001; Gupta & Gregg, 2015; Hens et al., 2007; Housez et al., 2014), the measured fabric performance of a building is often higher than predicted, leading to a discrepancy known as the ‘performance gap’. Rye and Scott (Rye & Scott, 2012) suggested that U-values used to evaluate the energy performance of dwellings can often be notably overestimated, a contributing factor of which can be due to assumptions made when using them (Li et al., 2015). This generally large discrepancy between predicted and measured fabric performance can significantly impact energy usage in domestic buildings as well as their $CO_2$ emissions. If the model or design of a dwelling is correct, but the as-built performance of the dwelling does not meet that, the building will not perform well, and measures need to be taken to close that gap.

In 2015, Johnston et al. presented results from co-heating tests (Johnston et al., 2015), explained later on in this chapter in section 2.4.1, which were undertaken on 25 newly built dwellings, built to Approved Document (AD) L1a 2006[1] standard or better, in order to quantify the size of the performance gap between the predicted fabric performance and the measured fabric performance. They found that the measured fabric performance was greater than the predicted fabric performance in all 25 of the newly built dwellings, resulting in a wide range in fabric performance and, in most of the properties, a large performance gap. The measured HTC was just under 1.5 times the HTC predicted at steady state, whilst the measured whole building U-value was over 1.6 times greater than predicted. As a result, when these domestic buildings are in use, there is likely to be significant implications for the amount of energy usage and $CO_2$ emissions.

A year later, Johnston at al. released another paper looking to ‘bridge that gap’ and examine the difference between the predicted fabric performance and the measured fabric performance of three new-build case-study dwellings based in the UK, by performing a selection of in-depth building fabric thermal performance tests (Johnston et al., 2016). These tests included co-heating tests, pressurisation tests and heat flux measurements. The results showed that the measured fabric performances of the three case-study dwellings were very close to their predicted

[1] Approved Documents provide practical guidance, regarding how to meet the requirements set out in The Building Regulations, and present what may be reasonable provisions for compliance with these requirements under ordinary circumstances. Approved Document L1a, for example, provides guidelines including limiting fabric parameters such as U-values and air permeability.

fabric performances. This disagreed with other previous work which revealed that there is a large discrepancy between the measured and predicted fabric performance seen in new-build dwellings in the UK. The authors attributed this good performance to three key factors, including the fact that all three of the dwellings were looking to gain Passivhaus Certification[2], they were all built by highly skilled people who took care with the design and construction of the dwellings, and, finally, the development of the buildings was subject to media attention and so could not afford to fail in terms of their fabric performance.

Fabric performance testing is often carried out on both older dwellings, to provide insight into their current performance and potential retrofitting requirements, and newer dwellings, to examine whether a newly built dwelling's measured in situ thermal performance performs as well as its design thermal performance predicts. In the same year, Johnston and Siddall used the co-heating method to investigate whether Passivhaus Certified dwellings actually performed as well in situ as predicted (Johnston & Siddall, 2016). Co-heating tests were performed on seven dwellings from 5 different Passivhaus developments, allowing for a range of dwelling sizes and construction types to be tested from different locations around the UK. The measured in situ HTC from each dwelling, determined from the co-heating test, was compared to the dwelling's predicted steady state HTC. It was found that in all the dwellings, except one, the measured in situ HTC was greater than the predicted HTC and that there was a performance gap, however this gap was minimal. However, at the more extreme end of things, this gap (in terms of absolute heat loss) would more than likely have important implications in terms of an increase of energy consumption. Despite this, it was concluded that the dwellings performed within the acceptable boundaries expected from Passivhaus Certified dwellings. Taking into consideration the current lack of measured

[2] Dwellings that have Passivhaus Certification use very little energy for heating and cooling but are still able to provide a high level of comfort to the dwelling's occupants. Simply put, according to BRE, a house that meets the Passivhaus standard is well insulated with minimal thermal bridging, makes use of passive internal heating and solar gains, and also has excellent air tightness as well as a good indoor air quality (BRE, 2019). There are more than 1000 Passivhaus certified dwellings in the UK, a considerably small number when compared to volume house builders (Passivhaus Trust, 2018).

Passivhaus fabric performance data, they determined that Passivhaus dwellings could potentially be constructed where their measured in situ fabric performance approximately performs as expected from their steady state predictions.

Whilst shortcomings in construction can be held accountable for the differences between predicted and measured fabric performance, Marshall et al. demonstrate in their paper that the modelling and measurement process of fabric performance can contribute as well (Marshall et al., 2017). A standard model of a typical pre-1920s UK end terrace house was built in DesignBuilder in order to determine the performance gap, using co-heating tests to determine the measured mean HTC of the dwelling. The aim was to then try and reduce the performance gap by calibrating the model with in situ data. The measured mean HTC of the dwelling from the co-heating tests was found to be 219.6 $W{\cdot}K^{-1}$, whilst the standard model, using assumed U-values, produced a mean HTC of 260.2 $W{\cdot}K^{-1}$, therefore creating a performance gap of 18.5%. However, by calibrating the standard model with newly obtained values of air permeability and U-values, the new predicted mean HTC became 224.9 $W{\cdot}K^{-1}$, reducing the performance gap to 2.4%. As such, this shows that the performance gap of a domestic building can be attributed to multiple factors: i) discrepancies in fabric performance and assumed values, ii) assumptions due to modelling software.

## 2.3 Fabric Performance

The research in this thesis focuses on measuring the fabric performance of a domestic building, in particular determining the HTC. However, the performance of the building fabric of a dwelling can be examined by taking both qualitative and quantitative measurements. All of these measurements have strengths and weaknesses and varying reliabilities. Some of the trusted key measurements most commonly made to determine fabric performance, and that are used in this thesis, are outlined in this section, split into disaggregate (individual element) and aggregate (whole house) measurements.

### 2.3.1 Disaggregate Measurements

2.3.1.1 U-values

A U-value, or thermal transmittance, as defined in ISO 7345 (BSI, 2018, p. 4), is the *"heat flow rate in the steady state divided by the area and by the temperature difference between the surroundings on both sides of a flat uniform system"*. U-values, however, have been around since the late 1800s, where Box originally defined it in his book as the heat loss from a building exposed on all sides to air, measured in units of per square foot per hour (Box, 1880). Today, a U-value has units of Watts per square meter per Kelvin ($W{\cdot}m^{-2}{\cdot}K^{-1}$) and are often measured by employing heat flow meters, or heat flux plates, to determine the heat flux density ($W{\cdot}m^{-2}$) of the element being measured, such as a wall. Dividing the heat flux density by the internal-external temperature difference (K) provides a value for the element's thermal transmittance (U-value). This is the standard method laid out in ISO 9869-1 (BSI, 2014).

In about 300 domestic buildings in England, during 2015, the Building Research Establishment (BRE) undertook U-value assessments of dwelling walls (Hulme & Doran, 2015), using the standard method laid out in ISO 9869-1 (BSI, 2014). Based on assumptions that had been made, as well as already known information, theoretical U-values of the dwellings were also determined. The measured U-values were then compared against the calculated theoretical U-values and against typical RdSAP U-values.

RdSAP stands for Reduced Data Standard Assessment Procedure and is used when a complete set of data is unavailable for Standard Assessment Procedure (SAP) calculations (BRE, 2012). SAP is used to calculate the energy performance of dwellings (BRE, 2014). RdSAP was developed by the UK government to be applied in already existing domestic buildings, whilst all newly built dwellings have to be assessed using SAP. In the RdSAP process, firstly the data set is filled in so that it becomes a complete data set, and then the SAP calculations are applied. The data in the BRE report was compared with the accepted RdSAP values at the time, where a standard, as-built, solid brick wall had an RdSAP U-value of 2.1 $W{\cdot}m^{-}$

$^{2}$·$K^{-1}$, as documented in Appendix S: Reduced Data SAP for existing dwellings (BRE, 2009), which was applicable from 2012.

For all the wall types investigated by Hulme and Doran (Hulme & Doran, 2015), it was found that there were wide variations in the measured U-values, which could be attributed to variations in the walls and/or the process of taking U-value measurements. Additionally, and most importantly, for a standard, solid brick wall, the median measured U-value was 1.59 W·$m^{-2}$·$K^{-1}$, whilst the theoretical U-value was calculated to be 1.92 W·$m^{-2}$·$K^{-1}$. Both of these, in particular the measured U-value, were significantly lower than that of the RdSAP value. Similar findings were presented for the other examined wall types. It was realised, that oversimplifying the way U-values were calculated using the RdSAP methodology, lead to the overestimation of the RdSAP U-values. This has since been accounted for and altered. The most current edition of RdSAP, at the time of writing this thesis, has been applicable since 2019, and provides a U-value of 1.7 W·$m^{-2}$·$K^{-1}$ for a standard, as-built, solid brick wall (BRE, 2012). The findings of this research obviously caused significant changes to the assumed energy performance of dwellings with solid walls (i.e., they were assumed to perform worse than they actually were), leading to the potential skewing of reported results, such as the effectiveness, of Government-supported insulation programmes (Hulme & Doran, 2015). Additionally, if homeowners believed that the walls of their houses were performing worse than they realistically were, they may have made unnecessary decisions to improve their wall insulation, etc.

#### 2.3.1.2 Infrared Thermography

According to ISO 13187 (BSI, 1999), thermography is the use of thermal images - images produced by an infrared (IR) radiation sensing system - in order to measure the IR radiant density from a surface, so that the surface temperature distribution can be determined or represented. There are some drawbacks with the use of IR thermography, such as occasional difficulty in focusing the image if conditions are not ideal, reflections and heat prints from touching a surface about to be measured.

- <u>Qualitative IR Thermography</u>

IR thermal imaging can often be used in the qualitative examination of building envelopes to show areas of more or less heat loss, as well as other irregularities. A standard method for this is laid out in ISO 13187 (BSI, 1999). For example, a surface showing up blue in a thermal image demonstrates that that particular area of the surface may be colder and so there is likely to be more heat loss in that area. Kirimtat and Krejcar, explored and reviewed the use of different thermographic methods, including qualitative IR thermography, in examining building fabric performance (Kirimtat & Krejcar, 2018). In the article, it was shown that qualitative IR thermography is most useful in determining the location of, as well as analysing, thermal bridges, the structural performance of the building fabric, air leakage, and areas of high moisture content.

- <u>Quantitative IR Thermography</u>

According to Kirimtat and Krejcar, quantitative IR thermography is the most frequently used IR thermography method (Kirimtat & Krejcar, 2018). One example of the quantitative use of IR thermography is demonstrated in the recent development of the Heat3D app (BTS, 2021a). Developed by the companies BTS and Electric Pocket, along with the University of Salford, Heat3D is a new app and method that allows for the rapid measurement of the U-values of walls. A Heat3D survey consists of firstly having an Augmented Reality 3D model of the room under examination created in the app on an iOS device. Using a FLIR One Pro IR camera inserted into the iOS device, thermal images of the walls are then mapped onto the 3D model. Using the thermal images, room temperature and reflected temperature measurements are recorded on the Heat3D app, where the total heat transfer across each wall is then calculated. An hour-long time lapsed survey is taken in order to measure the U-value of a wall in a heated room. In comparison to the standard method of calculating U-values using heat flux plates, detailed in ISO 9869-1 (BSI, 2014), which takes a minimum of three days to undertake, the Heat3D method takes one hour to calculate the U-value of a wall. When testing the accuracy of the method it was found that 85.7% of the surveys taken (out of a total of 42) fell within the accepted combined uncertainty interval provided by ISO 9869-1 (BSI, 2014), however it was found that the method struggled when attempting to measure

U-values below 0.2 W·m$^{-1}$. Theoretical U-values are generally used in the design and building process of dwellings, rather than the U-value being measured. However, as shown in the BRE report (Hulme & Doran, 2015), theoretical, or pre-determined, U-values are not always the same as the actual as-built, measured U-values. This can lead to the performance of the dwellings being over or underestimated. Heat3D provides a solution to address this and other issues. By providing a rapid U-value measurement, this can then be used for quality assurance and for better informing the management of building and retrofit processes.

### 2.3.2 Aggregate Measurements

2.3.2.1 Air Leakage

The air permeability of a building is the *“air leakage rate per the envelope area across the building envelope”*, as explained in ISO 9972 (BSI, 2015b, p. 1). The ventilation heat loss of a dwelling can be found by multiplying the air change rate of the dwelling under normal conditions by the volume of the dwelling and the specific heat capacity of air. The standardised $n_{50}$/20 ‘rule of thumb’ is used to convert the air change rate at 50 Pa, determined by an air leakage test, to the air change rate under normal conditions

One common way of determining the air permeability of a dwelling is through the use of a blower door test. The blower door test is an internationally recognised method for testing the air permeability of buildings with both an ISO standard (BSI, 2015b) and a USA standard (ASTM, 2010). According to ISO 9972, the blower door setup consists of a large fan that is mounted in an external doorway (BSI, 2015b). The building is then either pressurised or depressurised, allowing for air to either flow out of the building through all the unsealed cracks and gaps in the building envelope (pressurisation) or flow into the building (depressurisation). During the test, measurements such as the air flow rate and the internal-external air pressures are taken. Sometimes, thermal imaging cameras or tracer gas may also be used to look at the building fabric in order to see where air is leaking in or out.

Whilst it is one of the more commonly used methods of determining the air permeability of buildings, there is also an element of uncertainty associated with the blower door test. For example, Delmotte and Laverge investigated the reproducibility and repeatability of the blower door test, where they established that, at 50 Pa, the method achieved 2.7% reproducibility and 3.7% repeatability (Delmotte & Laverge, 2001). In 2016, Carrié and Leprince looked to quantify the uncertainties caused by steady wind whilst performing building pressurisation tests. It had been found that as wind speed increased, the degree of uncertainty during the test increased also, and Carrié and Leprince found that when performing the test at lower pressure, that level of uncertainty was more evident (Carrié & Leprince, 2016). As such, despite being perhaps currently the most common method to determine air permeability, the blower door test does face issues around uncertainty.

Another method of determining the air permeability of a building is through the use of the Pulse method, which was developed by Build Test Solutions (BTS) in 2018 based upon work originally undertaken at the University of Nottingham. The Pulse method (BTS, 2021b) is used to measure the amount of air leakage in a building at 4 Pa. Firstly, before the test starts, the background pressure of the building is measured as a baseline. Air is then released into the building and the rate of the air release is measured; the pressure of the building generally reaches its peak at 10 Pa. The air flow from the Pulse tank is less than the air flow through the building fabric, thus leading to the pressure in the building steadily decreasing. This is then used to measure and calculate the amount of air leakage through the building fabric. The air permeability of the building is calculated by comparing the pressure in the building, whilst it is steadily decreasing, to the amount of air that is released by the Pulse tank. Once the test finishes, the pressure in the building returns to normal as a result of the air leakage through the building fabric. The background pressure is measured once more as another baseline. Much testing has been carried out to validate the Pulse method (see (BTS, 2018; Feeley, 2018; Holden & Randall, 2019; Zheng & Smith, 2020) and Pulse has been verified and validated by the BRE.

In 2021, Hsu et al. compared the indoor air pressure distribution created using the blower door method and the Pulse method (Hsu et al., 2021). The uniformity of the pressure distribution found during a Pulse test had previously been called into question due to its dynamic and fast nature. However, in this comparison, uniform pressure distributions inside the test dwelling were found for both test methods.

Additionally, both methods provided good agreement with each other with regard to the calculated air permeability, with an observed deviation of 3.93% at 7.1 Pa up to a 4.56% deviation found at 10.6 Pa. Another observation was that the location of the Pulse tank within the dwelling slightly impacted the calculated air permeability.

In general, both methods present good reliability at determining the air permeability of a building with the blower door test being a very commonly used method, and the Pulse method showing a lot of promise to contend with this, having been developed over recent years.

#### 2.3.2.2 Heat Transfer Coefficient

The heat transfer coefficient (HTC) is defined as the *“heat flow rate divided by temperature difference between two environments”* in ISO 13789 (BSI, 2017d, p. 2). In other words, it is a measure of the rate of heat loss from the thermal envelope of the house in Watts (W), divided by the internal-external temperature difference in Kelvin (K) (Alzetto, Farmer, et al., 2018), where the thermal envelope of a building is the ‘conditioned’ area within the house (i.e., the heated or cooled spaces within the dwelling, excluding any loft or underfloor spaces).

In 2017, Farmer et al. presented findings that contained the first acknowledged measurement of a HTC obtained under steady-state conditions (Farmer et al., 2017). The test house that was being investigated was retrofitted in stages, with the HTC measured at each retrofit stage using a co-heating test. Retrofitting is the act of upgrading a dwelling in order to reduce the dwelling’s energy consumption (Swan et al., 2017). The authors found that it was not possible to compare, with accuracy, the predicted values of the HTC at each retrofit stage against the corresponding measured values, as not all thermal bridges were taken into account. A thermal bridge occurs where the thermal resistance of part of the building envelope is considerably altered by: i) the building envelope being penetrated by materials with different thermal conductivities, ii) differences between the internal and external areas of the building envelope, often found at junctions etc., iii) differences in the fabric thickness of the building envelope (BSI, 2017b).

## 2.4 Whole House Heat Loss Test Methods

Most of the measurements outlined above were used in Annex 71 (Bauwens et al., 2021; Fitton, 2021; Reynders et al., 2021), a recent set of reports, with work undertaken internationally, which looked to examine building energy performance based on measurements made in situ. Subtasks 1 and 4 (Fitton, 2021), in particular, looked at the inputs and outputs of data analysis methods, with notable emphasis on HTC measurement. Also assessed and compared were currently used testing methods for measuring the HTC.

### 2.4.1 The Co-heating Method

The 'electric co-heating' method was initially developed in North America in 1979 by Sonderegger and Modera (Sonderegger & Modera, 1979). The development of the method came about because of a need for a way to experimentally verify the effects of energy-savings measures applied to the building envelope of a dwelling or the heating systems within. Portable heaters were used to heat the property as well as the regular heating system in the dwelling, thus deriving the name 'co-heating'. The net heat gain to the dwelling was illustrated by the measured load reduction experienced by the portable heaters, this was then divided by the measured energy used by the heating systems to provide a value for the net efficiency of the heating system. In this paper, the 'electric co-heating' method was presented as a positive method which enabled a system's (made up of any appliance and a house) net efficiency to be measured. A year later, Sonderegger et al. published another paper depicting the further development of the 'electric co-heating' method (Sonderegger et al., 1980). Other capabilities of the method were reported with the in situ aspect of the method emphasised. Additionally, key advantages of the method were outlined and discussed, including the method's ability to perform in realistic operating conditions.

Whilst there is no official standard for carrying out the method, today a more recent version of the co-heating method is used, developed by Leeds Beckett University (then known as Leeds Metropolitan University) (Johnston et al., 2013), and is the most recognised established method. The current method spans 1-3 weeks and uses portable electric heaters and ventilation fans to homogenously heat up an unoccupied dwelling to an elevated internal temperature under quasi steady state conditions (i.e., the internal temperature is kept at a constant static state, whilst the external conditions remain dynamic and variable). During the test, the total electrical input to the building, internal temperatures, relative humidity, and the external climatic conditions, including the external temperature, are measured. The daily heat input to the dwelling is then plotted against the daily internal-external temperature difference and the resulting gradient of the plot provides a raw, uncorrected value of the HTC. This method uses an energy balance equation, modified from (Everett, 1985):

$$Q + R \cdot S = (\Sigma A \cdot U + \ C_V) \cdot \Delta T$$

*Equation 2.1*

Where the sum of the space heating (Q) and the solar gains (R·S) is equal to the sum of the fabric heat loss ((ΣA·U)·ΔT) and the air infiltration ($C_V$·ΔT).

However, the practicality and reliability of this method was called into question due to its long testing duration and uncertainty in measuring the HTC. A report reviewing co-heating test methodologies was published by the National Housing Building Council (NHBC) Foundation (Butler & Dengel, 2013). The report outlined the results and conclusions accrued after six teams performed co-heating tests, generally based on the guidelines provided by Leeds Beckett University, performed on different dates on two identical houses (A and B). One house was a control house, the other was the test house. Additionally, the teams attempted to derive the solar aperture of the dwellings. The teams had differing levels of experience when it came to performing co-heating tests and analysing the data. Some teams used different equipment, for example some used standard thermostats to control temperatures whilst another team used industrial digital temperature controllers. For the most part, all teams used an analysis method known as the Siviour method or, if not, something very similar. Furthermore, a few teams opted to analyse the data over different periods, in contrast to the proposed midnight-midnight in the guidelines, with one defining a day from 06:00-06:00, another defining it as from 09:00-09:00, and the other 18:00-18:00. It was found that the accuracy and repeatability of the co-heating tests were significantly impacted by the external weather conditions, including solar radiation, causing it to be difficult to attain proper steady state conditions. Changeable weather over the long testing period meant it was hard to achieve true steady state conditions, however shortening the testing period would also cause the test to become less accurate. This said, the results also suggested that by analysing the co-heating data from the night-time periods, the uncertainty that resulted from solar gains to the property may be reduced. Overall, the variability in the results obtained was rather small, however the reliability of the co-heating test continued to remain in question and still needed confirmation.

In a similar vein, Stamp assessed the uncertainty within the co-heating method, looking at both case-study field tests and simulated tests that applied the co-heating method (Stamp, 2015). In particular, experimental, weather driven, and statistical uncertainties were examined. To summarise, it was found that weather conditions during testing, especially solar radiation, particularly influenced estimates of the HTC. These estimates were also impacted by secondary heat flows, causing variation in the HTC. In addition, it was determined that large systematic uncertainties were likely if experimental uncertainties, such as irregular internal temperatures or errors from measuring equipment, were left unchecked.

In 2018, Jack et al. were able to provide the first evidence that co-heating tests were reliable, as well as establishing recommendations for the best way to undertake a co-heating test, including the positioning of the heaters and fans in each room within the test dwelling (Jack et al., 2018). Similar to the NHBC tests discussed previously, seven teams performed co-heating tests in the same test house, with slight variations in the way they conducted the tests (i.e., using different numbers of heaters and fans, taking different types of measurements, etc.,). Furthermore, different data analysis methods were applied, where some teams accounted for solar gains or windspeed, and other teams did not. When comparing results, six of the seven teams had recorded final HTC values within 10% of the mean HTC. Unfortunately, the seventh team experienced equipment failure during the testing phase and so were omitted from the final results. It was found that estimation of the solar gains caused the largest difference in the testing and analysis processes, thus leading to the conclusion that the method used for estimating the solar gains to the property should be stated when presenting the results of a co-heating test. By following the recommendations in carrying out co-heating tests outlined in the author’s paper, along with the co-heating guidelines initially established by Leeds Beckett University (Johnston et al., 2013), it should be possible to accomplish repeatable data collection.

Whilst the reliability and repeatability of the co-heating test is no longer in question, problems still arise around seasonality. In the UK, and in countries with similar climates, the method can only be used to determine the HTC in the colder, winter months where it is possible to achieve the required internal-external temperature differences. Meanwhile in cooling dominated climates, being able to achieve a temperature difference between the internal and external environments of at least 10 K must be extremely challenging.

Unfortunately, and possibly as a result of the currently used co-heating method having been developed in the UK, there are very few articles and reports documenting the use and results of co-heating tests outside of the UK, or indeed Europe (such as (Francisco et al., 1998)). However, in 2020, Law and Wong expressed the findings of using the co-heating method in different regions and times of the year in Australia (Law & Wong, 2020). The aim of the research was to examine how accurately the HTC could be estimated in different locations and times of the year in Australia through the use of simulated co-heating tests. It was found that, whilst the test could be used in most of the climate zones in Australia, the most accurate period in which to conduct a co-heating test and estimate the HTC was in the cooler May-September months, when significant internal-external temperature differences could be achieved. However, in the four most northerly (and hence warmest) zones under examination, the HTC was unable to be estimated with the use of the co-heating method. This was as a result of the warmer climate in the northern zones making it difficult to achieve and maintain a suitable temperature difference between the internal and external environments.

#### 2.4.1.1 Sources of Uncertainty

In his thesis, Stamp assesses the sources of uncertainty that arise when performing and analysing results from co-heating tests (Stamp, 2015). This section briefly discusses a couple of the key considerations that were highlighted in his thesis.

- Aggregation Interval

One such uncertainty that Stamp draws attention to is the aggregation interval (Stamp, 2015). A daily cycle of measurement can be aggregated across different intervals of the same length, for example, two commonly used intervals aggregate data between midnight-midnight or dawn-dawn. One of the earliest acknowledgements of which may be a more preferable aggregation interval can be found in Everett's report 'Rapid Thermal Calibration of House' (Everett, 1985). He suggests that a dawn-dawn aggregation may be a better choice since solar radiation stored in the fabric of the house during the day may not be entirely released until dawn the following day. Stamp himself reaches a similar conclusion that a sunrise-sunrise aggregation approach may be purer, though careful thought and consideration is always advised (Stamp, 2015).

On the other hand, tests recorded in the NHBC Report (Butler & Dengel, 2013) used a variety of aggregation intervals from 06:00-06:00, 09:00-09:00, 18:00-18:00 and midnight-midnight. The current co-heating guidelines set out by Leeds Beckett University (Johnston et al., 2013) state that the aggregation interval used is dependent on the type of building being assessed. For example, it is assumed that a lightweight or mediumweight dwelling (i.e., a dwelling that is perhaps made of timber), would release the solar radiation stored in its fabric by midnight of the day it was absorbed, and so a midnight-midnight aggregation would be preferable. Meanwhile, a heavyweight dwelling (such as one built from concrete), would be more likely to re-radiate its stored solar radiation by dawn the following morning, and therefore a dawn-dawn aggregation would be more suitable.

- Forced Intercept

Stamp also reveals that there has been much debate regarding whether a forced or an unforced intercept is better when plotting power against temperature difference in order to determine the HTC (Stamp, 2015). Johnston et al. suggest forcing the regression line through the origin, as this then assumes that when there is no internal-external temperature difference, there is no heating required inside the property (Johnston et al., 2013). However, it is also stated that it is still a possibility that, despite there being a zero temperature difference, there might still be some heat loss due to radiative cooling during the night, which may cause a non-zero intercept.

### 2.4.2 Other Heat Loss Test Methods

In addition to the co-heating method, there are other heat loss test methods that can be used to determine the HTC of a dwelling. This section discusses just some of these.

#### 2.4.2.1 The QUB Method

The QUB method was originally proposed by Mangematin et al. in 2012 (Mangematin et al., 2012), and patented a few years later as the Quick U-value of Buildings (QUB) method in a report written by Bouchié et al. (Bouchié et al., 2015). It is a dynamic method based around a resistor-capacitor model and is carried out during the winter months, over the course of one night, so that solar radiation can be neglected and will not skew the results from the test. The dwelling, which must be unoccupied, is heated up using constant power, calculated from an estimate of the HTC, for a period of time (for example, several hours). The dwelling is then allowed to cool naturally, using little-to-no power input, for the same period of time. The gradients of the resulting temperature profile over the night, along with the internal-external temperature differences, are then used to estimate the HTC of the dwelling, see (Alzetto, Pandraud, et al., 2018; Meulemans et al., 2017). Whilst this method is faster than the co-heating method there is still disturbance caused to the occupants so that the house can be measured unoccupied. There is also some ambiguity when it comes to measuring the gradients of the resulting temperature profiles; one person's interpretation of the steepness of the gradient may be different to someone else's.

#### 2.4.2.2 The PSTAR Method

The Primary and Secondary Term Analysis and Renormalisation (PSTAR) method is similar to the co-heating method, and, in some ways, also to the QUB method, in that it consists of a heating period and a cooling period. It was initially developed by Subbarao, a member of the Energy Research Institute, and presents a logical and convenient way of categorising the energy flows of the dwelling in to HTC, building mass, and area of solar gain (Subbarao, 1988). The method, which is dynamic, normally lasts between 2-4 days and can only be performed in the coldest months of the year. It begins with the property undergoing a co-heating-like test during the first night, and then a cooling down period during the second night. After these steps, data regarding the solar gains are collected during the day, which is sometimes followed by another night consisting of a heating system test. When compared to the co-heating test it had a deviation of up to 35%, however in general it has been shown to have a good overall accuracy and a repeatability of 5% (Bouchié et al., 2015). The method does require the dwelling to be unoccupied, causing inconvenience to the dwelling's occupants. It also could not be applied in warmer months due to the co-heating-like tests performed as part of the method.

#### 2.4.2.3 The ISABELE Method

The In Situ Assessment of the Building EnveLope performancEs (ISABELE) method was developed by Centre Scientifique et Technique de Bâtiment (CSTB) (Bouchié et al., 2014). Its duration lasts a minimum of 5 days, up to, at most, 15 days and can only be applied to an unoccupied dwelling. In the first step of the method, no heating power is applied to the dwelling so that the thermal energy stored in the thermal mass of the dwelling at the very start can be measured. The second step is to apply heating power to the dwelling so that it reaches a set internal temperature. This temperature is determined by using the average internal temperature measured in the first step, in order to increase it by a minimum of 10 K. To best achieve this temperature difference, it could be recommended that the method be undertaken during a colder time of the year. In the third and final step, the internal temperature is allowed to decrease naturally with no power input. Measurements, such as temperature, power input to heat the dwelling, external temperature, etc., are used in assessing the fabric performance of the dwelling and, ultimately, provide a value of the HTC (Bouchié et al., 2014, 2015). It has been generally found to provide an accuracy between 5-20% in comparison to a pre-determined reference HTC (Fitton, 2021). This method would be less useful in warmer months, due to the requirement of achieving a significant internal-external temperature difference. Furthermore, this method also requires the dwelling to be unoccupied, causing disturbance to the occupants.

#### 2.4.2.4 Integrated Co-heating and On-Board Monitoring

In 2016, Farmer et al. presented a methodology whereby the HTC of an unoccupied dwelling was obtained by using the dwelling's heating system. This method was referred to as 'integrated co-heating' (Farmer et al., 2016). The data from the integrated co-heating method was compared to electric co-heating data and results showed that there was good agreement between the HTCs. The paper concluded that the integrated method allowed for in situ quantification of both the dwelling's heating system and fabric performance, thus indicating that it may provide a more representative HTC of how the dwelling performed in-use, as well having the potential to be more cost-effective. This method was very similar to the co-heating method in the way it was carried out, with the key difference being the use of the dwelling's heating system rather than electric resistance heaters.

More recently, other methodologies have looked at using a dwelling's heating system without the need for the dwelling to be unoccupied and determining HTCs whilst the dwelling is in-use. (Allinson et al., 2022) released a technical evaluation of the SMETER technologies (TEST) project. SMETER (Smart Meter Enabled Thermal Efficiency Ratings) technologies use smart meter data from an occupied home in order to calculate the HTC of that dwelling by employing algorithms. Phase two of the project, as reported in the technical evaluation, involved carrying out field trials on thirty dwellings of varying constructions, typical of those found in the UK, all built during the twentieth century. Along with smart meters, temperature and humidity sensors were installed in a number of rooms in each dwelling. Before using the SMETER technologies, the measured as-built HTCs of the dwellings were determined by carrying out a modified version of the co-heating test in each of the dwellings whilst they were unoccupied. The dwellings were then occupied and monitored, with the occupant's permission, using select SMETER technologies assigned to each dwelling. The data collected from these technologies, after a period between several months to almost a year, were then used in the algorithms to determine the HTCs of each home. Each SMETER product was evaluated; firstly by a direct comparison to the measured HTC, with a successful estimate of the HTC occurring if the confidence intervals between the measured and estimated HTC overlapped, and secondly by looking at the difference between each SMETER estimated HTC and its corresponding measured HTC. It is important to note here, however, that because of the way they are determined, the HTC obtained from a co-heating test is fundamentally different to the HTC measured when the house is occupied (e.g., measured via SMETER technologies).

Despite this difference, it was found that the SMETER technologies were successful for 70% to 97% of the dwellings tested, with an average confidence interval of 12% to 33%. Five of the participating organisations were more than 90% successful overall at providing SMETER HTCs. It was noted, however, that the suitability of a particular SMETER technology for a specific application would likely depend on the accuracy of the technology, the duration of testing and the cost, as well as convenience, of carrying out the test.

Previous to this, Senave et al. investigated how various characterisation techniques impact and result in differing estimates of the HTC of a dwelling (Senave et al., 2019). This was done by carrying out sensitivity analysis on the characterisation outcome of a case study dwelling. Senave recognised that there was increasing interest in potentially using on-board monitoring (e.g., using smart meters, etc.) and data-driven modelling in order to estimate the HTC of a dwelling. However key challenges came from being able to identify the input data that would be required, and the most appropriate data analysis techniques to use in order to estimate the HTC of particular dwelling types. Outcomes from their research showed that, depending on the amount of monitoring data available and the prior data used to establish the interior temperature of the dwelling, there were deviations up to 29.6% on the estimated HTC. The way the internal and solar heat gains were represented also significantly impacted the estimated HTC. In addition to this, the HTC estimated by the on-board monitoring was compared to the corresponding theoretical HTC, and large gaps were found between the values. Factors that may have contributed to these discrepancies were explored, such as the way the U-values were calculated and the variability in the internal temperature measured in different locations within the dwelling.

On-board monitoring to determine the HTC of a dwelling is a very recent method, and it is expected that further research will be carried out investigating its validity. However, a positive of this method could include not needing to set up additional equipment, aside from sensors, in order for it to be performed, given that data would be collected directly from the on-board technology already used within the dwelling. This would cut some of the costs in carrying the method out. In addition, the dwelling can be occupied during testing, resulting in minimal disruption to the occupants. This said, the occupants may not feel comfortable having their energy usage monitored over a long period of time.

## 2.5 The Issue of Seasonality

Whilst many whole house heat loss test methods have been developed and have been proven to work, in particular the co-heating method, these methods struggle with seasonality, being most commonly applied during colder periods of the year in order to achieve significant internal-external temperature differences. In particular there is a lack of a methodology that can be performed in warmer climates so that the issue of performance gap in those countries can be better handled. Annex 71 (Fitton, 2021) also brought to light this issue, mentioning that this is one thing that stakeholders would be keen to see addressed, given that on a global scale average performance gaps in countries across the world range from 11% up to 74% (though it is worth noting that these values come from a small number of countries in various climates and with various sample sizes). There is a clear need for a method to be developed that can cope with seasonality or at least can be performed in a warmer climate or during hotter summer months, highlighted by the paper written by Law and Wong investigating the application of the co-heating method in Australian climates (Law & Wong, 2020). The research documented in this report aims to develop a method that might make progress towards being able to measure performance gap in warmer climates.

## 2.6 Developing the Alternative Method

### 2.6.1 Considerations for the Development of the Alternative Method

Previous research, highlighted in this literature review, has shown that the co-heating method (Johnston et al., 2013) can be considered as one of, if not the most, reliable whole house heat loss test methods available (Jack et al., 2018; Stamp, 2015). However, as discussed in the previous section, an alternative method is required to be able to determine the performance of dwellings in warmer climates (Fitton, 2021), such as Australia, or outside of the winter months in temperate climates, such as the summer months in the UK.

In warmer climates, it is unreasonable to attempt to heat a house up in order to establish an internal-external temperature difference of at least 10 K as the extreme internal temperatures required to achieve and maintain this could cause damage to the materials of the dwelling. However, it would not be unreasonable to suggest that it might be possible to cool a house down when external temperatures are elevated.

Therefore, in this thesis, it is proposed that an alternative 'reverse co-heating' method, using cooling techniques rather than heating techniques, could be a possible solution to the problem. In order to develop this alternative method, certain considerations had to be accounted for first, regarding both when the method could be performed and how, leading to a series of variables that could be explored:

Q1. When would be the ideal time to perform the alternative method?

Q2. What sort of weather and solar conditions would be the most suitable?

Q3. What would be the minimum internal-external temperature difference that would allow for the alternative method to work?

Q4. What would be the ideal test period length and aggregation interval for the method?

Q5. How would the construction type and built form of a dwelling impact the performance of the method?

Q6. What equipment should be used to carry out the cooling process?

In order to begin answering these questions the considerations regarding a co-heating test were first reviewed, using the guidelines suggested by Johnston et al. and Stamp (Johnston et al., 2013; Stamp, 2015).

Co-heating tests, as previously established, are best applied over a two-week period during the ‘heating season’, or coldest months of the year, in order to create an indoor-outdoor temperature difference of at least 10 K (Johnston et al., 2013). In addition, Stamp, suggests performing the test over a range of weather conditions, e.g., a mix of both sunny and overcast days (Stamp, 2015). The construction type and built form (i.e., whether the building is detached, semi-detached, etc.) of the dwelling must be considered, as this can impact, for example, how much and for how long solar radiation is stored in the fabric of the dwelling. This in turn impacts which aggregation interval is the most suitable, as using the wrong aggregation interval can lead to an underestimation bias (Stamp, 2015).

These considerations were then applied to the questions listed above. Given that the aim of the method was to determine the performance of a dwelling in cooling dominated climates, the alternative method would ideally be performed when external temperatures are significantly elevated. Since the development of the alternative method would be carried out through performing DesignBuilder simulations, questions Q1-Q4 could begin to be explored by compiling a selection of weather data from previous years and performing simulations using this weather data, hopefully then covering a range of weather conditions and extreme and average temperature profiles. This would also mean that different test period lengths could be investigated. The simulations in DesignBuilder would all still be carried out on the Zed House model, allowing for the performance of the alternative method to be investigated on a ‘high-performance’ dwelling, therefore beginning to answer Q5. It would provide some insight as to whether increased solar gains, a likely potential problem in summer months, would have more of an impact on the model than in the baseline co-heating simulation. Q6 would need to be answered through research of current cooling methods and equipment, to see which would prove the most effective at performing the alternative method. Results from each simulation would then be used to calculate the corresponding HTC and, by taking into account particular protocols, such as statistical validity, the most suitable of these would then be compared to the baseline HTC, found from the co-heating test simulation in DesignBuilder.

### 2.6.2 Initial Proposal of How the Alternative Method Would Work

The purpose of the alternative method is to determine the HTC of a dwelling that is located in a warmer climate. Air conditioning units could be employed to decrease the internal temperature of the dwelling to a setpoint so that there is an internal-external temperature difference. It must be accounted for that achieving a significant temperature difference, such as 10 K, during warmer external conditions and where the dwelling is being cooled down, will be more challenging than heating up a building in colder external conditions, such as during a co-heating test. This is because there is often a minimum temperature limit on cooling systems like air conditioning units (discussed further in section 3.8.1.1), so that in climates where average temperatures may reach somewhere in the late teens to early 20°Cs, only smaller internal-external temperature differences can be achieved. This would most likely be less of a problem in climates that achieve much higher external temperatures.

The test would occur over a period of time (to be determined) and during this time, the power input to the air conditioning unit would be measured. All heating and cooling systems have a coefficient of performance (COP) which indicates that system's efficiency. A more in-depth definition and explanation into the importance of a system's COP is provided later in this chapter. Since the air conditioning unit would have a COP greater than 1, the output from the system would be greater than the input. Consequently, either the values of input power and COP could be used to calculate the output power (see *Equation 2.2* in section 2.6.3.1) (simple simulation only), or a device that could separately measure the cooling output could be employed (more likely in reality due to additional heat gains from the cooling system).

From this, the power output needed to maintain the cool temperature of the dwelling could be plotted against the internal-external temperature difference to determine a raw value of the HTC. Measurements of solar irradiance could then also be used, through multiple linear regression (see section 3.5.3) in order to calculate a solar corrected value of the HTC.

### 2.6.3 Consideration of Air Conditioning Systems

In order to determine the type of air conditioning system that would be most effective for the level of cooling required in the alternative method, careful consideration of the types of air conditioning systems available had to be undertaken. (McMullan, 2012) and (Chadderton, 2013) provide examples of different types of refrigeration cycles and air conditioning systems.

#### 2.6.3.1 Refrigeration Cycles

The absorption refrigeration cycle does not require the use of moving parts and can operate without a compressor. The refrigerant in the system, for example, ammonia, is pressurised and circulated by a boiler. The boiler heats up a concentrated solution of the refrigerant in water and, in doing so, the refrigerant is evaporated into a vapour so that the water is left behind. As the refrigerant vapour passes through the condenser (where heat is released from the system) it becomes a liquid again. It then passes through the evaporator (where heat is absorbed into the system) and once again becomes a vapour. The cycle repeats itself as the refrigerant vapour moves through the absorber and is redissolved into water that is flowing from the boiler (McMullan, 2012). This cycle often burns gas in order to work and produce cooling, and also has a COP of 1, making it a more expensive refrigeration cycle to run compared to its counterpart: the vapour compression refrigeration cycle (Chadderton, 2013).

The vapour compression refrigeration cycle is electrically driven by a compressor which then also circulates the refrigerant in the system. Latent heat, which is extracted from the surroundings of the evaporator and thus causes the evaporator to act as a cooler, forces the liquid refrigerant in the system to evaporate into a vapour. The electrically driven compressor then increases the pressure, and hence also the temperature, of the refrigerant vapour. Once the vapour cools and reaches a temperature below that of its boiling point it condenses back into liquid refrigerant. The condenser acts as a heater as it emits the latent heat from this process back into the surroundings. The pressure of the liquid refrigerant is decreased as it passes through an expansion valve and moves towards the evaporator, where it is evaporated once again and the cycle repeats (McMullan, 2012). This cycle generally has a COP in approximately the range of 2-3, making it the more commonly used refrigeration cycle as it is simpler and cheaper to operate (Chadderton, 2013). A diagram of a vapour compression refrigeration cycle, interpreted from (McMullan, 2012), is shown in *Figure 2.1*.

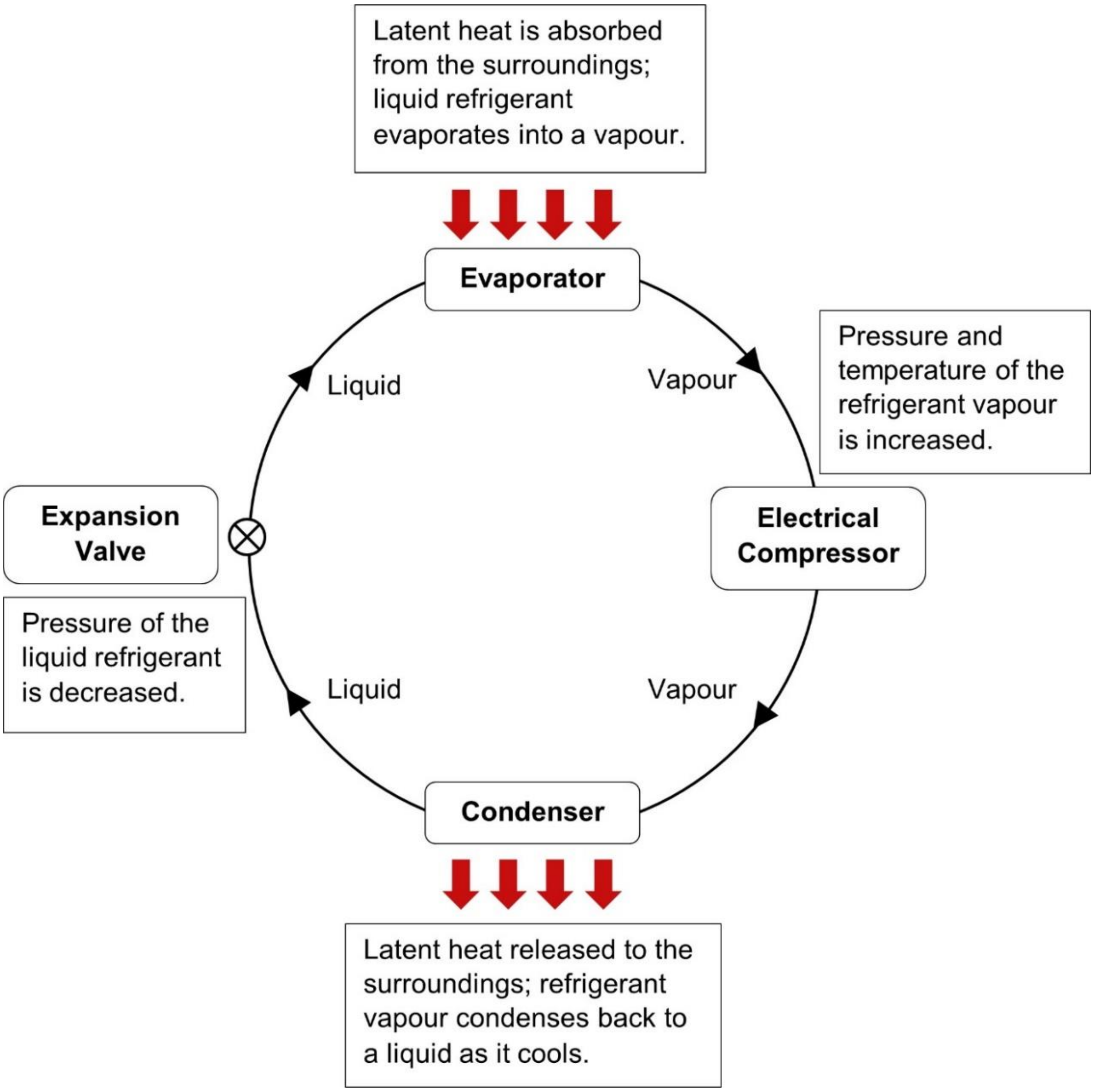


*Figure 2.1 The vapour compression refrigeration cycle, interpreted from (McMullan, 2012, p. 110)*

Refrigeration cycles are the same as heat pump cycles, except refrigeration cycles are used to cool the surrounding air (with the evaporator) and heat pump cycles are used to heat the surrounding air (with the condenser). The COP indicates a cycle's efficiency and can be calculated as a theoretical ratio for a system, the measured performance of a system, the ideal performance of a system (from test data provided by the manufacturer), or as a seasonal average for a system (Chadderton, 2013).

The equation, as demonstrated in (McMullan, 2012), used to determine the COP is:

$$COP = \frac{Heating/Cooling\ energy\ output\ (W)}{Pump\ energy\ input\ (W)}$$

*Equation 2.2*

In other words, the COP for a cycle is the 'heat' or 'cooling' energy output from the system (in Watts), divided by the energy inputted to the system (in Watts). Since the COP is a ratio, it has no units. Heaters, and, as mentioned previously, absorption refrigeration cycles, generally have a COP of 1, meaning that the power output from the system is the same as the power input to the system. Vapour compression refrigeration cycles, on the other hand, have COPs approximately between 2-3, meaning that the power output from the system is greater than the power input to the system, making them a more efficient, and thus cheaper, system to use.

#### 2.6.3.2 Air Conditioning Systems

*Table 2.1* provides information around common types of air conditioning systems that are used (Chadderton, 2013).

*Table 2.1 (Covered on pages 82-84) Common types of air conditioning systems along with the types of buildings they are generally used in and how they work*

| *Air Conditioning (AC) System* | *Where it is most commonly used* | *How it works* | *Notes* |
|---|---|---|---|
| Single-duct system | Large rooms or groups of rooms with a similar demand for AC. | Air, at a constant temperature, is sent to the terminal units in the system. A variable air volume (VAV) system in the AC system controls the quantity of air flow in response to a room air temperature sensor. An air stream forms a boundary across the ceiling which incorporates the room air for thorough air mixing. | Sometimes, when the VAV decreases the quantity of air flow, the boundary layer may not be maintained due to inadequate air velocity. As a result, cool air can ‘drop’ from the ceiling boundary layer onto the room’s occupants, causing discomfort. |
| Dual-duct system | Multi-room buildings where there are a wide range in heating and cooling demands. | In summer: the hot duct mixes fresh and recirculated air; the cold duct contains cooled and dehumidified air.<br>In winter: the cold duct contains untreated mixed air; the hot duct contains air that is increased in temperature.<br>The two air streams from the hot and cold ducts are mixed in varying proportions (controlled by a room air detector) before being supplied to the room(s). | Fan noise and air turbulence are muted by an acoustic silencer in the system. The system does not provide close humidity control so it can be used for comfort air conditioning; it can quickly react to changes in heating or cooling demand. |

| *Air Conditioning (AC) System* | *Where it is most commonly used* | *How it works* | *Notes* |
|---|---|---|---|
| Induction | Multi-room buildings. | Primary fresh air is injected into an induction unit in each room. Due to the high velocity of the air jets, the pressure within the unit decreases and air from the room is pulled into it. This air mixes with the primary fresh air and creates a secondary air flow that is then supplied to the room. The temperature of the secondary air flow can be adjusted with either hot or cold water passed through the coil in the system. | Recirculation is kept within the room, reducing the cost of ducts and service duct space requirements. This makes it a cheaper alternative to single- and dual-duct systems. |
| Fan coil units | Multi-room buildings. | Similar to induction systems, however, fan coil units are used when the required heating and cooling loads are too much for an induction system to handle. Separate fan and coil units are fitted into the false ceiling of each room, with a removeable access hatch beneath the unit for easy maintenance access. All recirculation is confined within the room, much like an induction system. | Provides better air filtration than an induction unit. Any fan-generated noise can be matched to that required of the environment. |

| *Air Conditioning (AC) System* | *Where it is most commonly used* | *How it works* | *Notes* |
|---|---|---|---|
| Packaged unit | Houses, offices, commercial buildings, etc. | Self-contained and made up of a refrigeration compressor, evaporator, condenser, electric resistance heater battery, filter, and automatic controls. They work using the vapour compression refrigeration cycle. These units are fitted to an external wall and have a change-over valve that reverses the refrigerant flow direction. The unit can cool internal air in summer and cool external air (heat internal air) in winter. | Noise levels are comparable with that of the accepted background acoustic environment. |
| Split system unit | Houses, offices, commercial buildings, etc. | The same as a packaged unit except it also has a separate condenser installed outside the building. | The internal and external equipment boxes are connected by two refrigerant pipes which gives more choice in where the compressor unit can be installed. |

2.6.3.3 Selecting an Air Conditioning System for the Alternative Method Simulation

To carry out the cooling required for the alternative method, a split system unit air conditioning system was selected to be modelled in the simulation, as it uses the most simple and efficient refrigeration cycle: the vapour compression refrigeration cycle. It was originally considered that a portable air conditioning unit may be used, however this would not be powerful enough for the level of cooling that would be required, hence the larger split system unit would be much more effective in its cooling capabilities, whilst also still being flexible in its setup and installation (compared to the other systems listed in *Table 3.4*).

# Chapter 3

# Research Methodology

## Chapter Overview

This chapter describes and explains the methodology chosen to carry out the research in order to answer the research questions. It consists of the following sections:

- **3.1 About the Research**: outlines the aim and research questions that lead to the considerations of the methodologies, facilities and equipment used in the research.
- **3.2 Consideration of How the Research Would Be Undertaken**: discusses the methods that were considered in order to develop an alternative heat loss test method.
- **3.3 Selected Research Methodology**: explains why simulation was chosen as the selected research methodology.
- **3.4 Baseline Testing**: covers the co-heating method used to determine the baseline HTC, along with other methods of determining the fabric performance of the test dwelling.
- **3.5 Co-heating Analysis Methodology**: demonstrates how the HTC was calculated using multiple linear regression analysis as well as key considerations for sources of uncertainty.
- **3.6 Simulation Software**: provides an overview of the modelling software DesignBuilder and the model of the test dwelling.
- **3.7 Co-heating Simulation**: details the model data used to calibrate the model and simulate a co-heating test as well as how the weather file was created.

- **3.8 Alternative Method Simulation**: details the model data used to simulate the proposed initial alternative method and explains how components such as temperature conditions and testing periods were factored in.

## 3.1 About the Research

### 3.1.1 What the Research Aims to Achieve

The aim of the research laid out in this thesis is to determine whether it is possible to develop a heat loss test method capable of determining the HTC of a domestic building in warmer climates.

### 3.1.2 Research Questions

Consideration of the relevant literature has led to four key research questions, which could only be answered through careful consideration of which methodologies, facilities and equipment should be used to undertake the research.

1. Is there a need for a new heat loss test method to determine the HTC of a domestic building in warmer climates?
2. Is it possible to develop a heat loss test method that can determine the HTC of a domestic building in warmer climates?
3. What needs to be considered for a heat loss test method, which could be used to determine the HTC of domestic buildings in warmer climates, to be developed?
4. Is the developed heat loss test method capable of determining the HTC of a domestic building in warmer climates?

## 3.2 Consideration of How the Research Would Be Undertaken

### 3.2.1 Practical Testing Vs. Simulations Carried Out in DesignBuilder

Whilst considering how to undertake the research, a handful of testing options were considered. A baseline test, or ‘grounded truth’, would be required for the test dwelling(s) (i.e., a reliable test would have to be carried out in order for a baseline HTC to be determined) which could then be compared against once the alternative method was developed and tested. Reviewing the relevant literature outlined the commonly used co-heating method's good reliability in determining the HTC of a dwelling (Butler & Dengel, 2013; Jack et al., 2018), thus this method was chosen to establish a baseline.

From here, the way in which an alternative method could be developed, for use in warmer climates including warmer months in temperate climates, was considered. As part of this process details such as weather conditions, time of year in which to carry out the alternative method, the length of the testing period, aggregation interval, and equipment to be used, all needed to be considered.

Once these details had been considered, there were two possible ways in which to develop and test the alternative method. The first idea was to carry out practical tests in the test dwelling(s), making use of actual equipment, which would have to either be bought or specially commissioned, along with sensors and data loggers to measure elements such as internal and external temperature, solar irradiance, and any other relevant measurements specific to the alternative method. Alternatively, simulations could be executed in a modelling software specific to buildings in which data regarding the environmental performance of the modelled dwelling could be calculated. Using this modelling software, the test dwelling(s) could be modelled, and simulated co-heating tests could be performed in order to compare against the practical baseline. Then, using the considerations mentioned above, the alternative method could be developed using the modelling software and simulated quickly with immediate results. Both options mentioned here would possibly require an element of trial and error.

### 3.2.2 Test Facilities

Two dwellings were considered for carrying out the research in this thesis. These were the Barratt Zed House and the Salford University Energy House. Both of these properties were located on the University of Salford's main campus, so were easily accessible, whilst also either being already unoccupied or could easily become unoccupied, with minimal inconvenience caused to the occupants. They were also an opportunity to potentially compare two extremes in terms of construction, with one classed as a heavyweight dwelling and built in a climatic chamber (Energy

House) and the other classed as a light-to-medium weight dwelling built in an outside dynamic environment (Zed House).

#### 3.2.2.1 The Barratt Zed House

The primary dwelling that would be used for this research was the Barratt Zed House, shown in *Figure 3.1*. It was designed to be a net zero-carbon operational home and was constructed by one of the UK's biggest housebuilders, Barratt Developments Ltd. Built off-site and then assembled on the University of Salford's Peel Park campus, the Zed House, which is monitored by Energy House Laboratories, is a two-storey detached house, with an internal volume of 282.2 $m^3$ and a total floor area of 115.9 $m^2$. The house provides charging points for electric vehicles and battery storage, and also uses PV solar panels. Air source heat pumps provide low carbon heating alongside other new heating methods such as IR heating panels and skirting board heating (that emits heat via hot water through a pipe). The house contains over 95 sensors, which not only measure temperature and humidity, but also variables such as the air quality inside the dwelling and the way the different smart technologies installed inside the house interact with each other. These measurements are important in the future of designing zero-carbon homes, particularly when looking at building these homes in sustainable areas which are nature-friendly. Over 40 partnering companies were involved in the project, alongside about 15 consultants and designers (Barratt Developments PLC, 2022). The floor plans of the ground and first floors of the Zed House are shown in *Figures 3.2a and b*.

*Figure 3.1 The Barratt Zed House*

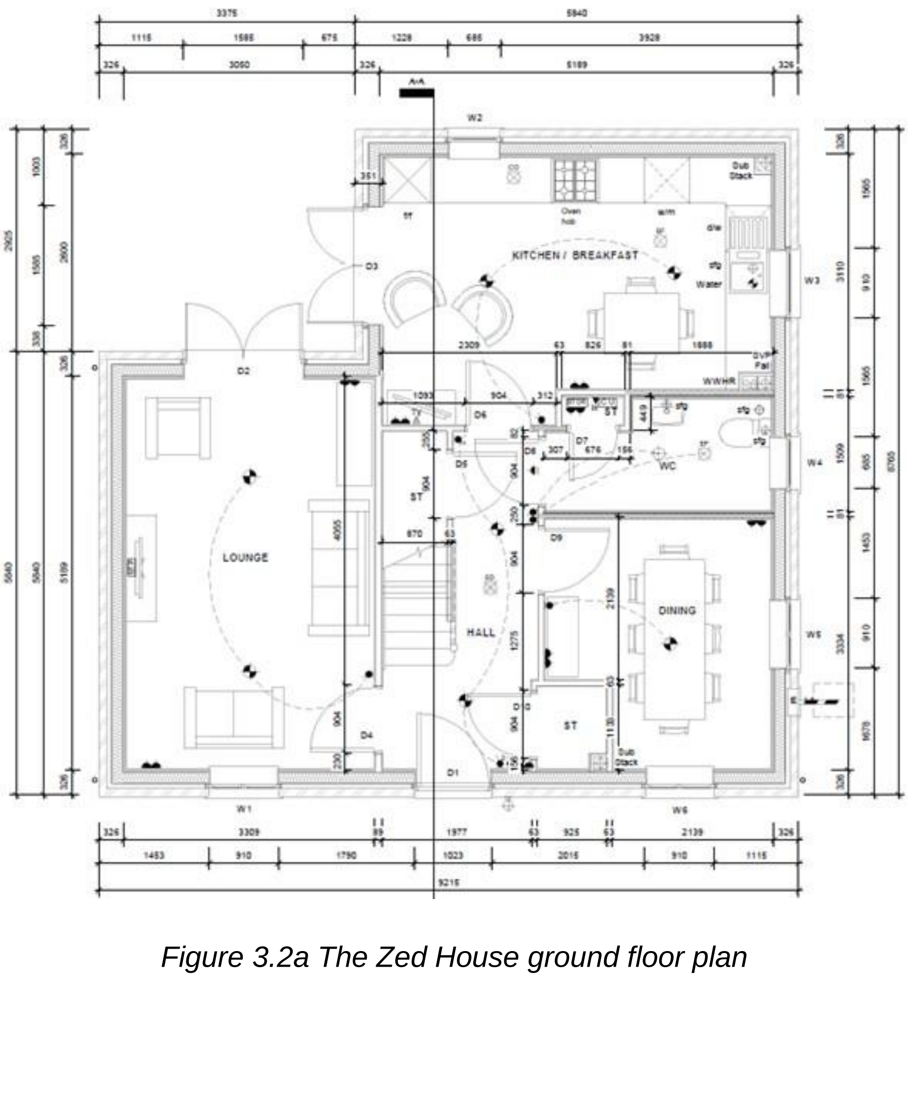


*Figure 3.2a The Zed House ground floor plan*

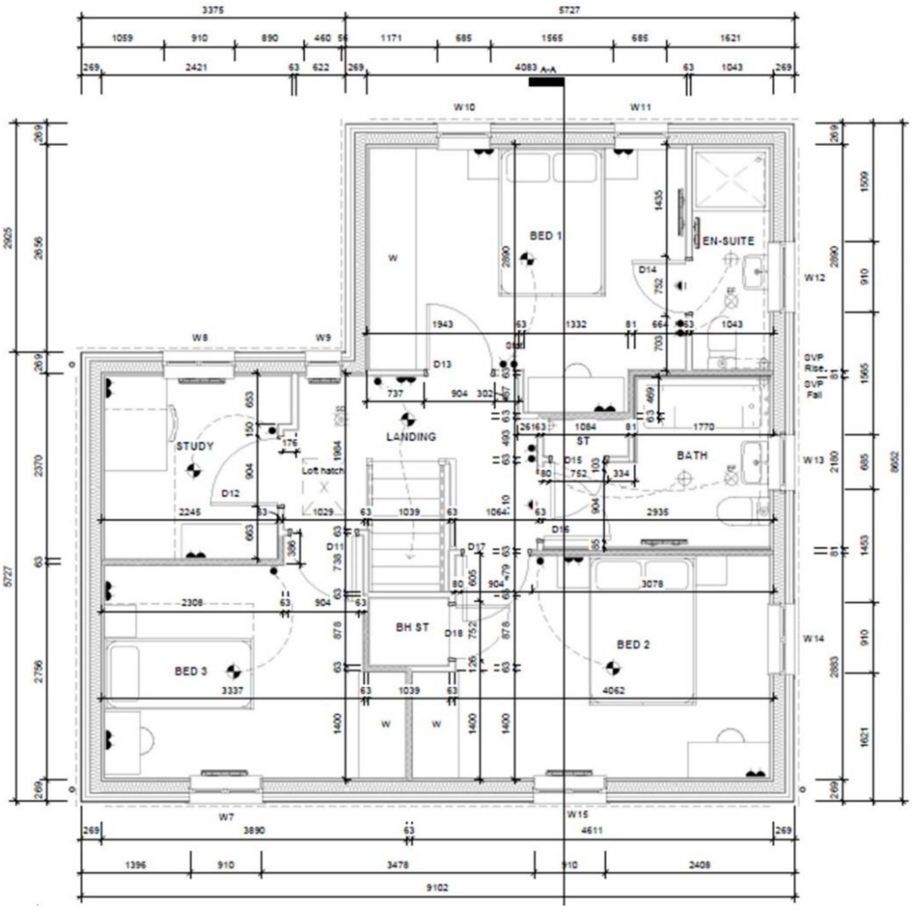


*Figure 3.2b The Zed House first floor plan*

*Table 3.1* compiles the key fabric heat loss characteristics of the Zed House, taken directly from the Zed House SAP documents, as well as the whole house metrics, including the design air permeability and design HTC of the dwelling, compared to the corresponding limiting values which are required for the property to comply with Approved Document (AD) L1a 2016, the Approved Document at the time of construction. This Approved Document provides a set of guidelines for how to comply with the requirements laid out in the 2010 Building Regulations for England, in this case specifically for fuel and power conservation in new dwellings (The National Archives, 2016). The values are also compared to the newest limiting values in the most recent Approved Document, valid from 2022, which will be the anticipated scenarios for the Future Homes Standard, due to be released in 2025 (The National Archives, 2023). The Zed House was built in response to this anticipated standard.

*Table 3.1 The key fabric heat loss characteristics and whole house metrics of the Zed House, taken from the Zed House SAP documents, compared to the limiting values laid out in AD L1a 2016 and the new proposed limiting values, valid from June 2022*

| *Element* | *Design from SAP* | *AD L1a* | *New Limiting Values (from June 2022)* | *Notes from SAP* |
|---|---|---|---|---|
| Ground Floor ($W \cdot m^{-2} \cdot K^{-1}$) | 0.15 | 0.25 | 0.18 | Jetslab Suspended System to achieve target U-value |
| External Walls - Brick ($W \cdot m^{-2} \cdot K^{-1}$) | 0.18 | 0.30 | 0.26 | 100 mm Brick, 65 mm Cavity TF200 thermo membrane, 100 mm Phenolic λ0.020 in 140 mm timber stud, Low E service void, Plasterboard |
| External Walls - Cladding ($W \cdot m^{-2} \cdot K^{-1}$) | 0.20 | 0.30 | 0.26 | Ventilated clad finish, membrane, 100 mm Phenolic λ0.020 in 140 mm timber stud, Low E service void, Plasterboard |
| Ceiling ($W \cdot m^{-2} \cdot K^{-1}$) | 0.09 | 0.20 | 0.16 | 100 mm λ0.044 Mineral Wool Laid Through Joists, 400 mm Mineral Wool Laid Over |
| Windows ($W \cdot m^{-2} \cdot K^{-1}$) | 1.20 | 2.00 | 1.60 | Double Glazed, Low-E Coated BFRC G-Window Value: 0.31 |
| Doors - Solid ($W \cdot m^{-2} \cdot K^{-1}$) | 1.00 | 2.00 | 1.60 | Glazed tall window (composition not stated on SAP sheet) |
| *Whole House Metrics* | | | | |
| Air Permeability ($m^3 \cdot h^{-1} \cdot m^{-2}$) | 4.00 | 10.00 | 8.00 | Measured value on SAP sheet: 3.98 |
| Y-value | 0.076 | 0.08 | 0.08 | Accredited Construction Details Used for 2013 Compliance |
| Heat Loss ($W \cdot K^{-1}$) | 105.5 | 181.2 | 160.3 | |

#### 3.2.2.2 The Salford University Energy House

Research was also considered to be carried out in the Salford University Energy House (see *Figure 3.3*), subject to its availability. Built in 2011, using reclaimed materials and methods of its time, the Energy House is a pre-1920's end-terrace house with a section of neighbouring property known as the Conditioning Void, which is capable of simulating neighbours living next door. The Energy House, which contains over 200 sensors, represents about 21% of the UK housing stock, and is classed as 'hard to treat'. It is built in a climatic chamber where it is possible to replicate weather conditions that would not otherwise be replicable in the field. The chamber can reach temperatures from -12°C up to +30°C (± 0.5°C) and can create solar profiles, rain up to 200 mm per hour, wind up to 10 m·s$^{-1}$, and snow (Energy House Laboratories, 2021; Ji et al., 2014). The floor plans for the ground and first floors are displayed in *Figures 3.4a and b*.

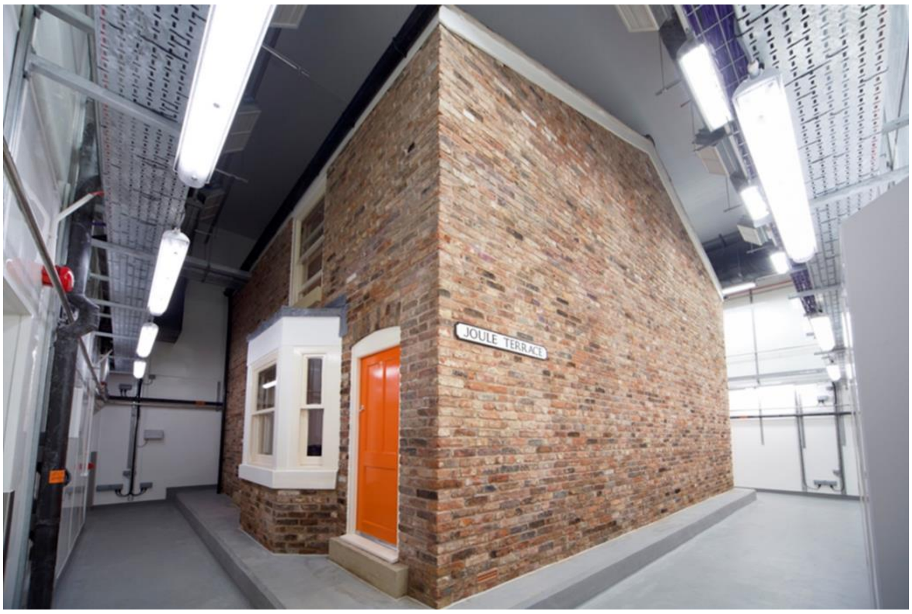


*Figure 3.3 The Salford University Energy House (University of Salford, 2014)*

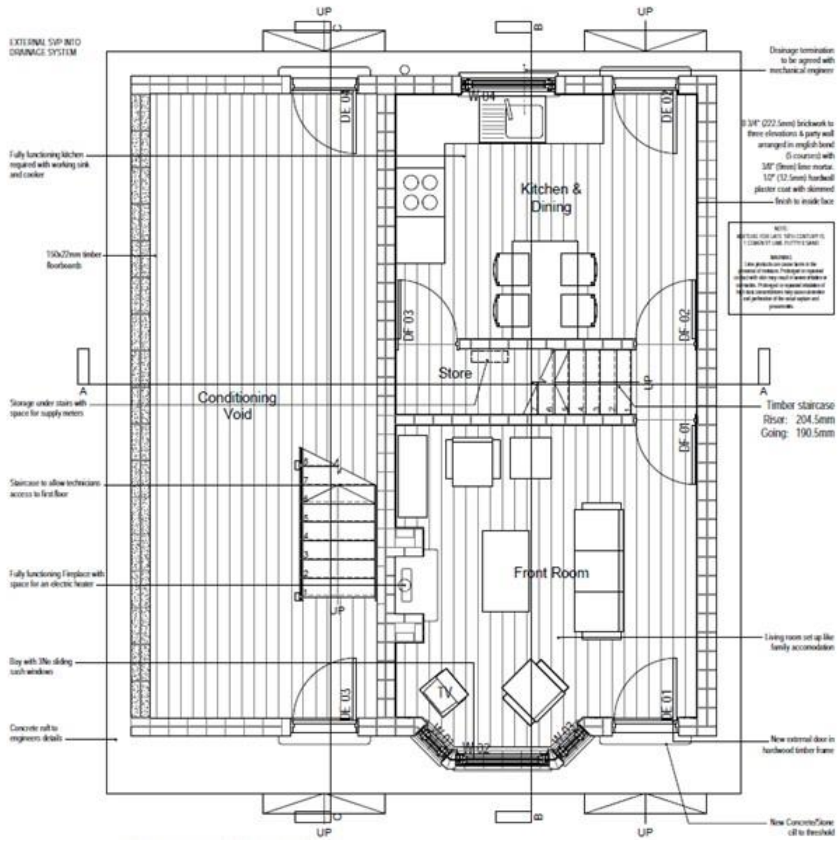

*Figure 3.4a The Energy House ground floor plan*

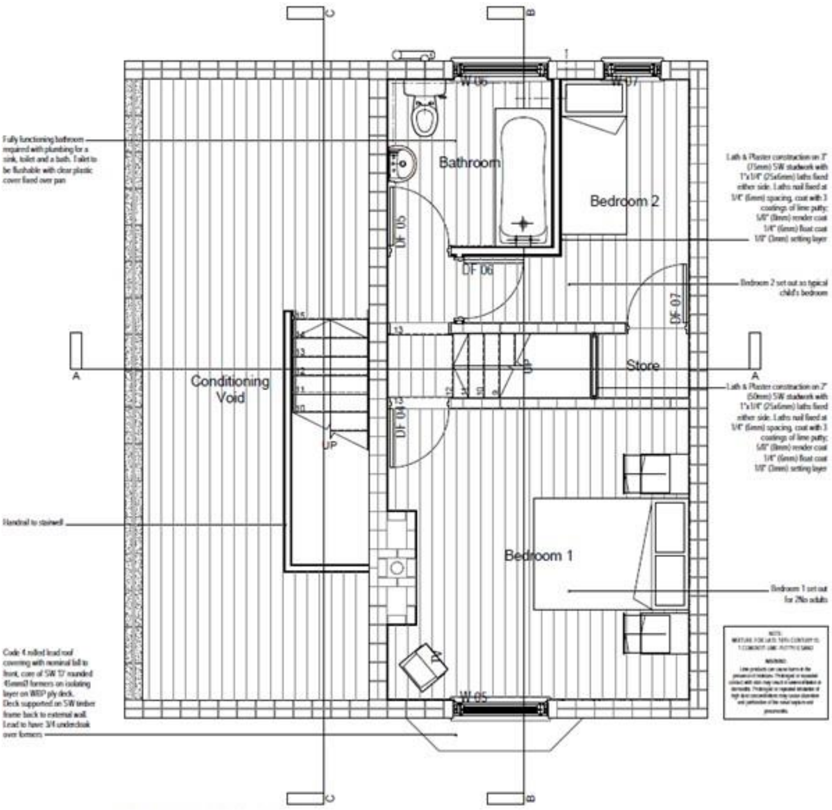


*Figure 3.4b The Energy House first floor plan*

## 3.3 Selected Research Methodology

It was decided that in order to carry out the development of the alternative method, the use of simulations through an energy modelling software would be the most efficient method. Firstly, it would be more cost effective, given that no physical equipment would then need to be bought in order to test the alternative method. Furthermore, it would also be more time effective, given that running a simulation would take a matter of, at the most, minutes, whereas running a full practical test would take at least a couple of days, or possibly even a couple of weeks, as with the co-heating method, in addition to the time it would take to set the equipment up in the dwelling. By simulating the test on a model property, if the test did not work the way it was anticipated, or the results did not seem quite right, it would be possible to quickly adjust the model data and simply run another simulation.

DesignBuilder was selected as the simulation software of choice for this research as it was readily available and it's capability of being able to simulate whole house heat loss test methods, namely the co-heating method, had been previously established by Marshall et al. in 2017 (Marshall et al., 2017).

Due to the lack of availability of the Salford University Energy House, testing could only be carried out on the Barratt Zed House. However, only having one dwelling to model and test, rather than two, decreased the amount of time needed for baseline testing and modelling, so that more time could be spent researching the alternative method and simulating it.

## 3.4 Baseline Testing

### 3.4.1 The Co-heating Method

In the field, co-heating tests are performed during the 'heating season'; in the UK this is during the colder winter months. This is to ensure that a minimum 10 K (Kelvin) internal-external temperature difference can be established so that most of the heat flow within the dwelling moves from the internal environment to the external environment (Johnston et al., 2013).

The co-heating test was undertaken in the Barratt Zed House. Monnit temperature and humidity sensors were placed on tripods in the centre of each room within the dwelling, at approximately chest height. Each room was then equipped with a heater and circulation fan. The heaters, placed on fire blankets in accordance with the risk assessment, were each connected to a temperature control box, set to a setpoint of 21°C, and were positioned so that they were not facing directly at the temperature sensors. The temperature control boxes had a built-in temperature sensor; when the temperature in the room dropped below 21°C, the temperature control box would turn the heater on. The heater would automatically be turned off again as soon as the room reached the required temperature. The fans were positioned to ensure homogenous air flow throughout each room and the dwelling as a whole. All external doors and windows were shut, and any window vents closed, whilst all curtains and blinds were drawn or closed to minimise the impact of solar gains within the dwelling. Additionally, extractor fans in the bathrooms and kitchen were sealed with air flow tape. Internal doors were left open, and any cupboard or wardrobe doors were also left open to ensure the air could move freely, including the fridge and freezer which had been emptied. All electric circuits within the dwelling were isolated at the distribution board, including the air source heat pump, with the exception of the lights and the sockets. All the lights were turned off at their switches and the hot water tank was also turned off and emptied. Examples of the co-heating setup in the Zed House are displayed in *Figure 3.5*.

The test was initially set up and data began recording on Wednesday 15th December 2021, with temperature measurements being monitored to ensure the air temperatures within the dwelling were homogenous and that there was no temperature stratification. Minor adjustments were made during the following days until the equipment was set up to the specifications outlined by Jack et al. and Johnston et al. (Jack et al., 2018; Johnston et al., 2013). Official data was recorded from Thursday 23rd December 2021 00:00 until Monday 10th January 2022 00:00, allowing for the minimum required two-week testing period. During the co-heating test, internal temperature, power input, and external conditions (such as external ambient temperature and solar irradiance) were measured and recorded. The internal temperature data was monitored remotely throughout the test period to ensure that the rooms were maintaining the desired 21°C internal temperature.

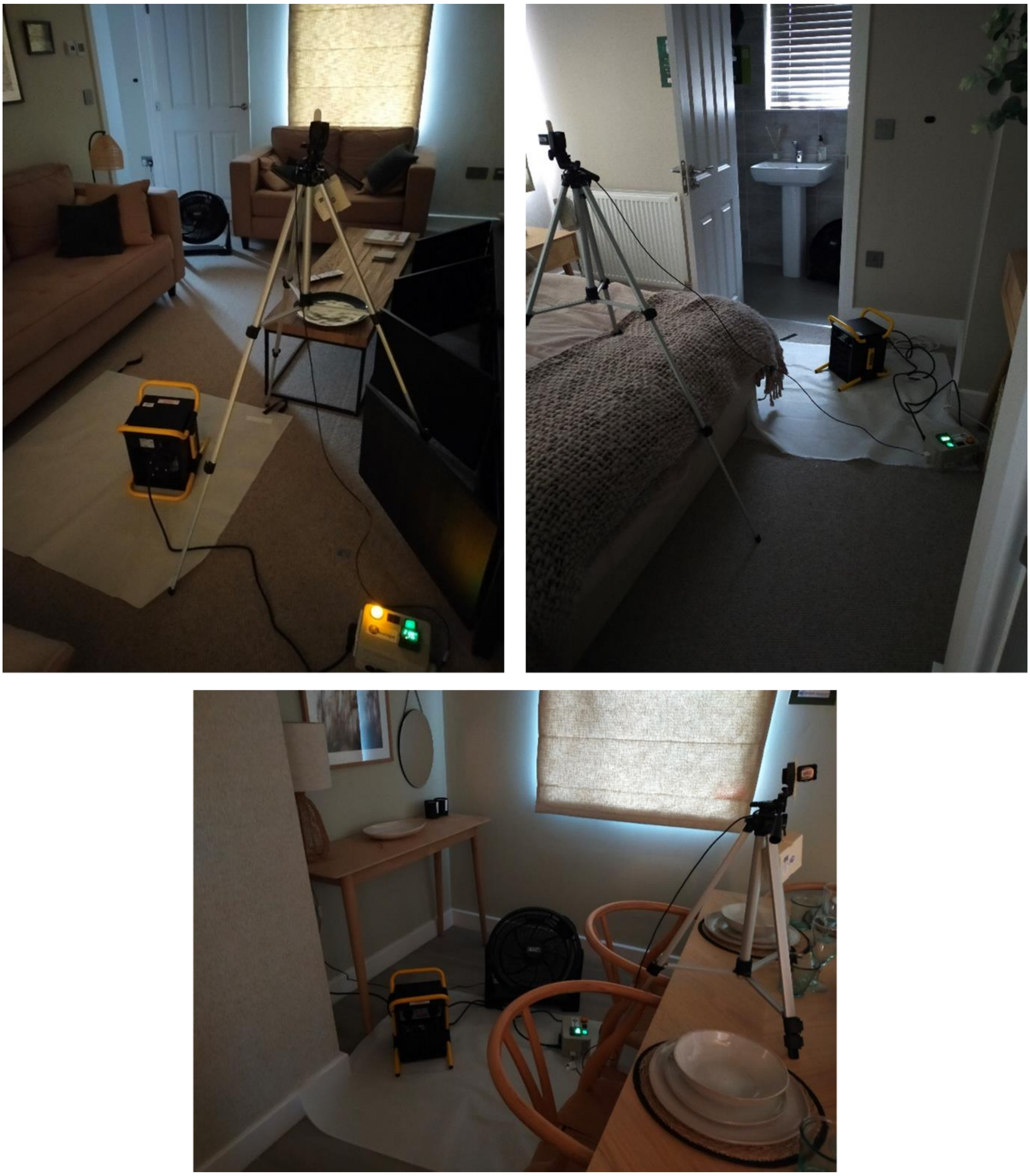

*Figure 3.5 Examples of the co-heating test setup in the Zed House living room (top left), bedroom one (top right) and dining room (bottom)*

### 3.4.2 Infrared Thermography

In order to visually assess the quality of the Zed House's thermal envelope, baseline thermographic surveys were carried out using a FLIR T660 thermal imaging camera, following the guidelines laid out in ISO 6781-3 (BSI, 2015a). This was to identify, under standard daily conditions, any areas within the envelope of significant heat loss such as thermal bridges and any areas with inconsistent or patchy insulation.

### 3.4.3 Air Permeability (Blower Door) Test

Time constraints between the Zed House being unoccupied and the beginning of the co-heating test meant, unfortunately, there was not enough time to perform a blower door test prior to the start of the co-heating test in order to determine the airtightness of the dwelling. Instead, a blower door test was performed in the Zed House on Thursday 13$^{th}$ January 2022, following the end of the co-heating test. The equipment for the test consisted of a fan, capable of depressurising and pressurising the dwelling, and devices for taking measurements such as the pressure and air flow rate. All windows and external doors in the dwelling, except the front door, were closed. Any vents were also closed, and extractor fans sealed with air flow tape. The frame structure which supports the fan was set up in the open front doorway, and then the flexible panel which holds the fan was tucked around the frame before the frame was locked into place. The fan, which has variable speeds, was then slotted into the flexible panel, facing outwards from the dwelling, ready for depressurisation. Air flow tape was taped around both sides of the frame, sealing it so that there could be no air leakage around the frame. The fan was then connected to a laptop which recorded the internal and external pressures as well as the airflow. *Figure 3.6* shows the blower door setup in the Zed House.

Before the depressurisation test began, IR thermal images were taken of the dwelling to provide a baseline to which IR images taken during the testing could be compared to. IR images were captured of both the inside of the dwelling as well as the outside of the dwelling.

The Zed House was then depressurised, whereby the fan decreased the air pressure within the dwelling by pulling air from inside and allowing the higher-pressure air from outside to flow through any unsealed cracks or gaps within the house, such as the electric sockets. During the test, the air permeability at 50 Pa was recorded. Once the depressurisation test was complete and the data recorded, the fan was set to a 60 Pa pressure difference, to allow time for an IR survey to be undertaken of the inside of the dwelling, focusing on areas showing abnormal cold spots, particularly in comparison to the previous IR survey taken before testing began. The IR images were taken on a FLIR camera, alongside normal optical photographs taken of the same areas for reference.

The fan was then taken out of the flexible panel and turned to face into the dwelling in order for a pressurisation test to be carried out. The fan increased the air pressure within the dwelling so that the now higher air pressure inside would flow through any unsealed openings to the lower air pressure outside. As with the depressurisation test, the air permeability of the dwelling at 50 Pa was recorded. Following the test, the fan's speed was set to 60%, which was approximately a 60 Pa pressure difference between the inside and outside, allowing for another IR survey to be carried out on the outside of the dwelling, looking for areas highlighting abnormal warm spots, where the warmer internal air was seeping through any unsealed gaps in the building fabric. Optical photos were also taken of the same areas for reference. Both blower door tests were carried out following the Air Tightness Testing & Measurement Association (ATTMA) guidelines (ATTMA, 2021) which in turn is based on ISO 9972 (BSI, 2015b).

*Figure 3.6 The blower door test setup in the Zed House ready for depressurisation (left) and pressurisation (right)*

### 3.4.4 In situ U-Value Measurements

In order to assess whether the design thermal performance of select thermal elements within the Zed House were representative of their as-built measured performance, in situ U-value measurements were taken, following the guidance set out in ISO 9869-1 (BSI, 2014), and using Hukseflux HFP01 heat flux plates.

Unfortunately, only limited in situ U-value measurements were able to be taken due to time constraints, which came about as a result of setting up the test prior to the Christmas shutdown period. Additionally, there was a limit on the number of available heat flux plates because of other tests being run by the facility at that time. Heat flux plates were placed on the floor in the kitchen, the ceiling in the study and the north facing external wall in bedroom three. Two heat flux measurements were taken at the locations of the external wall and ceiling elements, since the initial thermographic survey of the dwelling, under normal conditions, suggested that certain areas of these elements were subject to a greater increase in heat loss than was expected. Therefore, for these two regions, one heat flux plate was placed over an area deemed representative of the element construction, and another heat flux plate was placed over an area showing disproportionate thermal bridging.

## 3.5 Co-heating Analysis Methodology

### 3.5.1 Raw HTC Analysis Method

According to Johnston et al. (Johnston et al., 2013), analysis of the data gained from a co-heating test can be carried out assuming that this energy balance equation applies:

$$Q + R \cdot S = \left(\Sigma U \cdot A + \frac{1}{3} nV\right) \cdot \Delta T$$

*Equation 3.1*

Where, on the left-hand side of the formula, *Q* is the total power input (W) to the dwelling, *R* is the solar aperture ($m^2$) of the dwelling and *S* is the south-facing solar irradiance to the dwelling ($W \cdot m^{-2}$). Meanwhile, on the right-hand side, $\Sigma U \cdot A$ is the total fabric heat loss ($W \cdot m^{-2}$) of the dwelling, *n* is the background ventilation rate ($h^{-1}$), *V* is the dwelling's internal volume ($m^3$) and $\Delta T$ is the internal-external temperature difference (K).

The energy balance equation can be rearranged so that a raw value of the HTC ($W \cdot K^{-1}$) can be determined:

$$\frac{Q}{\Delta T} = \left(\Sigma U \cdot A + \frac{1}{3} nV\right) - \frac{R \cdot S}{\Delta T}$$

*Equation 3.2*

When the total power input, *Q*, is plotted against the internal-external temperature difference, $\Delta T$, the gradient of the resulting graph provides a raw, uncorrected value of the HTC. However, in order to calculate a solar corrected value of the HTC, the solar gains ($\frac{R \cdot S}{\Delta T}$) to the property need to be accounted for, and in order to do this, the solar aperture needs to be determined, so that we have the following equation:

$$\frac{Q}{\Delta T} + \frac{R \cdot S}{\Delta T} = \left(\Sigma U \cdot A + \frac{1}{3} nV\right)$$

*Equation 3.3*

In order to find the solar aperture, multiple linear regression can be carried out.

### 3.5.2 Multiple Linear Regression Analysis

Solar gains to the dwelling during a co-heating test impact the power input to the dwelling. In order to account for these solar gains, values of solar corrected power need to be calculated, using the solar irradiance ($W \cdot m^{-2}$) measured by a pyranometer and a determined value of solar aperture ($m^2$).

The solar aperture can be determined by using a method known as multiple linear regression which estimates the relationship between a dependent variable, in this case power (W), and two independent variables: temperature difference (K) and solar irradiance ($W \cdot m^{-2}$).

The formula for the solar multiple linear regression adapted from (Bevans, 2020) is:

$$Q = \beta_0 + \beta_{\Delta T} \cdot \Delta T + \beta_S \cdot S + \varepsilon$$

*Equation 3.4*

Where $Q$ is the predicted value of the dependent variable, power (W), $\beta_0$ is the y-intercept, $\beta_{\Delta T}$ is the regression coefficient for the temperature difference, $\Delta T$, (K), $\beta_S$ is the regression coefficient for the solar irradiance, $S$, and $\varepsilon$ is the model error. In this case, the regression coefficient for the temperature difference is also equal to the HTC and the regression coefficient for the solar irradiance is equal to the solar aperture ($R$), leading to the equation adapted from (Bauwens & Roels, 2014):

$$\frac{Q}{\Delta T} = HTC - R \cdot \frac{S}{\Delta T}$$

*Equation 3.5*

The multiple linear regression analysis for this research was carried out in RStudio, an application that runs the programming language R which is often used for computer analysis. The code that was inputted, see Appendix A, performed the multiple linear regression and generated a summary (an example is shown in *Figure 3.7a*) including the estimated values of the y-intercept and both regression coefficients, along with the standard errors and statistical validity of the estimates. In addition to this, the relationships between the dependent variable and the independent variable were plotted with their corresponding regression line. A slightly altered code, also shown in Appendix A was used to determine the estimates of the regression coefficients whilst the intercept was forced through the origin. This then excluded the estimated value of the y-intercept from the summary, as shown in *Figure 3.7b*.

```
Call:
lm(formula = power ~ temp.difference + solar.irradiance, data = mlr.data)

Residuals:
    Min      1Q  Median      3Q     Max
-158.75  -63.76   15.22   58.82  132.27

Coefficients:
                 Estimate Std. Error t value Pr(>|t|)
(Intercept)      -53.4264   108.5657  -0.492   0.6323
temp.difference  141.5619     9.2746  15.263 9.49e-09 ***
solar.irradiance  -1.5515     0.7354  -2.110   0.0586 .
---
Signif. codes:  0 ‘***’ 0.001 ‘**’ 0.01 ‘*’ 0.05 ‘.’ 0.1 ‘ ’ 1

Residual standard error: 94 on 11 degrees of freedom
Multiple R-squared:  0.9569,    Adjusted R-squared:  0.949
F-statistic:   122 on 2 and 11 DF,  p-value: 3.1e-08
```

*Figure 3.7a An example summary output from RStudio of a multiple linear regression*

```
Call:
lm(formula = power ~ temp.difference + solar.irradiance + 0,
    data = mlr.data)

Residuals:
    Min      1Q  Median      3Q     Max
-166.06  -60.88   15.76   51.71  134.07

Coefficients:
                 Estimate Std. Error t value Pr(>|t|)
temp.difference  137.2029     2.6616  51.549 1.87e-15 ***
solar.irradiance  -1.4964     0.7035  -2.127   0.0548 .
---
Signif. codes:  0 ‘***’ 0.001 ‘**’ 0.01 ‘*’ 0.05 ‘.’ 0.1 ‘ ’ 1

Residual standard error: 90.98 on 12 degrees of freedom
Multiple R-squared:  0.9974,    Adjusted R-squared:  0.9969
F-statistic:  2284 on 2 and 12 DF,  p-value: 3.231e-16
```

*Figure 3.7b The output summary from the same data input with the regression line forced through the origin*

### 3.5.3 Solar Corrected HTC Analysis Method

Rearrangement of *Equation 3.5* provides an equation for the HTC:

$$\frac{(Q + R \cdot S)}{\Delta T} = HTC$$

*Equation 3.6*

Adding the product of the solar aperture, *R*, and the solar irradiance, *S*, to the total power input to the dwelling, *Q*, provides a value of the solar corrected power input, $Q + R \cdot S$. Plotting this against the internal-external temperature difference, $\Delta T$, produces a graph, the gradient of which is the solar corrected HTC.

Comparison to *Equation 3.3* shows that:

$$HTC = \left(\Sigma U \cdot A + \frac{1}{3} nV\right)$$

*Equation 3.7*

Taking U-value and area measurements of the dwelling fabric, as well as its background ventilation rate and internal volume, also allows for the HTC to be determined and compared to the solar corrected HTC as a way of confirmation.

### 3.5.4 Addressing the Sources of Uncertainty

Section 2.4.1.1 outlines sources of uncertainty that arise when performing and analysing results from co-heating tests, highlighted by Stamp in his thesis (Stamp, 2015). This section briefly discusses how these sources of uncertainty were addressed within the research presented in this thesis, as well as how the error analysis on the research results was conducted.

#### 3.5.4.1 Aggregation Interval

SAP (BRE, 2014), provides a table (see *Table 3.2*) which characterises a dwelling's thermal mass parameter, which can be found on the dwelling's SAP document.

*Table 3.2 The SAP table characterising a dwelling's thermal mass parameter (BRE, 2014)*

| *Thermal Mass Parameter ($kJ{\cdot}m^{-2}{\cdot}K^{-1}$)* | *Thermal Mass Characterisation* |
|---|---|
| 100 | Low |
| 250 | Medium |
| 450 | High |

The Zed House's SAP document reveals that its thermal mass parameter is 154.3675 $kJ{\cdot}m^{-2}{\cdot}K^{-1}$, therefore categorising the Zed House as having low-medium thermal mass. As such, this means that it is a light-mediumweight dwelling and so, following the recommendations laid out by Johnston et al. (Johnston et al., 2013), a midnight-midnight aggregation should be more appropriate. This said, both the midnight-midnight and dawn-dawn aggregations were analysed in this report for comparison purposes, and these are shown in the results section (section 4.1.1).

Dawn could be considered as a somewhat vague time of the day, differing depending on the time of year. To be able to undertake analysis using the dawn-dawn aggregation interval, the time dawn occurred during the testing period was determined as being approximately 7:00 (Time and Date AS, 2022c, 2022d).

#### 3.5.4.2 Forced Intercept

Since the co-heating test covered in this report follows the Leeds Beckett University co-heating protocol (Johnston et al., 2013), along with guidelines laid out by Bauwens and Roles and Jack et al. (Bauwens & Roels, 2014; Jack et al., 2018), HTC values were determined from graphs where the intercept was set to (0, 0). Despite this, and again for comparison purposes, the same graphs, without their regressions forced through the origin, were examined (see section 4.1.2).

#### 3.5.4.3 Error Analysis

Error analysis carried out during this research was conducted following the guidelines set out in the GUM method (JCGM, 2008), as well as following some of the basic guidance presented in a document provided by the University of Pennsylvania (University of Pennsylvania, 2017).

To calculate the uncertainties for the baseline test carried out in the Zed House, Type A uncertainty analysis, looking at statistical errors, was undertaken first. The standard deviations of the internal temperatures, external temperatures, power inputs and solar irradiances for each 24-hour timestamp were calculated using *Equation 3.8*. These were then used in calculating the standard uncertainties (see *Equation 3.9*) for the temperature differences, solar irradiances, and solar corrected powers (both with and without a forced intercept through the origin). In these equations $\sigma$ is the standard deviation, $x$ is the value from the population, $\bar{x}$ is the population mean and $n$ is the size of the population.

$$\sigma = \sqrt{\frac{\sum(x - \bar{x})^2}{n}}$$

*Equation 3.8*

$$A = \frac{\sigma}{\sqrt{n}}$$

*Equation 3.9*

These were then combined with the Type B standard uncertainties, found by dividing the quoted uncertainties ($Unc._{quoted}$) provided by the various sensors used during the test, such as the Monnit temperature sensor (0.25°C), smart meter (2%), and the pyranometer (10% according to (Campbell Scientific, 2020)), by the coverage factor, *k*, which in this case was equal to 2 (*Equation 3.10*). The combination of the Type A and Type B uncertainties (see *Equation 3.11*), following the GUM method (JCGM, 2008), provided the final standard uncertainties (for both k = 1 and k = 2 coverage) for the temperature differences and solar corrected powers that could then be used to create error bars on the corresponding HTC graphs.

$$B = \frac{Unc._{quoted}}{k}$$

*Equation 3.10*

$$Standard\ Unc. = \sqrt{A^2 + B^2}$$

*Equation 3.11*

## 3.6 Simulation Software

### 3.6.1 An Introduction to DesignBuilder

DesignBuilder is a modelling software in which buildings can be modelled with various environmental controls applied, in order to virtually observe and collect data pertaining to energy usage and comfort conditions through the use of the EnergyPlus whole building energy simulation engine. The software can also demonstrate dynamics such as solar shading during the course of a predetermined period of time (DesignBuilder Software Ltd, 2022).

Any model built in DesignBuilder is organised in a hierarchy, which is demonstrated in *Figure 3.8*. This allows for the model data to be inputted at the model's different levels, from Site Level down to Openings Level. Any data inputted at Building level is automatically inherited by the Block, Zone, and other levels below it. Any Block, Zone, Surface, or Opening-specific changes can then be made later at the relevant level, and will be inherited by any levels below it, but not above.

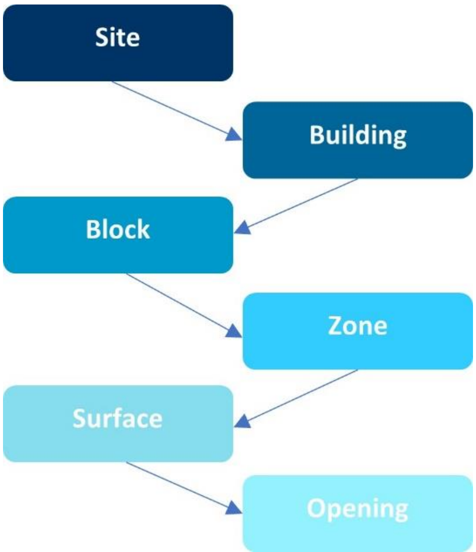


*Figure 3.8 The DesignBuilder hierarchy*

The software provides specific data input tabs, where data for the activity (occupancy) of the dwelling, construction details and HVAC systems can be loaded into the model as well as weather data at Site level. The model can then be simulated and the data output from the model, such as internal air temperature, internal gains and power input can be downloaded.

DesignBuilder, as well as any calculation engines it uses for determining the energy for space heating and cooling and the energy performance of buildings, such as EnergyPlus, all comply with the guidelines laid out in the documents listed in *Table 3.3*.

*Table 3.3 The documents that set out the guidelines which DesignBuilder and any calculation engines it uses must comply with*

| *Guidelines Document* | *Source* |
|---|---|
| EN ISO 12831-1:2017 | (BSI, 2017c) |
| BS EN ISO 15193-1:2017+A1:2021 | (BSI, 2017e) |
| BS EN ISO 52016-1:2017<br>(Formerly BS EN ISO 13790:2008) | (BSI, 2017f) |
| ASHRAE 140/BESTEST | (ASHRAE, 2004) |
| CIBSE TM33 | (CIBSE, 2006) |

### 3.6.2 The Zed House Model

3.6.2.1 Site Level

The Zed House model built in DesignBuilder is displayed at Site level in *Figure 3.9a* and *Figure 3.9b*. The model was built using the specifications laid out in the Zed House floor plans with the front of the model facing North, as per the orientation of the actual house.

In the Location tab, the location template was set to Salford. This then specifies, in the site location and site details segments, information such as the latitude and longitude of Salford, along with its elevation above sea level and ASHRAE climate zone. According to ASHRAE, Salford is classed as climate zone 5C which is defined as ‘Marine’ (OpenEI, 2009). The simulation weather data for the model can also be selected under the location tab. For the purposes of the Zed House model, actual Salford weather data was used. ASHRAE and CIBSE weather files were originally considered for this, however they were not freely available and due to budgetary constraints were discounted. How the weather file for the model was generated will be discussed later in this chapter in section 3.7.2.

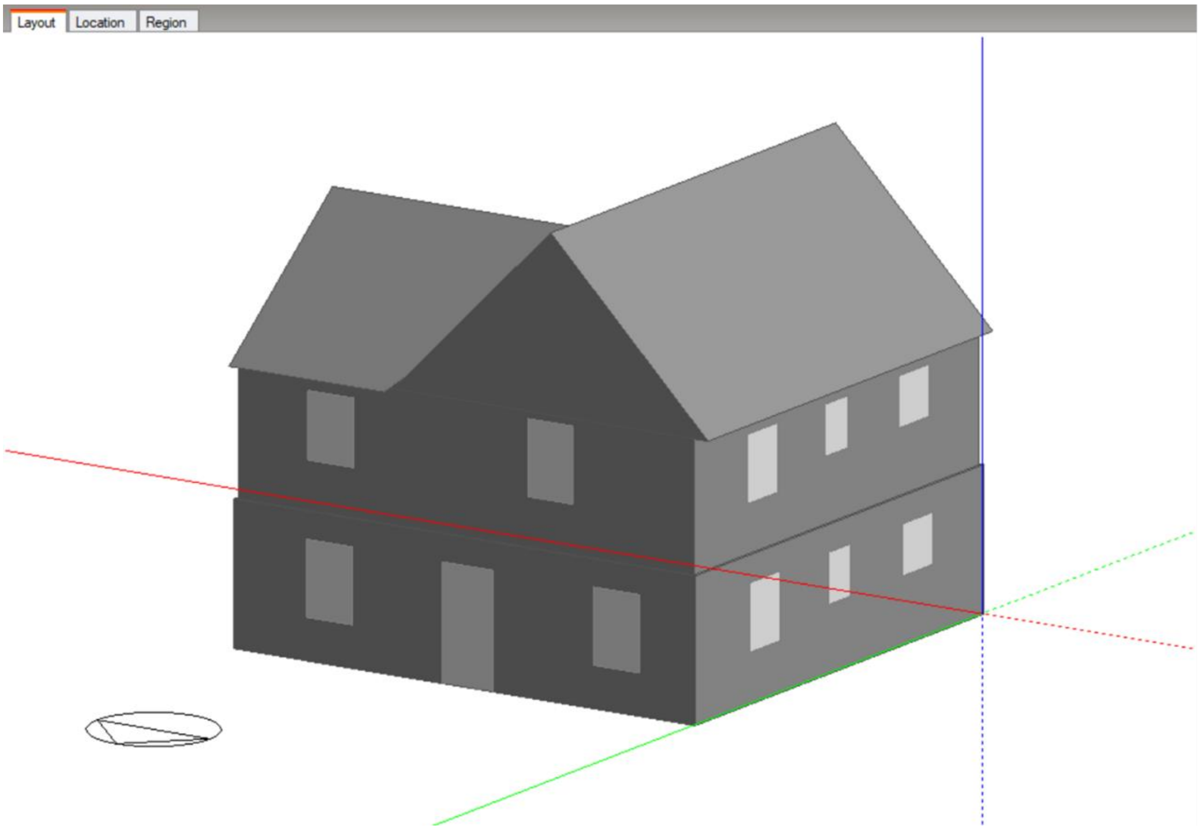


*Figure 3.9a The front angle of the Zed House model at Site level, built in DesignBuilder*

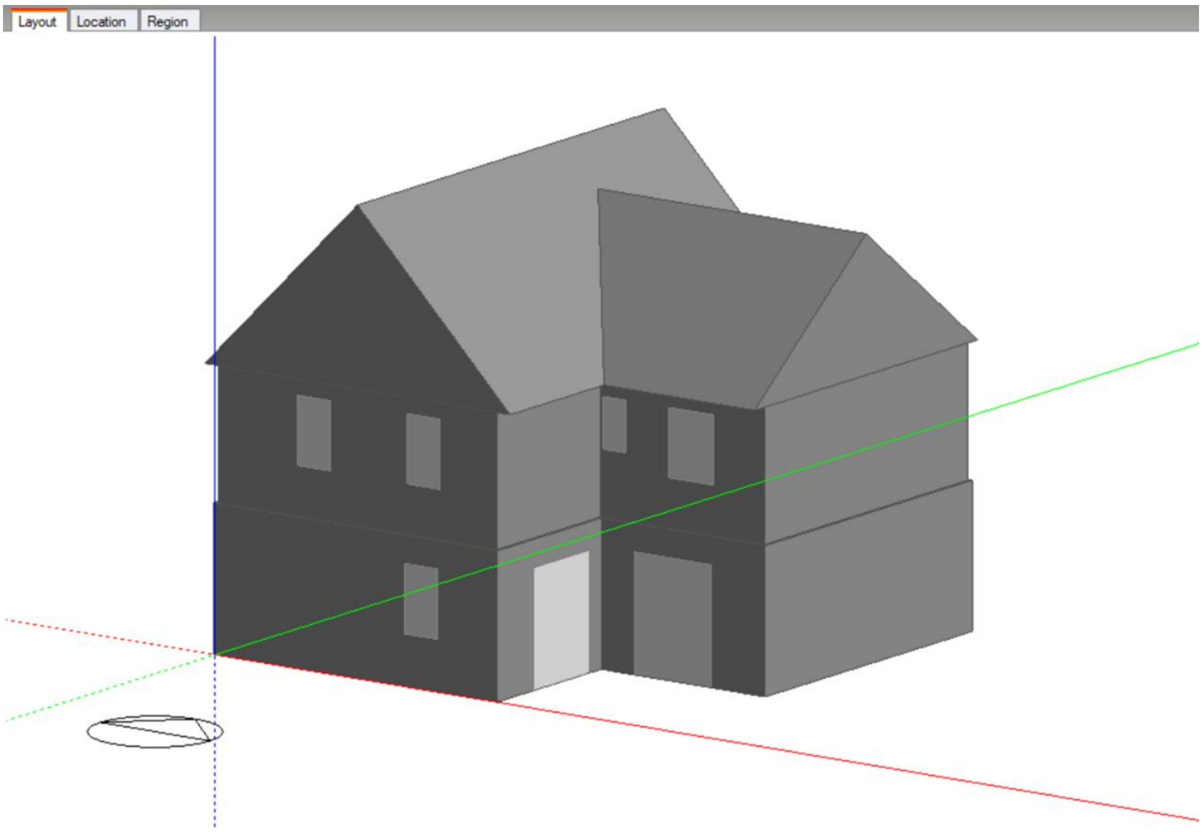


*Figure 3.9b The rear angle of the Zed House model at Site level, built in DesignBuilder*

### 3.6.2.2 Building Level - Construction

Under the Construction tab the ‘Project’ construction assemblies were replaced with Zed House-specific assemblies where necessary. Each of the Zed House-specific construction assemblies will be explained in further depth later in this chapter at their respective Block levels. The ‘Model infiltration’ box was checked under the Airtightness section and the constant rate (also known as air change rate - $ac{\cdot}h^{-1}$) was specified as the measured air change rate (under normal conditions) (0.29 ± 0.3% $ac{\cdot}h^{-1}$), found from performing the blower door test in the Zed House. How this figure was calculated is discussed in more depth in section 4.1.4.

### 3.6.2.3 Block Level - Construction: Ground Floor

*Figure 3.10* shows the layout of the ground floor of the Zed House. Since, for the purposes of any test simulations, the aim was to maintain a homogenous internal temperature within the entire dwelling, individual rooms were excluded. This was also done because the research presented in this thesis was intended to be a simple first run to see if the proposed alternative method might work on a fundamental level; putting a lot of time into creating an exact model if the method did not work at all could have been a potential waste of time and resources. It was postulated that if the method could work on a fundamental level on a simplified model, then further work could then look to apply it to a more complex and exact model. Originally, the plan was to do a simple, single block model of the whole house, without floors or rooms, with the roof on top. However, since the external wall construction of the Zed House ground floor is different to the external wall construction of the first floor (for example, the ground floor external surface is brick, whilst the first-floor external surface is Hardie plank cladding), and these different wall constructions have different U-values, the ground floor and first floor had to be modelled as separate blocks.

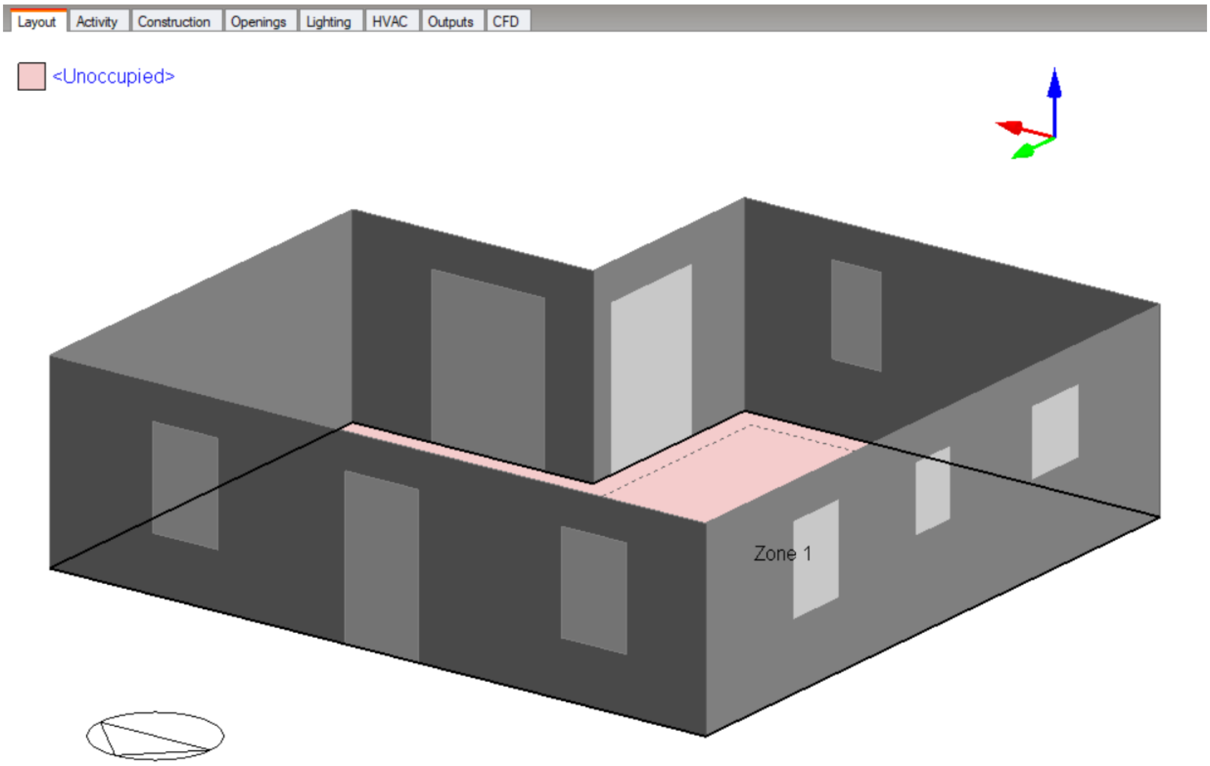


*Figure 3.10 The layout of the ground floor of the Zed House model at Block level*

Under the Construction tab, the External walls and Ground floor construction assemblies were custom created to match the specification laid out in the Zed House design diagrams and floor plans. Each of the layers of the External walls and Ground floor, from their external surfaces, through their insulation, to their internal surfaces, were specified as close to the materials provided by the Zed House SAP documents as possible, using the information available. The layers for the external wall and ground floor are displayed in *Figure 3.11*.

Since the design U-values of the building elements were known, these were manually set in the 'Edit Constructions' dialogue. The U-values for the External ground floor walls (U = 0.18 $W{\cdot}m^{-2}{\cdot}K^{-1}$) and the Ground floor (U = 0.15 $W{\cdot}m^{-2}{\cdot}K^{-1}$) were inputted, and DesignBuilder then automatically adjusted the thickness of the phenolic foam and the Jetfloor infill insulation block in the walls and floor, respectively. This way, both the makeup of the elements and their U-values were correct, although this alteration may not have completely matched the as-built thicknesses of the Zed House, however the model had to be built as best as possible using the resources and information available at the time. Design U-values were used due to the limitation on the number of in situ U-value measurements that could be taken in the Zed House. Additionally, thermal bridging heat loss could not be included in the model due to the Zed House SAP document not providing the individual psi values for each element required by DesignBuilder[3], and DesignBuilder not having an option to account for total thermal bridging heat loss or an input for the dwelling's design y-value (provided on the SAP document). As a result, the target HTC of the model was the sum of the design fabric and the measured ventilation heat losses of the Zed House, with the thermal bridging heat loss (21.1005 $W{\cdot}K^{-1}$) then subtracted.

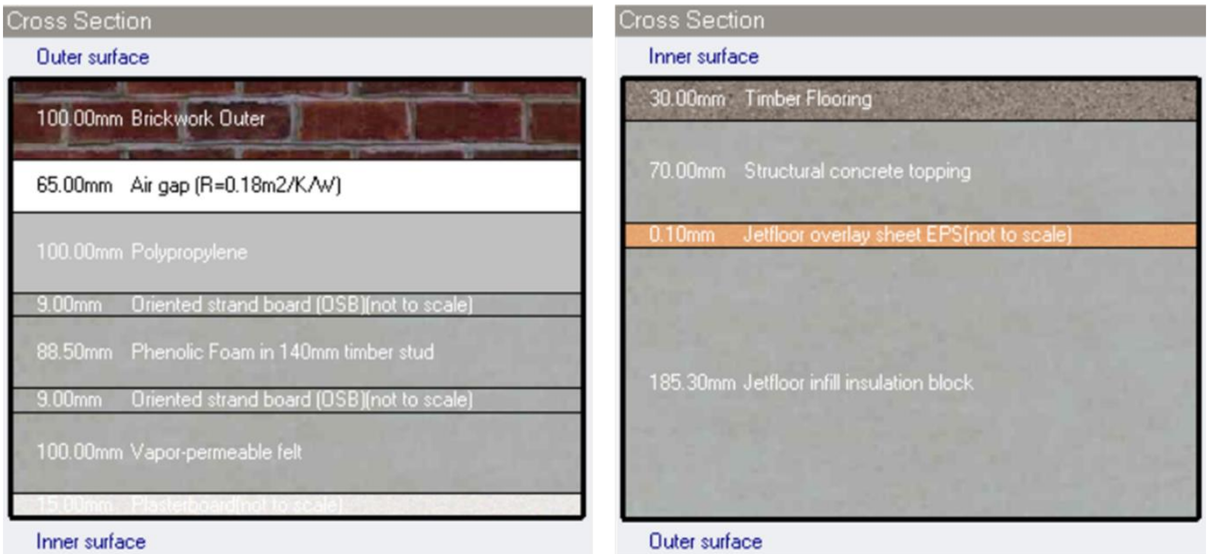


*Figure 3.11 The layers of the External wall (right) and Ground floor (left) elements of the Zed House ground floor block*

3.6.2.4 Block Level - Construction: First Floor

The layout to the first floor is shown in *Figure 3.12*. Similar to the ground floor external walls, the assembly of the first-floor external walls had to be custom created using the Zed House designs and floor plans as guidance. The U-value was also manually applied using the design U-value (U = 0.20 $W{\cdot}m^{-2}{\cdot}K^{-1}$). *Figure 3.13*

[3] The SAP document only provided a y-value for which accredited construction details were used for 2013 compliance. Unfortunately, the psi values and the element details used to calculate this y-value were not provided in the SAP document, and it was these that were required by DesignBuilder for it to factor in thermal bridging heat loss in the model.

demonstrates the layering in the external walls of the first floor. Comparison between the ground floor and first floor external walls show many similarities in their construction materials and layering.

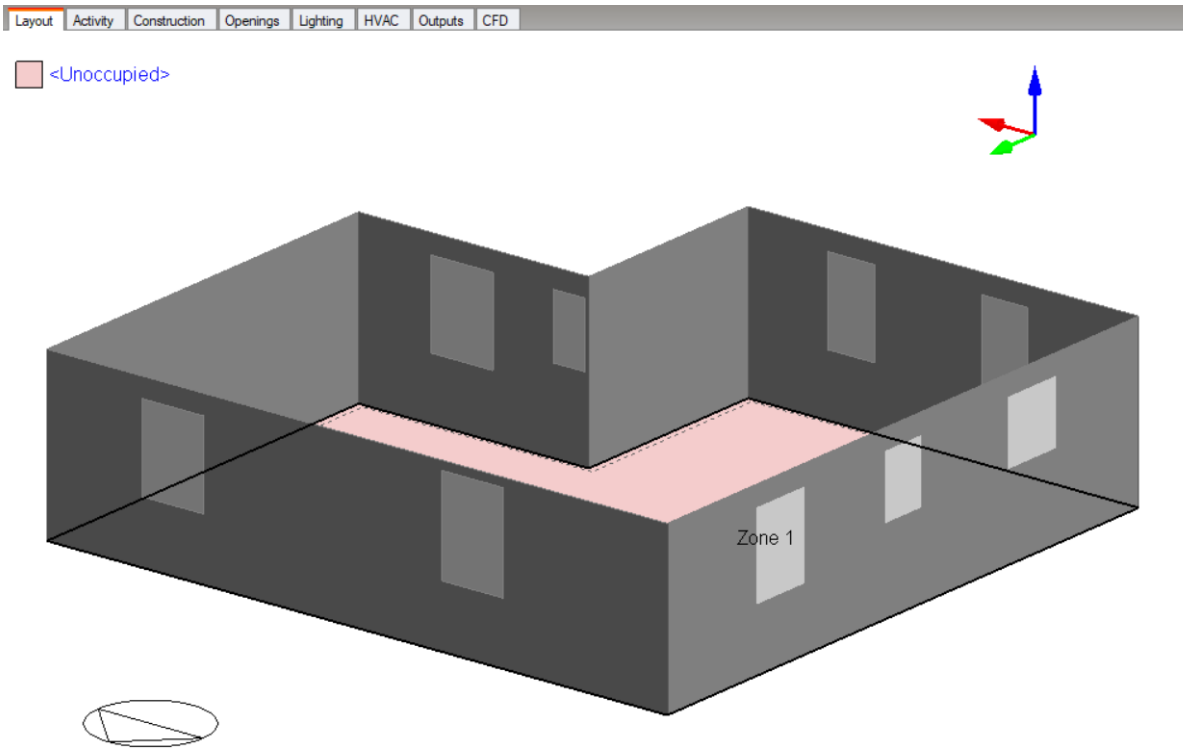


*Figure 3.12 The layout of the first floor of the Zed House model at Block level*

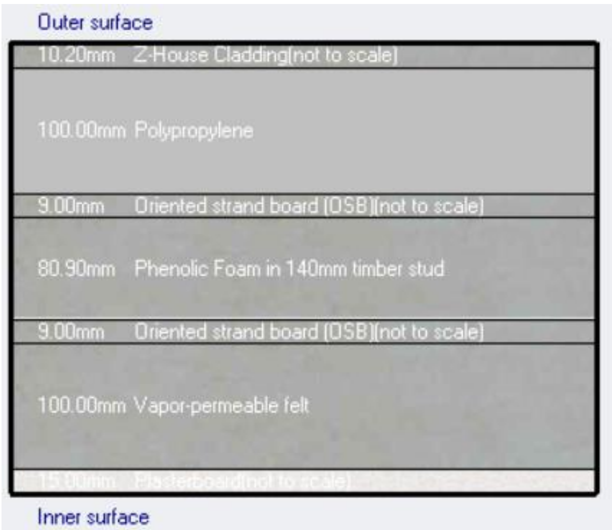


*Figure 3.13 The layers of the External wall elements of the Zed House model first floor block*

### 3.6.2.5 Block Level - Construction: Roof

The Zed House has a gable roof, with the larger section pitched at 45° and the smaller section pitched at 37.5°. The model of the roof at Block level is presented in *Figure 3.14*. The grey sections represent external wall elements; these had the same construction assembly as the first floor.

The composition for the Pitched roof and Ceiling construction assemblies are exhibited in *Figure 3.15*. It is worth noting that the air change rate did not match that of the rest of the dwelling. This is because the air permeability (blower door) test only measured the air change rate of the thermal envelope of the dwelling, and this excludes the roof space, which is classed as ‘unconditioned’. Therefore, the constant rate of the roof was set back to the ‘Project’ value rather than inheriting the measured value from the Building level, although it is accepted that this value is also unlikely to be correct, however was used in the absence of a measured value for that space.

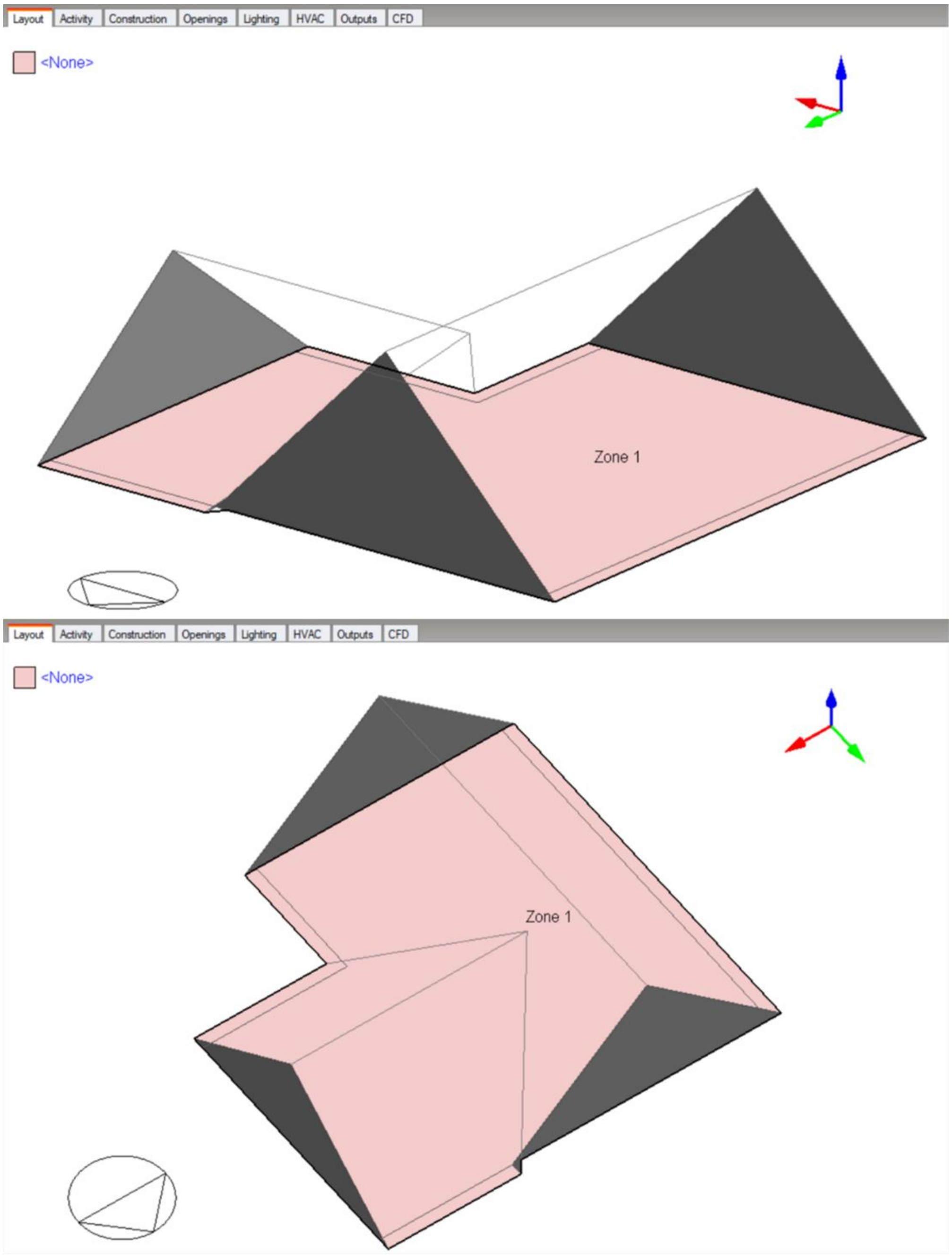


*Figure 3.14 The layout of the roof of the Zed House model at Block level*


*Figure 3.15 The composition of the Pitched roof (unoccupied) (left) and Ceiling (right) construction assemblies of the Zed House model*

### 3.6.2.6 Openings

The openings of the Zed House, which included any windows or doors, were applied to the model using the Zed House designs and floor plans. The Zed House SAP documents specified that the French doors at the rear of the property (found in the kitchen and living room) were to be treated as windows and therefore were inputted as such into the model. This is shown in *Figure 3.16*: the ground floor shown at Zone level, where windows are highlighted yellow, and doors are highlighted blue. The front door (and only 'door' in the model) did not have any specifications provided for it in the SAP documents other than its design U-value (U = 1.0 $W{\cdot}m^{-2}{\cdot}K^{-1}$). Therefore, the door construction assembly was set so that it matched the design U-value.

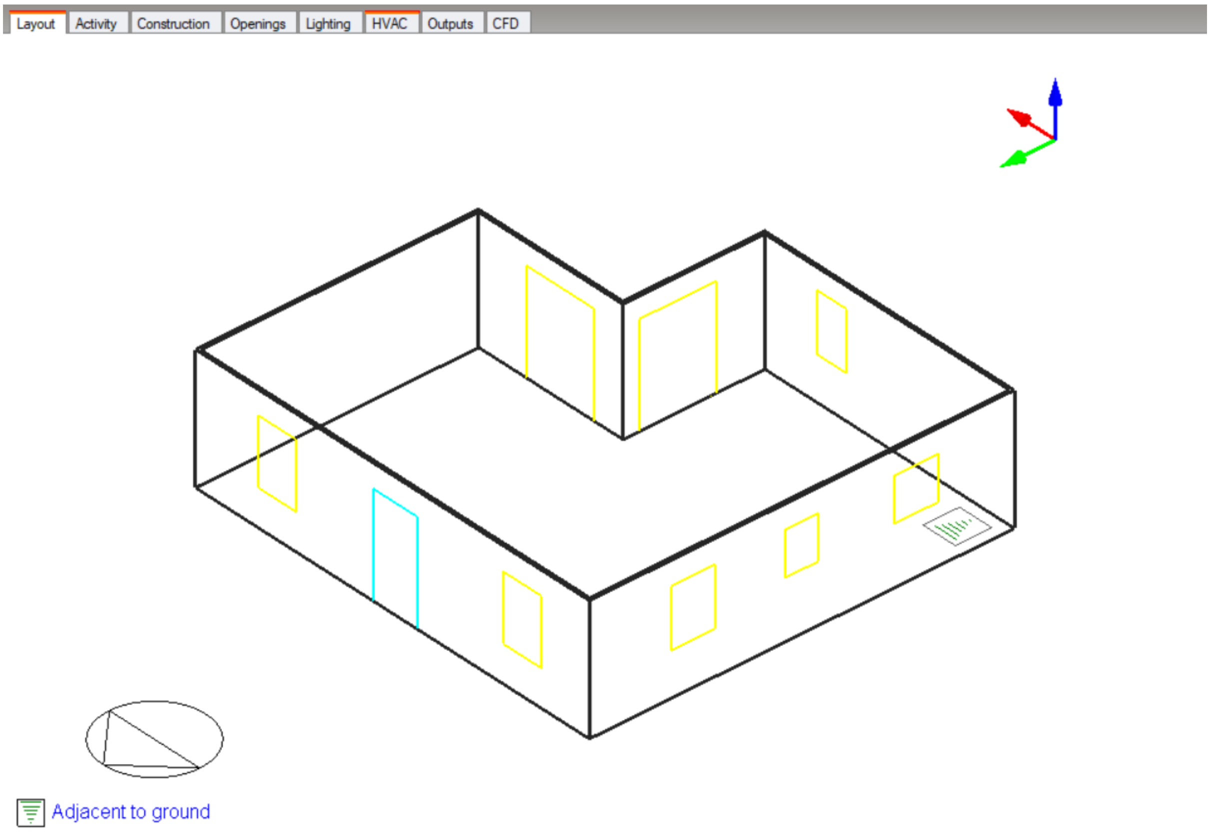


*Figure 3.16 The ground floor of the Zed House model at Zone level displaying windows (yellow) and doors (blue)*

In the Openings tab, it was possible to specify the type of glazing used in the property. The Zed House, according to the SAP documents, was installed with double glazed, low-E coated windows. This type of glazing was custom created in the ‘Edit Glazing’ dialogue, and the U-value set to the Zed House design U-value ($U = 1.2\ W{\cdot}m^{-2}{\cdot}K^{-1}$) - in much the same way as the construction assemblies discussed in the previous sections - and then applied, at Building level, to all the windows. It is accepted that, in an as-built setting, the U-value for each of the windows and French doors would vary depending on their size, however the Zed House SAP document specified that the design value for all was 1.2 $W{\cdot}m^{-2}{\cdot}K^{-1}$, and since this was the only value available, this value had to be used for the Zed House model.

Also in the Openings Tab, was an option to add shading to the windows. To minimise additional solar radiation through the windows during actual testing, all blinds and curtains were drawn constantly, therefore this was also applied to the model.

The type of shade used was dependent on the room. Most rooms used a shade roll that was fairly thick and therefore classed as medium opaque in DesignBuilder. This was applied accordingly at Building level, so that it could be inherited by the levels below it. However, in rooms such as the kitchen and bathrooms, venetian blinds were applied, whilst the French doors (modelled as windows) used drapes - in the kitchen fairly light drapes were used, and in the living room heavier drapes were used.

#### 3.6.2.7 Rendered View

*Figure 3.17* compares, side-by-side, the final rendered model of the Zed House model generated in DesignBuilder, against the actual Zed House built on the University of Salford’s main campus. The Visualise tab in DesignBuilder compiles the various construction details of the surfaces and displays them as a rendered model.

*Figure 3.17 Comparison of the final rendered Zed House model in DesignBuilder with the actual Zed House built on the University of Salford's Peel Park Campus*

## 3.7 Co-heating Simulation

### 3.7.1 Model Data and Model Calibration

3.7.1.1 Thermal Envelope

Information regarding the setup and conditions of a co-heating test were inputted into the model data tabs. Firstly, since co-heating tests are always performed in unoccupied dwellings, the activity template in the Activity tab was set to ‘Unoccupied’, so that the occupancy density of the dwelling was established as zero, and the schedule of occupancy was ‘Off 24/7’. Next, the heating temperature setpoints were inputted to match the same setpoints for the actual baseline co-heating test: 21°C. In DesignBuilder, the setback temperature is simply the temperature setpoint used during the night or when the dwelling is unoccupied, and therefore was set to 21°C as well, since the house would be simulated as unoccupied. Finally in the Activity tab, all computers, office equipment and miscellaneous power consuming items were kept off, and, as in a co-heating test, all electrical appliances - except those directly used in the undertaking of the co-heating test - were also switched off.

Under the lighting tab, all lights connected to the dwelling were switched off, including exterior lights as well as interior ones. Again, this follows with the setup of a co-heating test where all lights are turned off.

Electric radiators were selected as the HVAC template in the HVAC tab. These were a pre-made HVAC template available in DesignBuilder and closely represented the electric heaters used in the actual co-heating test. The heating in the dwelling was scheduled to be ‘On 24/7’ whilst cooling, domestic hot water (DHW), natural ventilation and mechanical ventilation were kept off and as per the conditions required for a co-heating test. The electric radiator template, provided by DesignBuilder, automatically included natural ventilation, so this had to be manually turned off.

3.7.1.2 Roof

The roof/loft space of a dwelling is generally not considered as part of the thermal envelope - it is not a conditioned space. As such, the model data tabs for the roof required different inputs. Firstly, the activity template in the Activity tab was set to 'None' representing that it was an unconditioned space. Also, in DesignBuilder, roof zones are automatically set as 'Semi-exterior unconditioned'. Additionally, the heating setpoints in this tab were left at their pre-set values. This is because, in the HVAC tab, the HVAC template was defined as 'No heating or cooling'. There were no HVAC inputs for the roof space, and, furthermore, there was no lighting, so these were kept off.

### 3.7.2 Weather File

In order to create the weather file that would run during the simulation, the software Elements was used. Elements can be used to custom create or edit weather files for use in energy modelling in buildings.

Weather data was copied into the relevant table columns in the software, displayed in *Figure 3.18*. Dry bulb temperature is the air temperature of the external environment and is also known as the ambient temperature. The same external temperature data collected during the actual co-heating test was inserted here, with one exception. To account for the short period of pre-heating (from 15$^{th}$ December-23$^{rd}$ December) in the simulation before the co-heating test began, Salford temperature data, prior to the two-week period over which the co-heating test was conducted, was gathered from Time and Date AS (Time and Date AS, 2022a). From here, relative humidity data for Salford over the whole co-heating period was also recorded. Due to set-up time constraints during the pre-heating period, the equipment used during the co-heating test to collect external weather conditions was set up towards the end of the pre-heating week, meaning external weather data was not collected for that full week, resulting in the decision to obtain the data from Time and Data AS. CIBSE were considered, however it was not freely available and therefore was discounted due to budgetary constraints.

The wet bulb and dewpoint temperatures were calculated automatically in the software following the addition of the dry bulb temperature data. At constant pressure, the lowest temperature at which evaporating water can cool the air is known as the wet bulb temperature (Razak, 2007), whilst the temperature that water vapour in the air, also at constant pressure, has to be cooled in order to become saturated is known as the dewpoint temperature (Camuffo, 2014). Elements automatically assumes that the atmospheric pressure of a location is 101.33 kPa, or 1 atmosphere.

During the actual co-heating test, global solar irradiance was measured using a pyranometer, oriented horizontally because, according to Kipp and Zonen most meteorological data is based on a horizontally oriented pyranometer (Kipp & Zonen, 2013), and this data was copied into the Elements weather file. Data regarding the normal and direct solar irradiance had not been recorded and so were not included in the file. On site wind speed had also not been recorded due to a failure with the anemometer. It could also not be obtained from Time and Date AS because the site provided inconsistent wind data, one of the drawbacks of using that particular source of weather data. However, following the recommendations demonstrated in calculations in ISO 6949 (BSI, 2017a), a 4 $m \cdot s^{-1}$ wind speed was used.

The completed weather file was then uploaded into DesignBuilder at Site Level and used for the co-heating simulation.

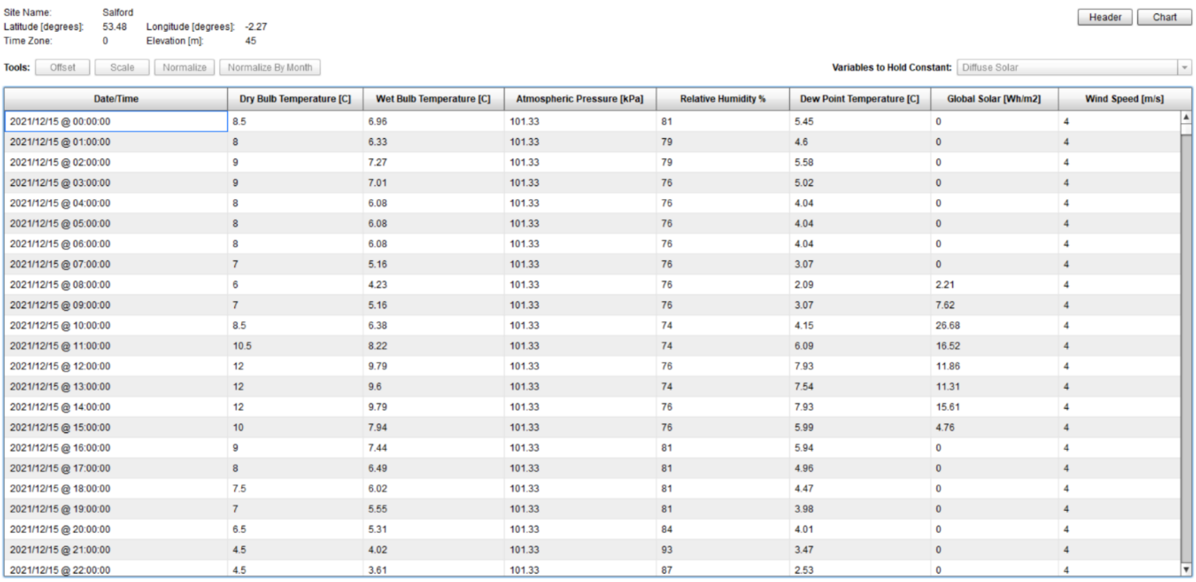

Site Name: Salford
Latitude [degrees]: 53.48 Longitude [degrees]: -2.27
Time Zone: 0 Elevation [m]: 45

Header Chart

Tools: Offset Scale Normalize Normalize By Month

Variables to Hold Constant: Diffuse Solar

| Date/Time | Dry Bulb Temperature [C] | Wet Bulb Temperature [C] | Atmospheric Pressure [kPa] | Relative Humidity % | Dew Point Temperature [C] | Global Solar [Wh/m2] | Wind Speed [m/s] |
|---|---|---|---|---|---|---|---|
| 2021/12/15 @ 00:00:00 | 8.5 | 6.96 | 101.33 | 81 | 5.45 | 0 | 4 |
| 2021/12/15 @ 01:00:00 | 8 | 6.33 | 101.33 | 79 | 4.6 | 0 | 4 |
| 2021/12/15 @ 02:00:00 | 9 | 7.27 | 101.33 | 79 | 5.58 | 0 | 4 |
| 2021/12/15 @ 03:00:00 | 9 | 7.01 | 101.33 | 76 | 5.02 | 0 | 4 |
| 2021/12/15 @ 04:00:00 | 8 | 6.08 | 101.33 | 76 | 4.04 | 0 | 4 |
| 2021/12/15 @ 05:00:00 | 8 | 6.08 | 101.33 | 76 | 4.04 | 0 | 4 |
| 2021/12/15 @ 06:00:00 | 8 | 6.08 | 101.33 | 76 | 4.04 | 0 | 4 |
| 2021/12/15 @ 07:00:00 | 7 | 5.16 | 101.33 | 76 | 3.07 | 0 | 4 |
| 2021/12/15 @ 08:00:00 | 6 | 4.23 | 101.33 | 76 | 2.09 | 2.21 | 4 |
| 2021/12/15 @ 09:00:00 | 7 | 5.16 | 101.33 | 76 | 3.07 | 7.62 | 4 |
| 2021/12/15 @ 10:00:00 | 8.5 | 6.38 | 101.33 | 74 | 4.15 | 26.68 | 4 |
| 2021/12/15 @ 11:00:00 | 10.5 | 8.22 | 101.33 | 74 | 6.09 | 16.52 | 4 |
| 2021/12/15 @ 12:00:00 | 12 | 9.79 | 101.33 | 76 | 7.93 | 11.86 | 4 |
| 2021/12/15 @ 13:00:00 | 12 | 9.6 | 101.33 | 74 | 7.54 | 11.31 | 4 |
| 2021/12/15 @ 14:00:00 | 12 | 9.79 | 101.33 | 76 | 7.93 | 15.61 | 4 |
| 2021/12/15 @ 15:00:00 | 10 | 7.94 | 101.33 | 76 | 5.99 | 4.76 | 4 |
| 2021/12/15 @ 16:00:00 | 9 | 7.44 | 101.33 | 81 | 5.94 | 0 | 4 |
| 2021/12/15 @ 17:00:00 | 8 | 6.49 | 101.33 | 81 | 4.96 | 0 | 4 |
| 2021/12/15 @ 18:00:00 | 7.5 | 6.02 | 101.33 | 81 | 4.47 | 0 | 4 |
| 2021/12/15 @ 19:00:00 | 7 | 5.55 | 101.33 | 81 | 3.98 | 0 | 4 |
| 2021/12/15 @ 20:00:00 | 6.5 | 5.31 | 101.33 | 84 | 4.01 | 0 | 4 |
| 2021/12/15 @ 21:00:00 | 4.5 | 4.02 | 101.33 | 93 | 3.47 | 0 | 4 |
| 2021/12/15 @ 22:00:00 | 4.5 | 3.61 | 101.33 | 87 | 2.53 | 0 | 4 |

*Figure 3.18 The completed Elements weather file ready to be uploaded and run in DesignBuilder via EnergyPlus*

### 3.7.3 Analysis of Simulation Data

#### 3.7.3.1 Data Analysis

The simulation was set to run over the same period as the actual co-heating test: 23rd December 2021 00:00-6th January 2022 00:00, displaying data sub-hourly (i.e., at half hour intervals).

Once the simulation had finished running, DesignBuilder displayed the simulation outputs in the Simulation tab. Zone heating for each conditioned zone (ground floor and first floor) was exported, along with the temperatures of each zone. These, along with the external ambient temperature and solar irradiance used in the weather file, were then used to calculate the HTC of the DesignBuilder Zed House model, in the same way as demonstrated in section 3.5.

#### 3.7.3.2 Error Analysis

Error analysis was carried out in the same way as presented in section 3.5.4.3, following the GUM method (JCGM, 2008). The only change came from the Type B uncertainties: since DesignBuilder and EnergyPlus do not provide standard uncertainties for their simulation results, these could not be included. Type B uncertainties for the external temperatures and solar irradiances remained the same however, since the weather data collected during the co-heating test performed in the Zed House was used in the weather file for the co-heating simulation in DesignBuilder.

## 3.8 Alternative Method Simulation

### 3.8.1 Model Data

3.8.1.1 Thermal Envelope

The DesignBuilder model of the Zed House that was used for the co-heating simulation was also used for the alternative method simulation, so that all construction elements remained the same, as well as any other known information about the Zed House, such as its air change rate. Openings, such as windows, doors, and vents, also remained closed or sealed, and the shading settings were all kept in place in order to minimise the amount of solar radiation coming into the dwelling via the openings. It was decided, similar to the co-heating test, that the alternative method would be carried out when the dwelling was unoccupied. As such, the activity template in the Activity tab was established as ‘Unoccupied’, thereby making the occupancy density of the dwelling zero and the scheduled occupancy ‘Off 24/7’. In addition, all computers, office equipment, and other miscellaneous power consuming devices, along with internal and external lighting, were kept off, so that only the power input to and output from the HVAC system - discussed further on in this section - would be measured.

Exploring the recommended and general minimum temperatures reached by most standard air conditioning units, found that 16°C should be the lowest setpoint temperature for the simulation (Air Con Direct, 2020; American Home, Water & Air, 2020; CIBSE, 2015; Dunklee, 2021; Watson, 2021). This was so that it would be as close to the temperature that could hypothetically be achieved if the test were to occur in real conditions. This also fell in line with the lowest internal temperature that could be achieved, on average, when looking at a psychometric chart (such as the one shown in *Figure 3.19*), where values of dew point temperature (automatically calculated in the Elements weather file, as discussed in section 3.7.2) and relative humidity were used to determine an approximate, suitable value of internal temperature: ~ 16°C. From this, 16°C was inputted as the setpoint and setback temperatures for the model.

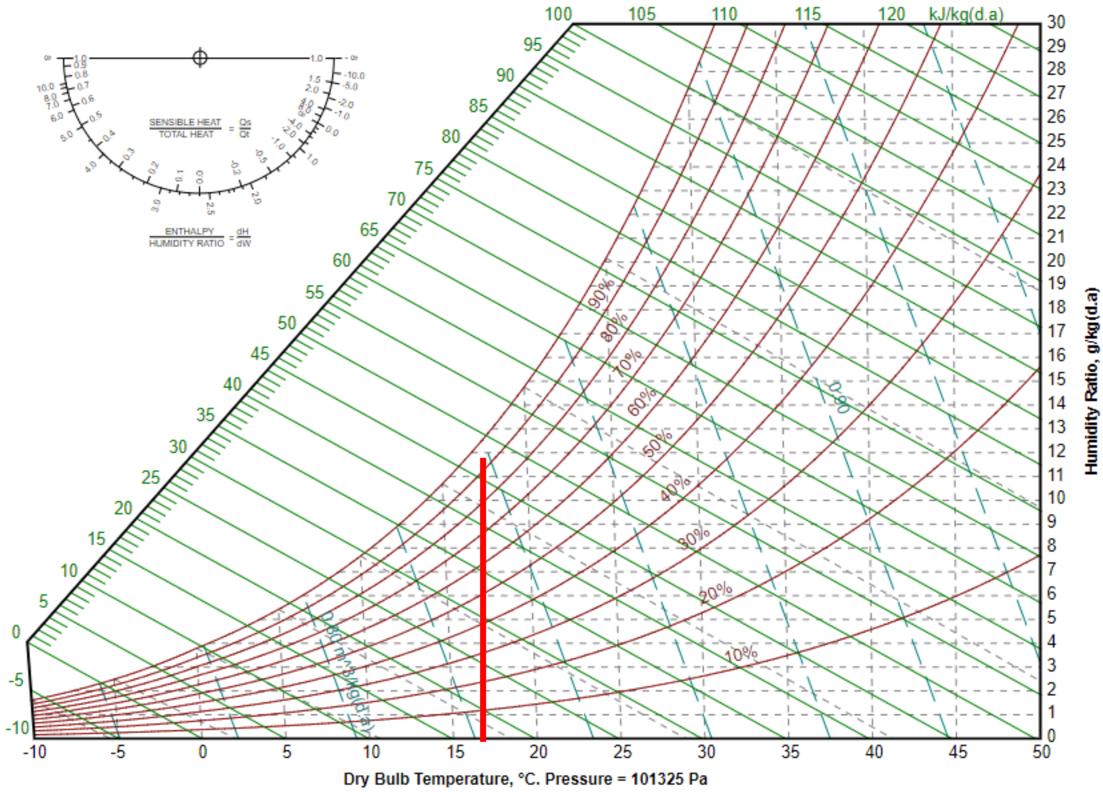


*Figure 3.19 A psychometric chart (FlyCarpet Inc., 2015)*

The ‘Split no fresh air’ HVAC template was selected in the HVAC tab. This denoted a split system air conditioning unit, as chosen in section 2.6.3.3, which did not allow any other natural ventilation to occur in the dwelling, so that the cooling effect would exclusively be down to the performance of the split system air conditioning unit. The default settings for the cooling system were not changed, so that it had a COP of 1.8, and a minimum supply air temperature of 12°C. The operating schedule for the system was set to ‘On 24/7’.

3.8.1.2 Roof

The settings for the roof/loft space remained the same as they were during co-heating simulation since that particular space was not considered to be part of the thermal envelope. Therefore, the activity template in the Activity tab was left as 'None' and the HVAC template in the HVAC tab was left as 'No heating or cooling' with all lights and other powered devices remaining turned off.

### 3.8.2 Compiling the Weather Data

Weather data, including external temperature, relative humidity and solar irradiance, was compiled from NASA and Time and Date AS (NASA, 2022; Time and Date AS, 2022a), covering five years-worth of data from 2017 up to 2021, inclusive. These sources were used instead of a simulation weather file provided by DesignBuilder because the closest simulation weather file to Salford was Aughton (26 miles away) and was therefore deemed as not representative of the weather conditions in Salford. Since a co-heating test is usually performed over a two-week period, it was deemed sensible to find the hottest two-week period from each year, as well as a two-week period that had temperatures approximately equal to the year's summertime average. This was because testing in a real-world environment would be more likely to occur during more average temperatures, as hotter temperatures would be harder to predict and plan for in advance. In order to calculate the summertime average, temperatures from the beginning of June up to the end of August were averaged, as these were shown to be the hottest months of a year. When finding the hottest two-week period from each year, it was found that periods containing 'hottest days' (days that contained the hottest temperatures) were not always the equivalent of periods of 'average hottest days' (i.e., a day that might contain the hottest temperature, did not necessarily average out to be as hot as other averaged days). As such, two sets of two-week periods covering extreme temperatures were found; one covering a two-week period containing the days that reached the hottest temperatures in that year, and one covering a period that was the hottest average two-week period in that year. Then, within these two-week periods, periods of average and both extreme temperatures over twelve days, one week, five days and forty-eight hours were determined (demonstrated in *Tables*

*3.4a-c*), chosen to cover a similar range of test periods used in other whole house heat loss test methods (highlighted in section 2.4). This provided a range of test periods to test over, whilst still conforming with the average or extreme temperatures being used, in order to explore test period length.

The corresponding external temperatures, relative humidities and solar irradiances for each two-week period in each average and extreme temperature category were inputted into weather files created in Elements, in the same manner as explained in section 3.7.2. To maintain consistency with the data available for the baseline co-heating simulation, wind speed was set to 4 $m \cdot s^{-1}$, once again following the recommendations presented in calculations in (BSI, 2017a). It is accepted that, in reality, wind speed would vary during the different seasons, so this standard wind speed may not be as applicable for the alternative simulations. However, ISO 2017a did not specify a particular time of year that 4 $m \cdot s^{-1}$ represented and that is why the standard value was also used for the alternative simulations. The completed weather files were then uploaded into DesignBuilder at Site Level and used in the corresponding simulations.

*Table 3.4a The test periods for the extreme day summertime temperatures*

**Periods of Extreme Day Summertime Temperature**

| Year | Period | 2 Weeks | 12 Days | 1 Week | 5 Days | 48 Hours |
|---|---|---|---|---|---|---|
| 2021 | 14/07/2021 | | | | | |
| | 15/07/2021 | | | | | |
| | 16/07/2021 | | | | | |
| | 17/07/2021 | | | | | |
| | 18/07/2021 | | | | | |
| | 19/07/2021 | | | | | |
| | 20/07/2021 | | | | | |
| | 21/07/2021 | | | | | |
| | 22/07/2021 | | | | | |
| | 23/07/2021 | | | | | |
| | 24/07/2021 | | | | | |
| | 25/07/2021 | | | | | |
| | 26/07/2021 | | | | | |
| | 27/07/2021 | | | | | |
| 2020 | 05/08/2020 | | | | | |
| | 06/08/2020 | | | | | |
| | 07/08/2020 | | | | | |
| | 08/08/2020 | | | | | |
| | 09/08/2020 | | | | | |
| | 10/08/2020 | | | | | |
| | 11/08/2020 | | | | | |
| | 12/08/2020 | | | | | |
| | 13/08/2020 | | | | | |
| | 14/08/2020 | | | | | |
| | 15/08/2020 | | | | | |
| | 16/08/2020 | | | | | |
| | 17/08/2020 | | | | | |
| | 18/08/2020 | | | | | |
| 2019 | 13/07/2019 | | | | | |
| | 14/07/2019 | | | | | |
| | 15/07/2019 | | | | | |
| | 16/07/2019 | | | | | |
| | 17/07/2019 | | | | | |
| | 18/07/2019 | | | | | |
| | 19/07/2019 | | | | | |
| | 20/07/2019 | | | | | |
| | 21/07/2019 | | | | | |
| | 22/07/2019 | | | | | |
| | 23/07/2019 | | | | | |
| | 24/07/2019 | | | | | |
| | 25/07/2019 | | | | | |
| | 26/07/2019 | | | | | |
| 2018 | 25/06/2018 | | | | | |
| | 26/06/2018 | | | | | |
| | 27/06/2018 | | | | | |
| | 28/06/2018 | | | | | |
| | 29/06/2018 | | | | | |
| | 30/06/2018 | | | | | |
| | 01/07/2018 | | | | | |
| | 02/07/2018 | | | | | |
| | 03/07/2018 | | | | | |
| | 04/07/2018 | | | | | |
| | 05/07/2018 | | | | | |
| | 06/07/2018 | | | | | |
| | 07/07/2018 | | | | | |
| | 08/07/2018 | | | | | |
| 2017 | 13/06/2017 | | | | | |
| | 14/06/2017 | | | | | |
| | 15/06/2017 | | | | | |
| | 16/06/2017 | | | | | |
| | 17/06/2017 | | | | | |
| | 18/06/2017 | | | | | |
| | 19/06/2017 | | | | | |
| | 20/06/2017 | | | | | |
| | 21/06/2017 | | | | | |
| | 22/06/2017 | | | | | |
| | 23/06/2017 | | | | | |
| | 24/06/2017 | | | | | |
| | 25/06/2017 | | | | | |
| | 26/06/2017 | | | | | |

*Table 3.4b The test periods for the extreme average summertime temperatures*

**Periods of Extreme Average Summertime Temperature**

| Year | Period | 2 Weeks | 12 Days | 1 Week | 5 Days | 48 Hours |
|---|---|---|---|---|---|---|
| 2021 | 13/07/2021 | | | | | |
| | 14/07/2021 | | | | | |
| | 15/07/2021 | | | | | |
| | 16/07/2021 | | | | | |
| | 17/07/2021 | | | | | |
| | 18/07/2021 | | | | | |
| | 19/07/2021 | | | | | |
| | 20/07/2021 | | | | | |
| | 21/07/2021 | | | | | |
| | 22/07/2021 | | | | | |
| | 23/07/2021 | | | | | |
| | 24/07/2021 | | | | | |
| | 25/07/2021 | | | | | |
| | 26/07/2021 | | | | | |
| 2020 | 05/08/2020 | | | | | |
| | 06/08/2020 | | | | | |
| | 07/08/2020 | | | | | |
| | 08/08/2020 | | | | | |
| | 09/08/2020 | | | | | |
| | 10/08/2020 | | | | | |
| | 11/08/2020 | | | | | |
| | 12/08/2020 | | | | | |
| | 13/08/2020 | | | | | |
| | 14/08/2020 | | | | | |
| | 15/08/2020 | | | | | |
| | 16/08/2020 | | | | | |
| | 17/08/2020 | | | | | |
| | 18/08/2020 | | | | | |
| 2019 | 22/07/2019 | | | | | |
| | 23/07/2019 | | | | | |
| | 24/07/2019 | | | | | |
| | 25/07/2019 | | | | | |
| | 26/07/2019 | | | | | |
| | 27/07/2019 | | | | | |
| | 28/07/2019 | | | | | |
| | 29/07/2019 | | | | | |
| | 30/07/2019 | | | | | |
| | 31/07/2019 | | | | | |
| | 01/08/2019 | | | | | |
| | 02/08/2019 | | | | | |
| | 03/08/2019 | | | | | |
| | 04/08/2019 | | | | | |
| 2018 | 26/06/2018 | | | | | |
| | 27/06/2018 | | | | | |
| | 28/06/2018 | | | | | |
| | 29/06/2018 | | | | | |
| | 30/06/2018 | | | | | |
| | 01/07/2018 | | | | | |
| | 02/07/2018 | | | | | |
| | 03/07/2018 | | | | | |
| | 04/07/2018 | | | | | |
| | 05/07/2018 | | | | | |
| | 06/07/2018 | | | | | |
| | 07/07/2018 | | | | | |
| | 08/07/2018 | | | | | |
| | 09/07/2018 | | | | | |
| 2017 | 13/06/2017 | | | | | |
| | 14/06/2017 | | | | | |
| | 15/06/2017 | | | | | |
| | 16/06/2017 | | | | | |
| | 17/06/2017 | | | | | |
| | 18/06/2017 | | | | | |
| | 19/06/2017 | | | | | |
| | 20/06/2017 | | | | | |
| | 21/06/2017 | | | | | |
| | 22/06/2017 | | | | | |
| | 23/06/2017 | | | | | |
| | 24/06/2017 | | | | | |
| | 25/06/2017 | | | | | |
| | 26/06/2017 | | | | | |

*Table 3.4c The test periods for the average summertime temperatures*

**Periods of Average Summertime Temperature**

| Year | Period | 2 Weeks | 12 Days | 1 Week | 5 Days | 48 Hours |
|---|---|---|---|---|---|---|
| 2021 | 30/06/2021 | | | | | |
| | 01/07/2021 | | | | | |
| | 02/07/2021 | | | | | |
| | 03/07/2021 | | | | | |
| | 04/07/2021 | | | | | |
| | 05/07/2021 | | | | | |
| | 06/07/2021 | | | | | |
| | 07/07/2021 | | | | | |
| | 08/07/2021 | | | | | |
| | 09/07/2021 | | | | | |
| | 10/07/2021 | | | | | |
| | 11/07/2021 | | | | | |
| | 12/07/2021 | | | | | |
| | 13/07/2021 | | | | | |
| 2020 | 15/08/2020 | | | | | |
| | 16/08/2020 | | | | | |
| | 17/08/2020 | | | | | |
| | 18/08/2020 | | | | | |
| | 19/08/2020 | | | | | |
| | 20/08/2020 | | | | | |
| | 21/08/2020 | | | | | |
| | 22/08/2020 | | | | | |
| | 23/08/2020 | | | | | |
| | 24/08/2020 | | | | | |
| | 25/08/2020 | | | | | |
| | 26/08/2020 | | | | | |
| | 27/08/2020 | | | | | |
| | 28/08/2020 | | | | | |
| 2019 | 02/07/2019 | | | | | |
| | 03/07/2019 | | | | | |
| | 04/07/2019 | | | | | |
| | 05/07/2019 | | | | | |
| | 06/07/2019 | | | | | |
| | 07/07/2019 | | | | | |
| | 08/07/2019 | | | | | |
| | 09/07/2019 | | | | | |
| | 10/07/2019 | | | | | |
| | 11/07/2019 | | | | | |
| | 12/07/2019 | | | | | |
| | 13/07/2019 | | | | | |
| | 14/07/2019 | | | | | |
| | 15/07/2019 | | | | | |
| 2018 | 03/08/2018 | | | | | |
| | 04/08/2018 | | | | | |
| | 05/08/2018 | | | | | |
| | 06/08/2018 | | | | | |
| | 07/08/2018 | | | | | |
| | 08/08/2018 | | | | | |
| | 09/08/2018 | | | | | |
| | 10/08/2018 | | | | | |
| | 11/08/2018 | | | | | |
| | 12/08/2018 | | | | | |
| | 13/08/2018 | | | | | |
| | 14/08/2018 | | | | | |
| | 15/08/2018 | | | | | |
| | 16/08/2018 | | | | | |
| 2017 | 19/07/2017 | | | | | |
| | 20/07/2017 | | | | | |
| | 21/07/2017 | | | | | |
| | 22/07/2017 | | | | | |
| | 23/07/2017 | | | | | |
| | 24/07/2017 | | | | | |
| | 25/07/2017 | | | | | |
| | 26/07/2017 | | | | | |
| | 27/07/2017 | | | | | |
| | 28/07/2017 | | | | | |
| | 29/07/2017 | | | | | |
| | 30/07/2017 | | | | | |
| | 31/07/2017 | | | | | |
| | 01/08/2017 | | | | | |

### 3.8.3 Simulation and Data Collection

Overall, fifteen separate simulations were run: three for each of the years (2017-2021) covering the average temperature period, the extreme day temperature period and the extreme average temperature period. Each simulation was set to run over the corresponding nominated two-week duration (see column three in *Tables 3.4a-c* in section 3.8.2), and the outputs were set to be recorded at sub-hourly, or half hour, intervals.

Following the completion of each simulation, the results were displayed in the Simulation tab. As explained earlier in this chapter, cooling equipment, such as split system air conditioning units, have a COP greater than 1, because their output is greater than their required input. For this reason, the Total Cooling (kW) measured was 1.8 (the value of the COP used in the simulation) times greater than the Electricity (kW) input. This is demonstrated in the example shown in *Figure 3.20* and also shows there were no additional gains to the house from heat given out by the air conditioning unit. In a real-world test environment this would likely not be the case, however, for all the DesignBuilder simulations carried out during this research, the simple HVAC system model was used. This meant that the system was defined using basic HVAC data descriptions. As such the heating and cooling loads were calculated using the idealised EnergyPlus “Ideal Loads” system (DesignBuilder Software Ltd, 2022). In addition, the Electricity and Cooling (Electricity) columns were exactly the same because the only power input to the dwelling was to the split system air conditioning unit. As such it was concluded that the idealised EnergyPlus “Ideal Loads” system and the simple HVAC system must have already accounted for any additional heat generation caused by the air conditioning unit, and thus factored it in to its calculation of the heating and cooling loads. The values in the Total Cooling column are negative to denote that the power was used for cooling rather than heating, thus, in calculations later on, the absolutes of these values were used.

The values of whole house thermal envelope power input and output were exported, along with the temperatures of each conditioned zone (ground floor and first floor).

Zed House, House

Analysis | Summary | Parametric | Optimisation | Data Visualisation

| Date/Time | Electricity (kW) | Cooling (Electricity) (kW) | Total Cooling (kW) |
|---|---|---|---|
| 04/08/2002 00:3... | 0.114973 | 0.114973 | -0.206952 |
| 04/08/2002 01:0... | 0.12226 | 0.12226 | -0.220067 |
| 04/08/2002 01:3... | 0.114647 | 0.114647 | -0.206364 |
| 04/08/2002 02:0... | 0.105518 | 0.105518 | -0.189933 |
| 04/08/2002 02:3... | 0.103528 | 0.103528 | -0.186351 |
| 04/08/2002 03:0... | 0.10204 | 0.10204 | -0.183672 |
| 04/08/2002 03:3... | 0.080814 | 0.080814 | -0.145464 |
| 04/08/2002 04:0... | 0.057996 | 0.057996 | -0.104393 |
| 04/08/2002 04:3... | 0.055693 | 0.055693 | -0.100248 |
| 04/08/2002 05:0... | 0.056822 | 0.056822 | -0.10228 |
| 04/08/2002 05:3... | 0.069144 | 0.069144 | -0.124459 |
| 04/08/2002 06:0... | 0.086526 | 0.086526 | -0.155746 |
| 04/08/2002 06:3... | 0.095479 | 0.095479 | -0.171862 |
| 04/08/2002 07:0... | 0.108377 | 0.108377 | -0.19508 |
| 04/08/2002 07:3... | 0.130366 | 0.130366 | -0.234658 |
| 04/08/2002 08:0... | 0.15945 | 0.15945 | -0.28701 |
| 04/08/2002 08:3... | 0.190037 | 0.190037 | -0.342066 |
| 04/08/2002 09:0... | 0.218865 | 0.218865 | -0.393957 |
| 04/08/2002 09:3... | 0.262363 | 0.262363 | -0.472254 |
| 04/08/2002 10:0... | 0.315186 | 0.315186 | -0.567335 |
| 04/08/2002 10:3... | 0.336734 | 0.336734 | -0.60612 |
| 04/08/2002 11:0... | 0.348435 | 0.348435 | -0.627183 |
| 04/08/2002 11:3 | 0.355281 | 0.355281 | -0.639505 |

*Figure 3.20 An example of the power inputs (Electricity and Cooling (Electricity)) and outputs (Total Cooling) from one alternative method simulation*

### 3.8.4 Analysis for the Alternative Method

3.8.4.1 Data Analysis

Once data from the simulations had been exported, the output power (Total Cooling), and the internal temperature data for each zone were used along with the external temperature and solar irradiance data used in the weather files. From here, analysis was very similar to that of the co-heating method and was conducted in Microsoft Excel (Excel).

Firstly, the average internal temperature for the building envelope at each sub-hourly timestamp was calculated by averaging the ground floor and first floor temperatures. Following this, timestamps for each day in the selected two-week period were created with a start and end time. Then, internal temperature, external temperature, and solar irradiance for each 24-hour time stamp in the two-week period were determined. Since the output power was negative the absolute values of average power were calculated. Meanwhile, the average internal and external temperatures were used to calculate the average internal-external temperature differences. A graph of power against temperature difference was then calculated, the regression line gradient of which provided a raw value of the HTC.

Multiple linear regression analysis was then carried out in R Studio, in the same way as explained in section 3.5.2. This accounted for solar irradiance during the test and provided the value of solar aperture ($m^2$). A value of solar aperture accounting for a zero intercept was also determined, in the same manner described in section 3.5.4.2.

A zero intercept (where the regression line passed through the origin) was used so the assumption could be made that when there was no internal-external temperature difference, cooling was not necessary within the dwelling and thus there was no cooling power input or output.

Using *Equation 3.6* from section 3.5.3, the solar aperture for a zero intercept was used to calculate the solar corrected power for a zero intercept (the numerator in the equation) for each 24-hour timestamp. These values were then plotted against their corresponding temperature difference and a regression line drawn through them to give a solar corrected value of the HTC for that particular simulation.

For each simulation, analysis was carried out over two-week, twelve-day, one-week, five-day and forty-eight-hour durations, in line with the test periods established in *Tables 3.4a-c*. Alongside this, different aggregation intervals were investigated. Daily cycles running from midnight-midnight, dawn-dawn, 06:00-06:00, midday-midday and 18:00-18:00 were considered for each test period conducted for each simulation. This was done to see whether increased hours and levels of sunlight during summer months impacted the dwelling's ability to release any solar radiation stored in its building fabric during each daily cycle. The time dawn occurred during each year's testing periods were found using Time and Date AS (Time and Date AS, 2022b).

### 3.8.4.2 Error Analysis

Error analysis for the data collected and values calculated for the alternative method was carried out following the GUM method, equivalent to the way it was undertaken in sections 3.5.4.3 and 3.7.3.2. As in section 3.7.3.2, DesignBuilder provided no Type B uncertainties, however Type B uncertainties for the real time weather data that was used, such as the external temperatures and solar irradiances, were found from Custom Weather and NASA Power (Custom Weather, 2022; NASA POWER, 2021).

# Chapter 4

# Results and Discussion

## Chapter Overview

This chapter presents the results of the research in the form of graphs and tables and discusses the possible reasons for these results. The chapter is made up of the following sections:

- **4.1 The Measured Performance of the Zed House**: reveals the measured, or as-built, HTC of the Zed House, whilst further backing up the choices that were made in the methodology section regarding the aggregation interval and use of forcing the regression line through the origin.
- **4.2 The Performance of the Zed House Model in DesignBuilder during the Simulated Co-heating Test**: reports the outcomes from running the simulated co-heating test on the Zed House model that was created in DesignBuilder, and compares these outcomes to the as-built and design performance of the Zed House and target performance of the Zed House model.
- **4.3 Results from the Alternative Method Simulations**: presents the findings from running the alternative method on the Zed House model, along with the protocols taken into consideration when determining the most appropriate HTC from the data sets to compare the simulated baseline and target HTCs against.

## 4.1 The Measured Performance of the Zed House

A co-heating test was performed on the Zed House, with data analysed during the period Thursday 23rd December 2021 00:00 to Thursday 6th January 2022 00:00. *Figure 4.1* displays the temperature profiles of each room in the Zed House during the heat-up and co-heating periods. After an initial couple of days of fluctuation whilst equipment was set up in the dwelling, most of the room temperatures stabilised around 21°C, which was the setpoint temperature. The hall sensor dropped out for a short period between the afternoon of 15th December and the morning of 16th December, and this caused the recorded temperature to show as 0°C. Additionally, the ensuite struggled to reach the setpoint temperature. The three peaks that can be seen during the heat-up period corresponds to solar gains through the ensuite's west facing window at a similar time to sunset on those days. A heater was added to the ensuite which then allowed its temperature to stabilise around the setpoint. *Figure 4.2* shows the difference between each room's temperature and the setpoint temperature (21°C). Whilst there is quite a lot of fluctuation during the heat-up period, adjustments made to the setup in the dwelling, either by moving the heaters and fans or adding some in, meant that the room temperatures stabilised to a maximum difference of ±1.0°C from the setpoint temperature during the co-heating period.

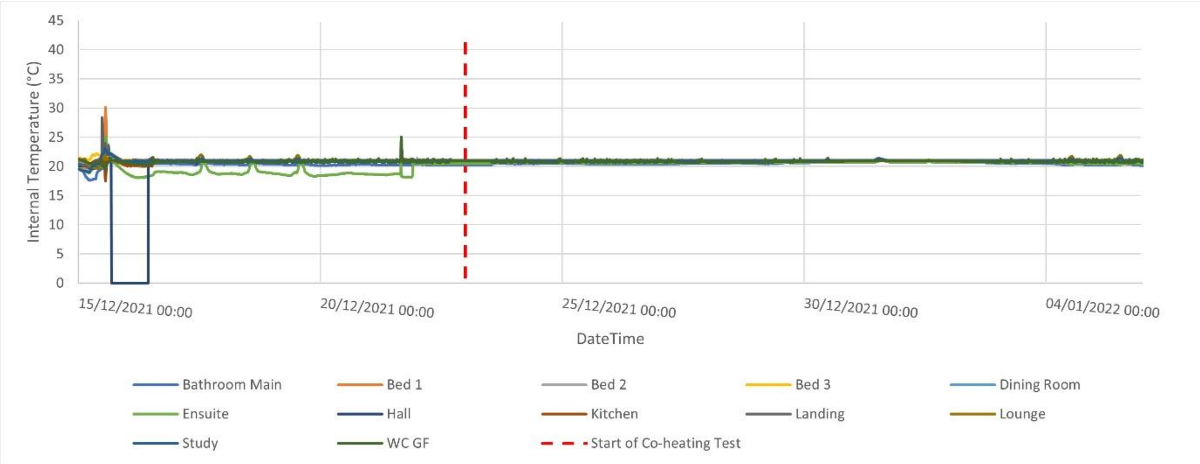


*Figure 4.1 The temperature profiles for each room in the Zed House during the heat-up and co-heating periods*

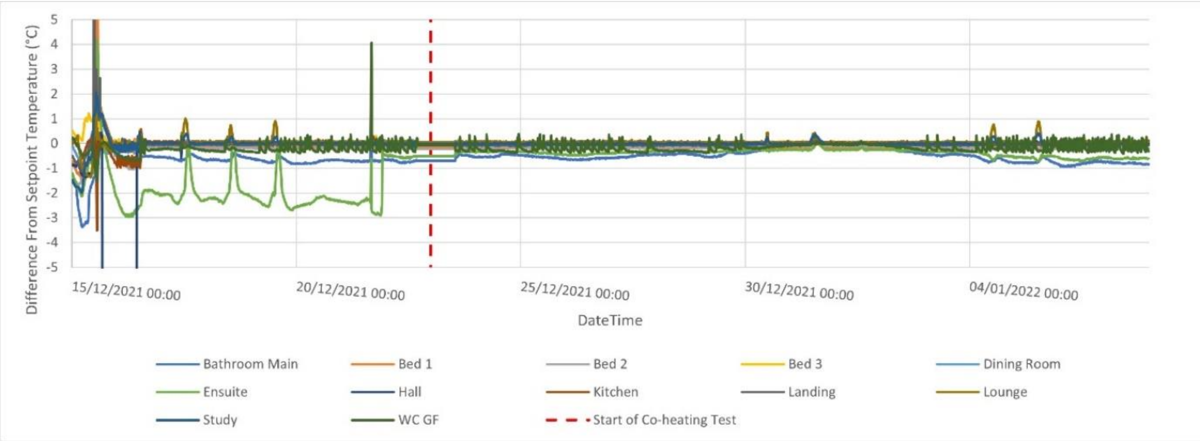


*Figure 4.2 A graph showing the difference between the internal temperatures of each room in the Zed House and the setpoint temperature (21°C) during the heat-up and co-heating periods*

### 4.1.1 Impact of Different Aggregation Intervals on the Measured HTC

As mentioned in section 3.5.4.1, two aggregation intervals were analysed for comparison purposes to see how much impact the two different aggregation intervals had on the measured HTC. Data was aggregated across midnight-midnight and dawn-dawn intervals and the results are plotted in *Figure 4.3*. The measured solar corrected HTC for the midnight-midnight aggregation interval was 137.2 $W{\cdot}K^{-1}$, whilst the dawn-dawn aggregation interval produced an HTC of 136.2 $W{\cdot}K^{-1}$.

This suggested that, in the case of the Zed House, analysing the data using a dawn-dawn aggregation interval over a midnight-midnight aggregation interval had very little impact on the resulting HTC. This could be expected, given that the Zed House can be classed as a light-mediumweight dwelling, and would therefore have re-radiated the majority, if not all, the solar radiation stored in its fabric by midnight the same day. In addition, the co-heating test was performed when days were very short, so there was a longer period between dusk and midnight, and the blinds were kept closed so there was no direct solar radiation on the internal fabric of the building, such as tiled floors. As such, when considering the measured HTC of the Zed House, the value determined from the midnight-midnight aggregation interval, 137.2 $W{\cdot}K^{-1}$, was selected and has been used and discussed in the rest of this report. This is for consistency purposes with the co-heating method developed by Leeds Beckett University (Johnston et al., 2013), reviewed in the literature .

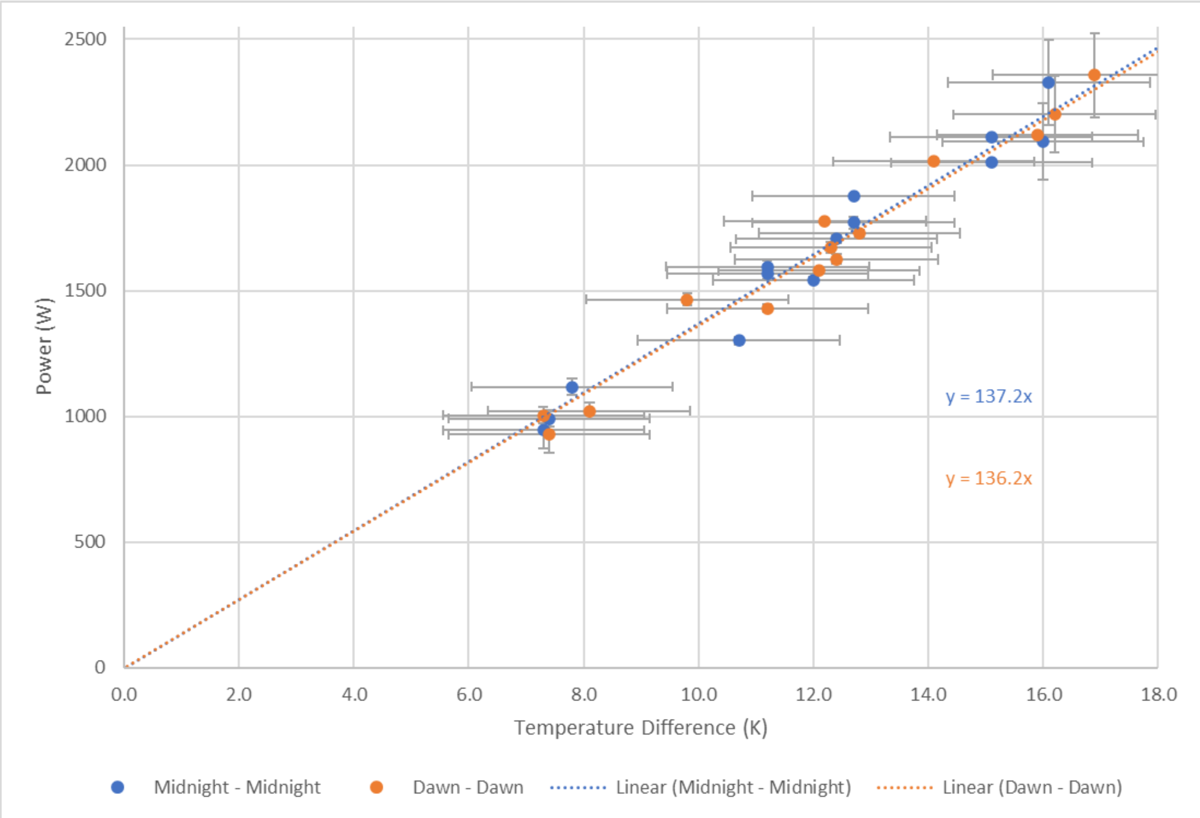


*Figure 4.3 A graph showing solar corrected power plotted against temperature difference for the midnight-midnight and dawn-dawn aggregation intervals along with the corresponding regression lines*

### 4.1.2 Impact of a Forced Intercept on the Measured HTC

In this section, comparisons are drawn between not forcing and forcing the regression line of the power against temperature difference plots through the origin and their impact on the value of the corresponding HTC.

*Figure 4.4* shows the raw and solar corrected power against temperature difference plots, along with their regression lines, which were not forced through the origin. The raw value of the HTC was slightly lower than the HTC which was corrected to account for solar radiation. Additionally, the values of the intercepts were not particularly high compared to the measured values of power plotted on the graph, therefore it would not be unreasonable to expect, in the case of the Zed House, that forcing the regression lines through the origin would not have a considerable impact on the measured values of the HTC. This thought process is verified in *Figure 4.5*, which shows the plots with their regression lines forced through the origin. Whilst the measured value of the HTC had decreased, by approximately 4.4 $W \cdot K^{-1}$ (3.1%) in the case of the solar corrected HTC and 1.3 $W \cdot K^{-1}$ (1.0%) in the case of the raw HTC, these were considerably small diminishments. A comparison between the unforced and forced solar corrected regression lines are displayed in *Figure 4.6*, which more clearly demonstrates the minor impact of forcing the solar corrected regression line through the origin in this instance.

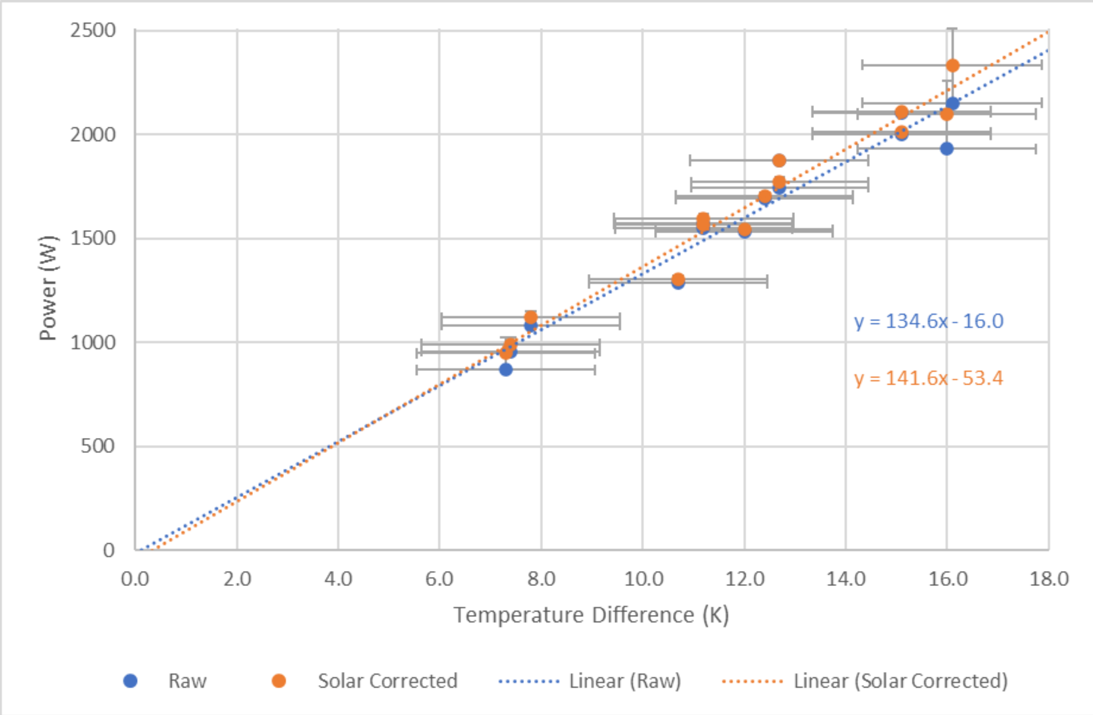


*Figure 4.4 A graph of raw power and solar corrected power plotted against temperature difference with the corresponding regression lines not forced through the origin*

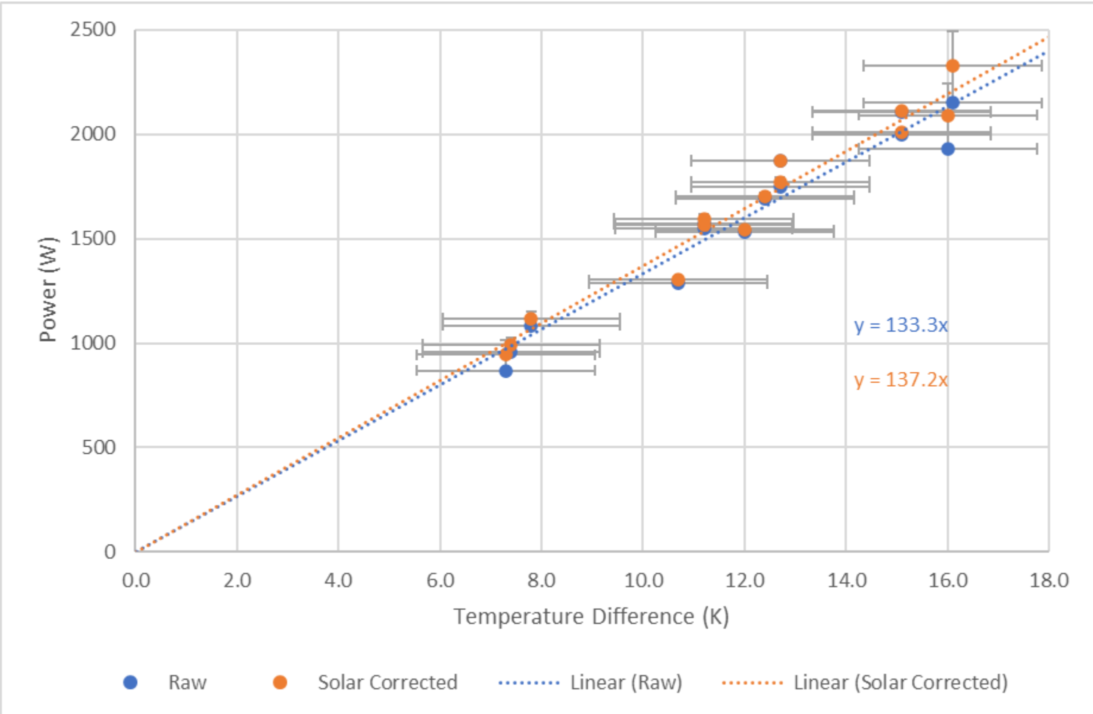


*Figure 4.5 A graph of raw power and solar corrected power plotted against temperature difference with the corresponding regression lines forced through the origin*

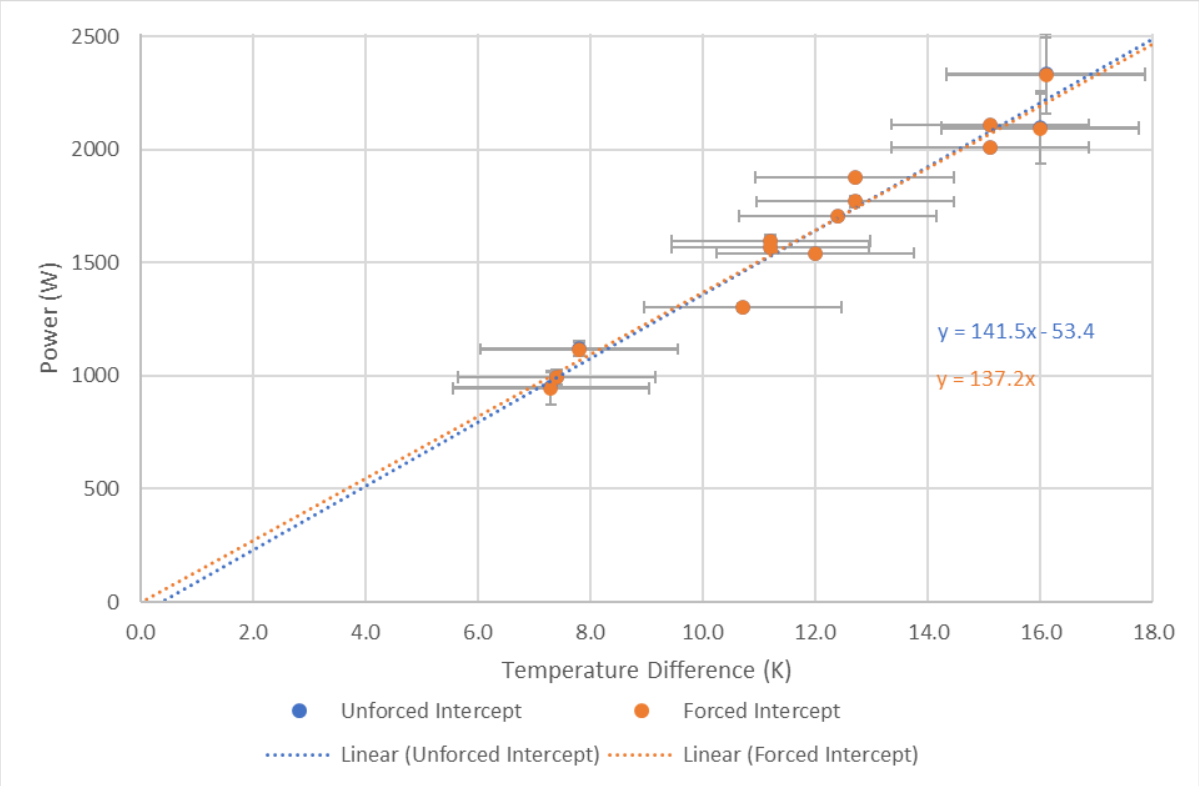


*Figure 4.6 Solar corrected power plotted against temperature difference comparing the regression lines being forced and unforced through the origin*

Despite this minor difference, and as explained in section 3.5.4.2, the value of the measured HTC determined from the regression line forced through the origin has been used in this report, in accordance with the guidelines laid out by Bauwens and Roles, Jack et al. and Johnston et al. (Bauwens & Roels, 2014; Jack et al., 2018; Johnston et al., 2013).

### 4.1.3 Measured HTC and Performance Gap

*Figure 4.7* displays the as-built raw and solar corrected HTCs of the Zed House which were determined from data collected during the two-week co-heating test. These values are also displayed in *Table 4.1* along with their calculated uncertainties. It is worth noting, in *Table 4.1* and subsequent tables, that “k = 2” is a coverage factor and provides a level of confidence of approximately 95%.

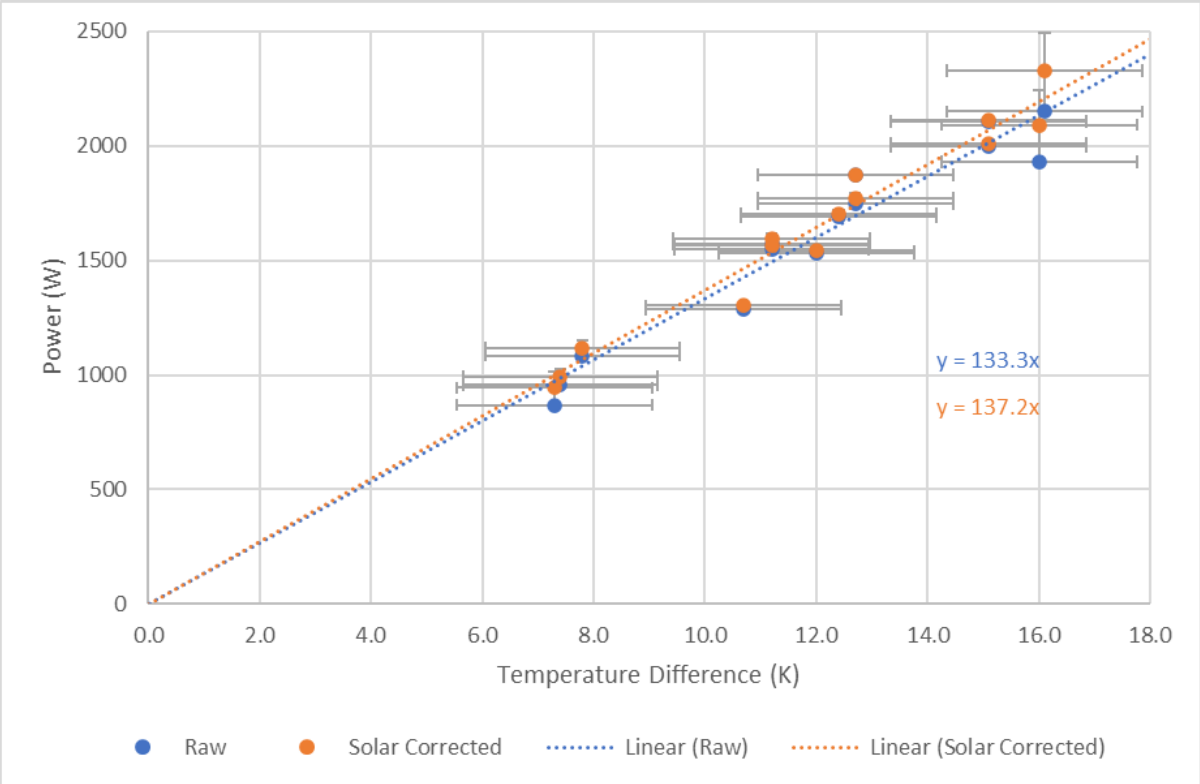


*Figure 4.7 The as-built raw and solar corrected powers plotted against temperature difference from the Zed House two-week co-heating test with the corresponding regression lines*

*Table 4.1 The calculated raw and solar corrected HTCs for the Zed House along with their calculated uncertainties (Note: k = 2 is a coverage factor and provides a level of confidence of approximately 95%)*

| | | | | *k = 2* | |
|---|---|---|---|---|---|
| *HTC Type* | *HTC ($W{\cdot}K^{-1}$)* | *Absolute Unc. ± ($W{\cdot}K^{-1}$)* | *Relative Unc. ± (%)* | *Absolute Unc. ± ($W{\cdot}K^{-1}$)* | *Relative Unc. ± (%)* |
| Raw | 133.3 | 8.7 | 6.6 | 20.0 | 15.0 |
| Solar Corrected | 137.2 | 5.3 | 3.9 | 12.2 | 8.9 |

In comparison to the calculated design (fabric and ventilation) HTC of 105.5 $W{\cdot}K^{-1}$, the as-built, or measured, HTC of 137.2 ± 12.2 $W{\cdot}K^{-1}$ is 31.7 $W{\cdot}K^{-1}$ higher, creating a performance gap between the design and as-built HTCs of 30%. On the other hand, the Zed House as-built HTC presents a 44.0 $W{\cdot}K^{-1}$ (24%) improvement on a dwelling of similar form, built to achieve the minimum requirements set out in AD L1a 2016 (The National Archives, 2016), meaning it performed better than the minimum standard dictated by building regulations at the time of construction. *Table 4.2* breaks down the individual heat loss components and their contributing performance gaps. The design fabric heat loss was determined from the design thermal bridging heat loss and the plane element heat loss (calculated from the design U-values). The design ventilation heat loss was calculated using the design air change rate at 50 Pa from the Zed House SAP document (discussed in more detail in the next section). Combining the design fabric and ventilation heat losses gave a value of the total design heat loss (HTC). The measured ventilation heat loss was then calculated (also discussed in the next section) and subtracted from the measured HTC to give the measured fabric heat loss. The measured ventilation and measured fabric heat losses contributed 8.3 $W{\cdot}K^{-1}$ (26%) and 23.4 $W{\cdot}K^{-1}$ (74%), respectively, to the design performance gap. The following sections in this chapter investigate the fabric and ventilation performance of the Zed House, looking at the outcomes of airtightness testing, U-value measurements, and thermography.

*Table 4.2 The fabric, ventilation and combined fabric and ventilation design and measured heat losses and their corresponding percentage performance gaps*

| *Heat Loss* | *Design ($W{\cdot}K^{-1}$)* | *Measured ($W{\cdot}K^{-1}$)* | *Performance Gap (%)* |
|---|---|---|---|
| Fabric | 86.7 | 110.1 ± 0.1 | 27.0 ± 0.01 |
| Ventilation | 18.7 | 27.1 ± 0.1 | 44.5 ± 0.1 |
| Fabric + Ventilation | 105.5 | 137.2 ± 5.3 | 30.1 ± 1.2 |

### 4.1.4 Air Permeability

Analysis of the results from the blower door test that was performed on the Zed House on Thursday 13th January 2022, revealed that the dwelling had an air permeability of 5.78 $m^3{\cdot}h^{-1}{\cdot}m^{-2}$ ± 0.3 %, and an air change rate at 50 Pa ($n_{50}$) of 5.81 $h^{-1}$ ± 0.3%[4]. This value of $n_{50}$ was then used to calculate n (the air change rate under normal conditions) of the Zed House.

[4] The uncertainties for the air permeability and air change rate at 50 Pa were taken directly from the Air Leakage Test Report, generated from the blower door test.

By employing the $n_{50}/20$ 'rule of thumb' and multiplying this by the Zed House's sheltered factor of 1 (determined from the assessment that the dwelling had no sheltered sides), the value known as n was calculated. The decision to use the $n_{50}/20$ 'rule of thumb' was made due to wanting to use a standardised, known method for repeatability. The rule was originally developed by (Kronvall, 1978) and (Persily & Linteris, 1983) when they were comparing infiltration rates that had been measured using a tracer gas method against results that had been gathered from carrying out a pressurisation test. Multiplying the value of n by the volume of the Zed House (282.2 $m^3$) and 0.33 $W{\cdot}h{\cdot}m^{-3}{\cdot}K^{-1}$ (the specific heat capacity of air, i.e., the energy (W·h) needed to raise one $m^3$ of air by 1 K) provided the measured ventilation heat loss of the Zed House. This was calculated to be 27.1 ± 0.1 $W{\cdot}K^{-1}$, (exhibited in *Table 4.2*).

Meanwhile, the design ventilation heat loss of the dwelling was established as 18.7 $W{\cdot}K^{-1}$ (also expressed in *Table 4.2* above), using the same calculation techniques described above, except using the design value of $n_{50}$ (4.0 $h^{-1}$) for the $n_{50}/20$ 'rule of thumb'.

The design ventilation heat loss was 8.4 $W{\cdot}K^{-1}$ less than its as-built equivalent, showing that the as-built ventilation heat loss of the Zed House was approximately 31% more than the designed target.

Visual comparisons of the measured air permeability to the AD L1a 2016 maximum, as-built SAP design, and design target values, are represented in *Figure 4.8*.

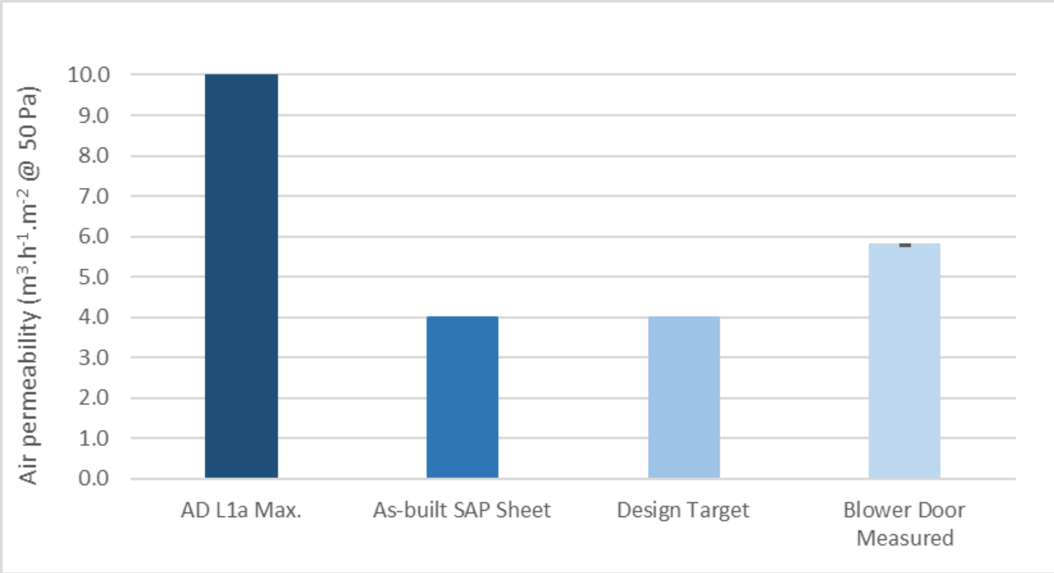


*Figure 4.8 Comparison of the measured air permeability of the Zed House to the design target, as-built SAP design and 2016 Part L1a maximum*

Multiple failures across the airtightness barrier of the Zed House were highlighted during the depressurisation phase of the blower door test with the use of IR thermography. Inadequate sealing of the cold roof space appeared to be the largest area for concern, along with the internal and external partition walls also being poorly sealed, which, by means of interconnected voids within the walls, intermediate floor, and service risers, allow for air movement and infiltration across both floors of the Zed House. These air paths result in heat loss from internal elements and have the potential to massively impact the U-values of external elements, as they allow for convective thermal bypassing of the thermal insulation layer. Some examples of these types of air movement and air infiltration points within the structure of the Zed House are demonstrated in the form of thermal images in *Figures 4.9-4.13*. However, it is worth noting that it was not always possible to fully identify air infiltration points and air paths within the structure using thermography due to the presence of second fix joinery, furnishings, and tiling.

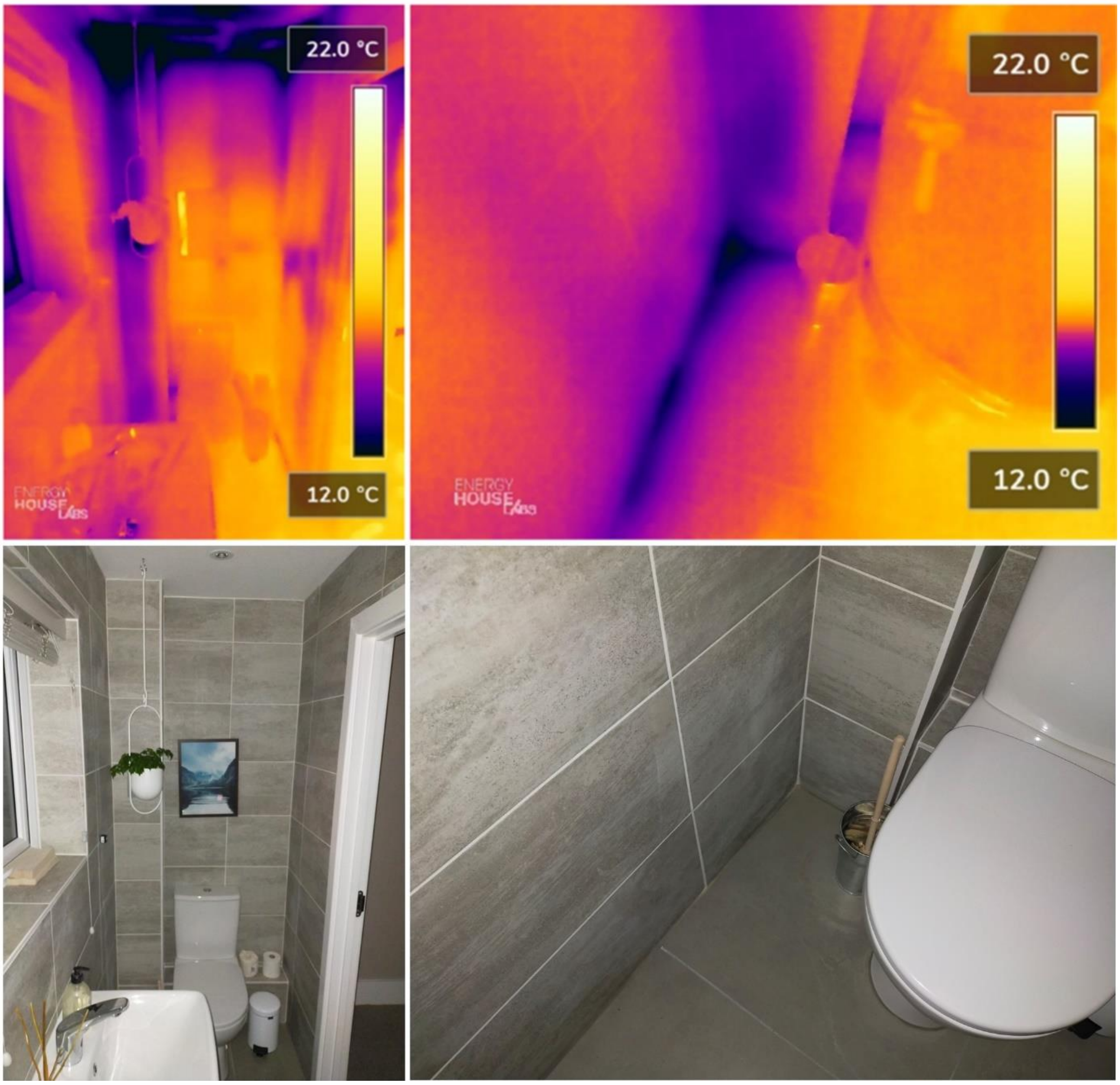


*Figure 4.9 Air movement within the SVP void in the first-floor bathroom (left) with some air infiltration evident at the interface between the void and intermediate floor (right)*


*Figure 4.10 Air movement possibly from the cold roof space into the SVP void in the kitchen on the ground floor. Air movement between the SVP void into the surrounding external wall and intermediate floor void was also evident.*


*Figure 4.11 Air movement from the cold roof space into the internal partition wall. Air infiltration into the habitable space was evident through the wall mounted services and at the junction with the intermediate floor (left and right). Direct air infiltration was evident around the loft hatch (left).*


*Figure 4.12 Examples of cold air movement from the loft space behind the plasterboard of the external (left) and internal (right) walls*


*Figure 4.13 Air infiltration was observed through closed trickle vents both prior to and during the blower door test (left). Air movement behind the plasterboard around the window and door was also revealed (left and right). Air infiltration into the dwelling from the door was revealed at the ground floor junction and through external wall mounted services via the plasterboard void (right).*

#### 4.1.5 In Situ U-Value Measurements

Five U-value measurements were taken between Tuesday 21st December 2021 and Tuesday 11th January 2022 across three locations: the kitchen, bedroom three and the study (see *Figures 4.14-4.16)*. These locations (which were determined from IR thermography), along with the element measured in each location are listed in *Table 4.3*, which then summarises and compares the measured U-Value of each element with their design and AD L1a 2016 maximum equivalents. The as-built absolute uncertainties are calculated using the ISO 9869-1 specification of 14% uncertainty (BSI, 2014).

As can be seen in *Table 4.3*, the as-built measurements taken at positions suggested by IR thermography that were representative of their corresponding element (HFPs 1, 2 and 4) were all within 0.04 $W{\cdot}m^{-2}{\cdot}K^{-1}$ of their design values and were also acceptably within the AD L1a 2016 maximums.

The in situ U-value measurements taken at locations showing disproportionate thermal bridging (HFPs 3 and 5) provide evidence that there were regions of the external walls and ceiling that exceeded both the design targets and the AD L1a 2016 limiting values. Increased thermal bridging, inconsistencies in the dwelling's insulation layer, and convective thermal bypassing were all possible contributors, whether individually or combined, to this lack of thermal consistency across the external walls and roof of the Zed House, which was also highlighted during the thermographic survey conducted prior to the blower door test. Examples of these thermal inconsistencies observed on the external walls and roof are provided in *Figure 4.17*.

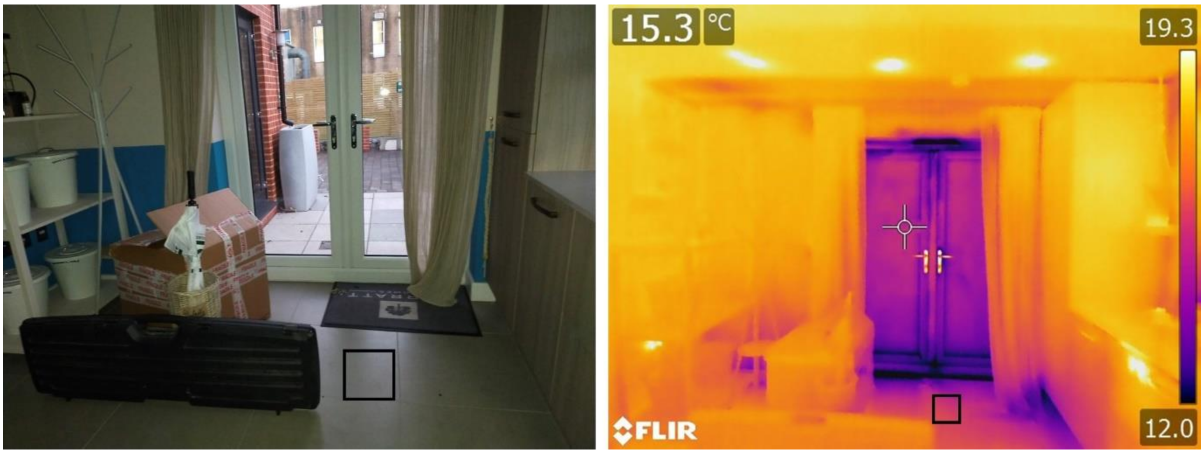


*Figure 4.14 The heat flux plate location on the kitchen floor. Unfortunately, these images were taken after the removal of the HFP*


*Figure 4.15 The locations of the two HFPs on the bedroom 3 wall. Unfortunately, the thermal image was taken after the removal of the HFPs*


*Figure 4.16 The location of the HFPs on the study ceiling. The thermal image was taken using a Flir iOS device attachment*

*Table 4.3 The location of each heat flux plate placed in the Zed House, the element they were measuring and the corresponding as-built, design and AD L1a 2016 maximum U-values*

| | | | *U-Value ($W{\cdot}m^{-2}{\cdot}K^{-1}$)* | | |
|---|---|---|---|---|---|
| *HFP* | *Room* | *Element* | *As-built* | *Design* | *L1a Maximum* |
| 1 | Kitchen | Floor | 0.19 ± 0.03 | 0.15 | 0.25 |
| 2 | Bedroom 3 | Wall - Cladding | 0.22 ± 0.03 | 0.20 | 0.30 |
| 3 | Bedroom 3 | Wall - Cladding | 0.31 ± 0.04 | 0.20 | 0.30 |
| 4 | Study | Ceiling | 0.11 ± 0.02 | 0.09 | 0.20 |
| 5 | Study | Ceiling | 2.79 ± 0.39 | 0.09 | 0.20 |


*Figure 4.17 Thermography under no artificially induced pressure differential. Thermal inconsistency was observed on a region of the external wall (left) and across the first-floor ceiling (right).*

## 4.2 The Performance of the Zed House Model in DesignBuilder during the Simulated Co-heating Test

### 4.2.1 HTCs from the Simulated Co-heating Test

The simulations were carried out on a model built using design-based U-values and the measured air change rate determined from the blower door test. Despite the internal thermal envelope temperature of the DesignBuilder Zed House model being set to 21°C in the co-heating simulation, it was found that when the simulation was run there were two peaks in both the ground floor and first floor air temperatures, found in the later stages of the simulation, as well as a smaller peak in the ground floor temperature found approximately two thirds of the way though the two-week test period (see *Figure 4.18*). The most likely cause for these peaks was overheating caused by increased solar gains, shown in *Figure 4.19* where the peaks in temperature corresponded with larger peaks in solar irradiance. These peaks in solar irradiance also corresponded to larger dips in the power, demonstrated in *Figure 4.20*.

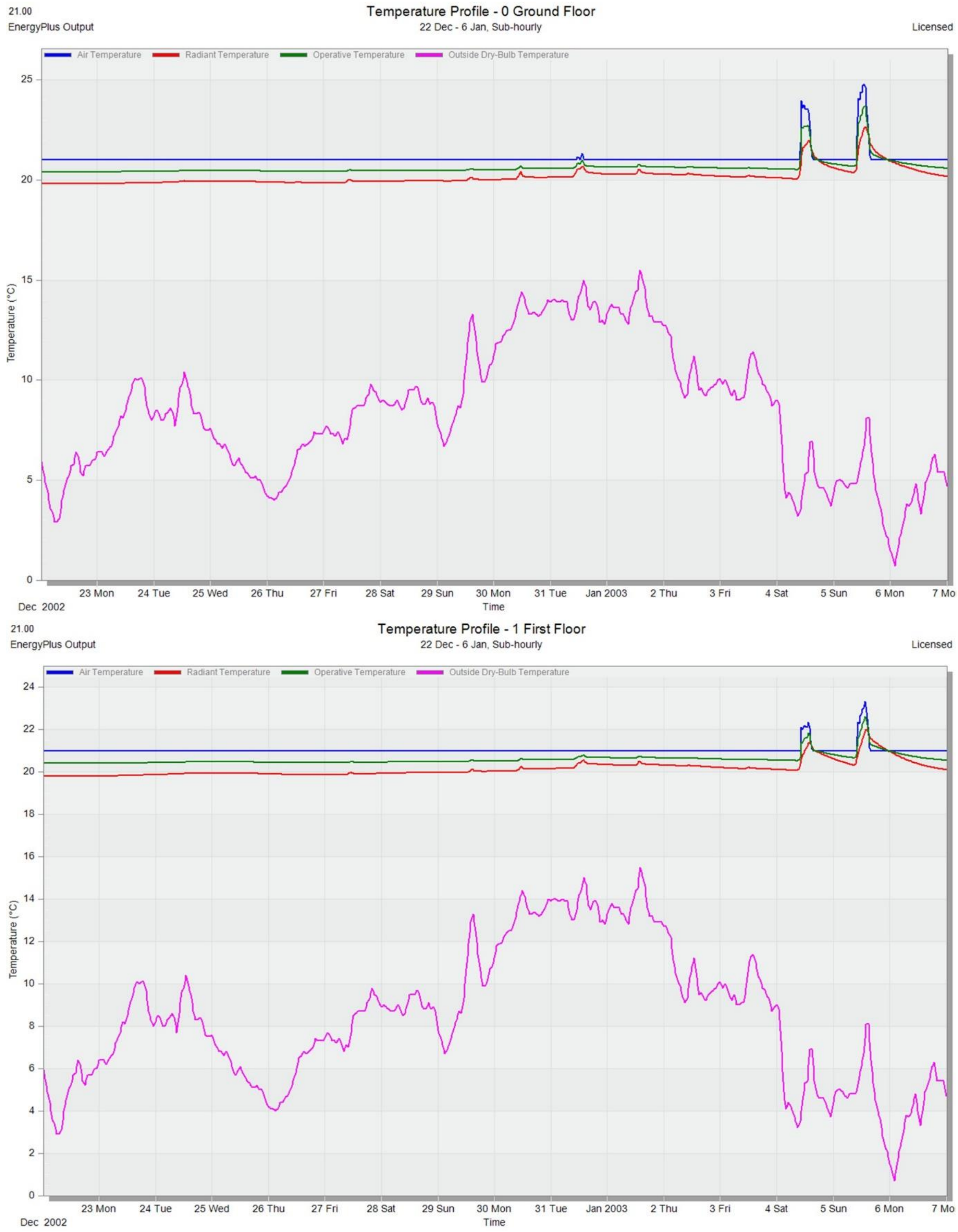


*Figure 4.18 The ground (top) and first floor (bottom) internal temperature profiles from the co-heating simulation performed in DesignBuilder. Note: Due to a quirk of DesignBuilder, all graphs are dated 2002, however the data used was from December 2021-January 2022*

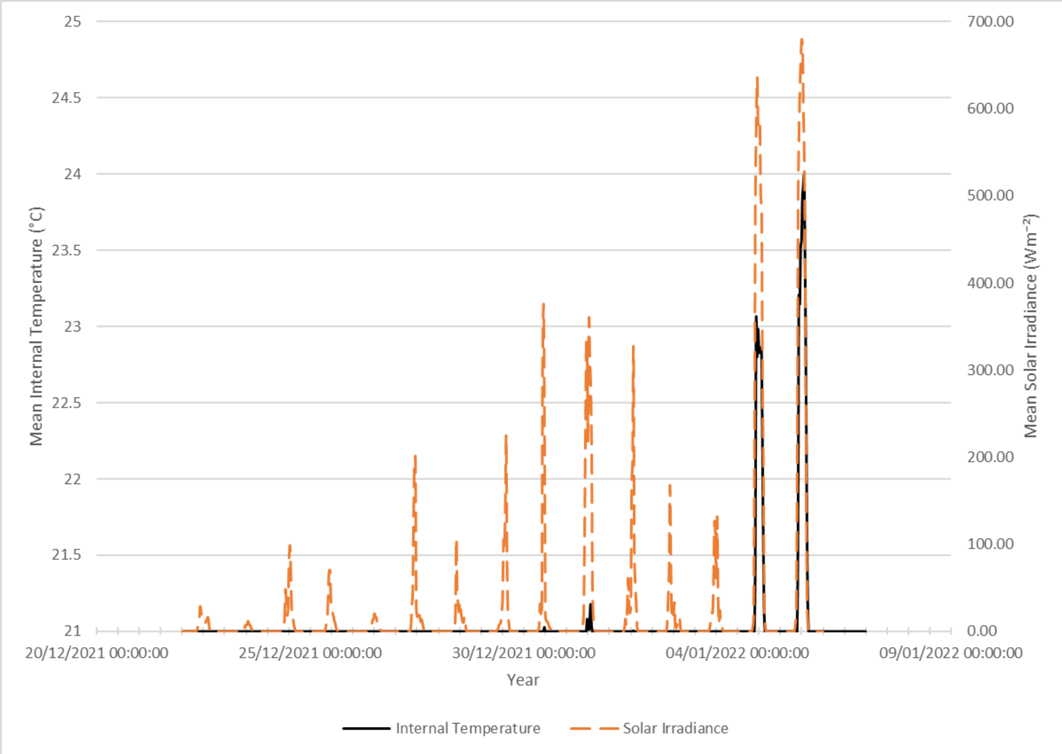


*Figure 4.19 Comparison between the mean internal temperature profile and mean solar irradiance profile over the two-week period from the co-heating simulation, with the temperature axis adjusted to allow for a clearer comparison*

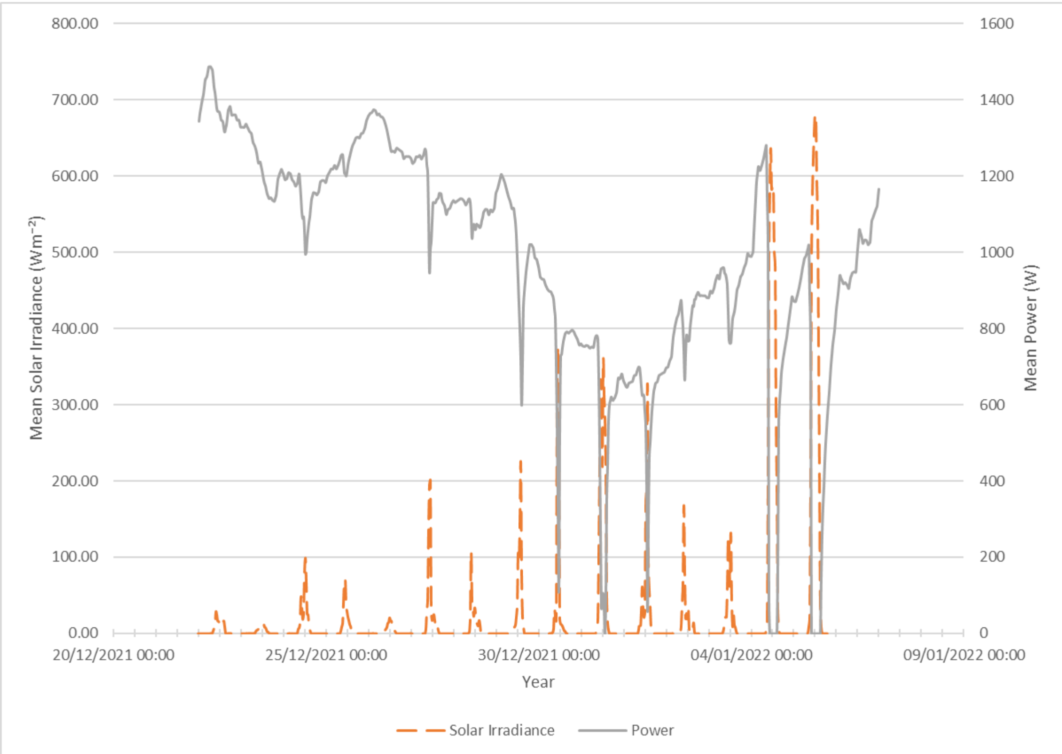


*Figure 4.20 Comparison between the mean solar irradiance profile and mean power profile over the two-week period from the co-heating simulation*

It was decided that analysis both accounting for, and discounting, this overheating would be undertaken in order to see how much of an impact the overheating had on the HTC derived from the simulated co-heating test.

Firstly, analysis of the data over the full two-week test period, from 23$^{rd}$ December 2021 00:00 - 6$^{th}$ January 2022 00:00, which accounted for the peaks in internal temperature, was conducted, resulting in the graph plotted in *Figure 4.21a*. The HTC for this set of data was calculated to be 93.6 ± 5.3 W·K$^{-1}$.

After this, analysis was performed over a twelve-day period between 23$^{rd}$ December 2021 00:00 - 4$^{th}$ January 00:00, therefore excluding the two larger peaks found on 4$^{th}$ January 2022 and 5$^{th}$ January 2022. This resulted in a calculated HTC of 88.4 ± 2.9 W·K$^{-1}$ as shown in the graph in *Figure 4.21b*.

Similar to this, a one-week period, between 23$^{rd}$ December 2021 00:00 - 30$^{th}$ December 2021 00:00, was analysed, which then excluded all values that did not equal 21°C. The calculated HTC from this analysis was 88.1 ± 6.1 W·K$^{-1}$ and *Figure 4.21c* shows the corresponding graph.

Finally, further analysis was conducted on the full two-week period, this time with all values of internal temperature set to 21°C, completely discounting the variations caused by overheating. It is accepted that, realistically, artificially setting the internal temperature to 21°C, whilst also using the same power and solar data, may not be helpful since only altering one factor that directly impacts the HTC would likely provide a misinterpretation of the dwelling's performance. However, despite this and despite overheating due to solar gains being something that is observed in co-heating tests, this was done to ensure that the small peaks in temperature were not as a result of how the model handled solar radiation. This produced an HTC of 93.3 ± 5.1 W·K$^{-1}$ which is shown in the graph displayed in *Figure 4.21d*.

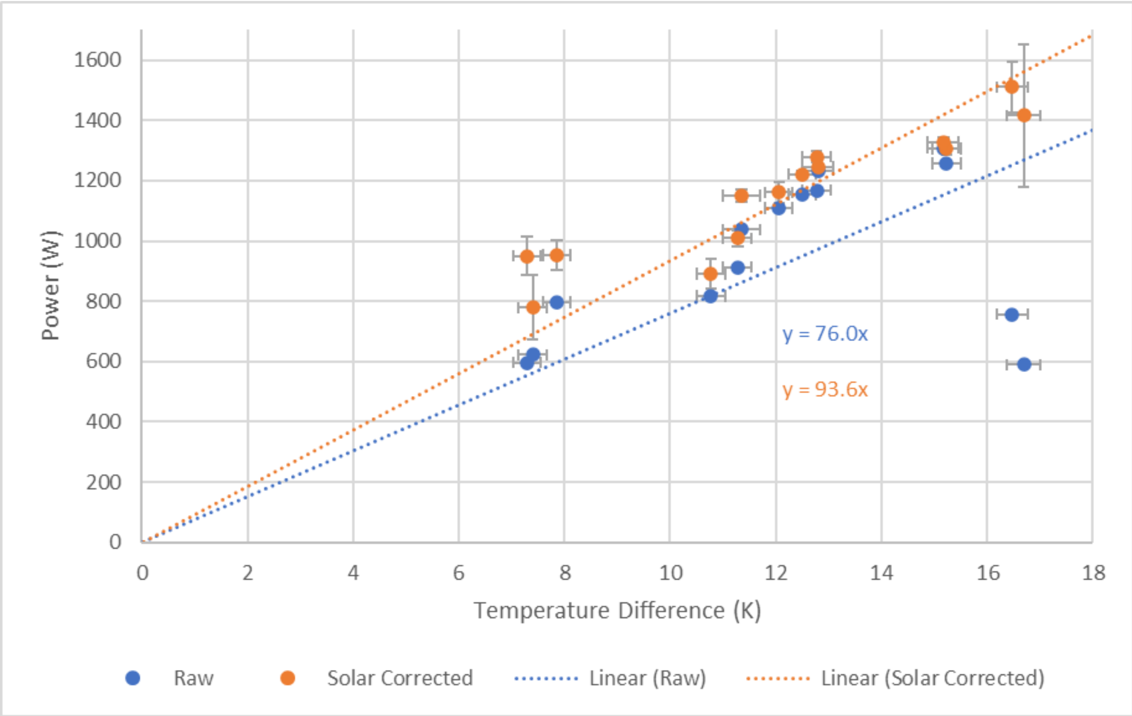


*Figure 4.21a The raw and solar corrected powers plotted against temperature difference for the full two-week period, accounting for the peaks in internal temperature*

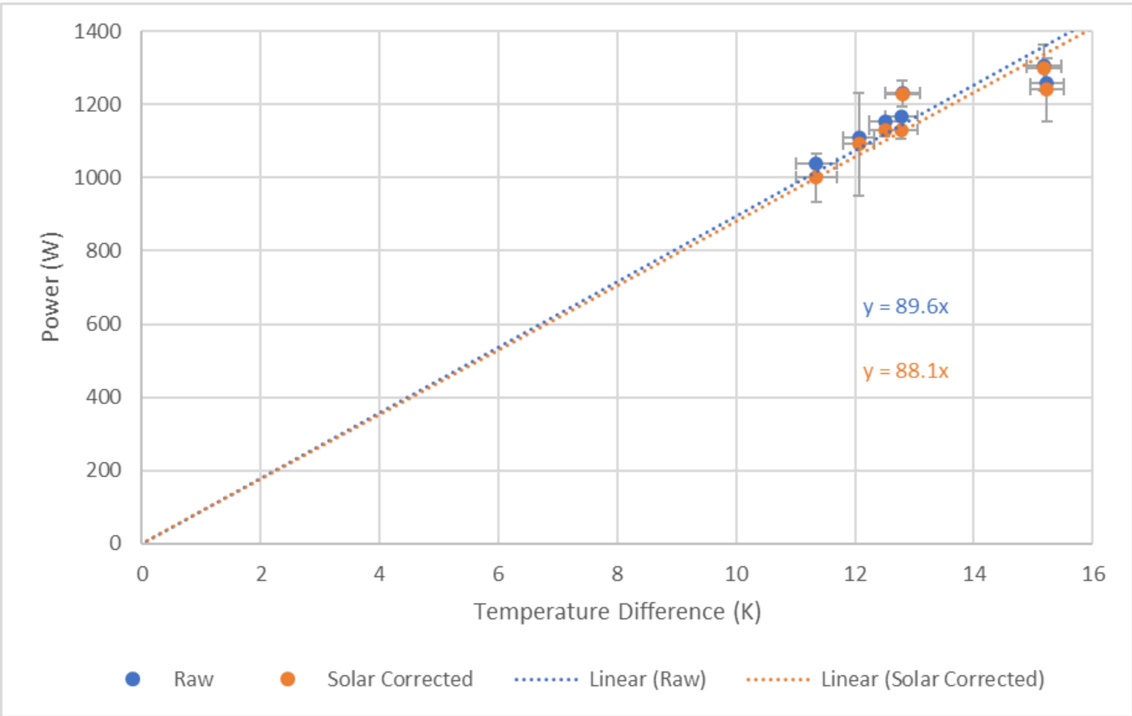


*Figure 4.21b The raw and solar corrected powers plotted against temperature difference for a one-week period, discounting the later peaks in internal temperature*

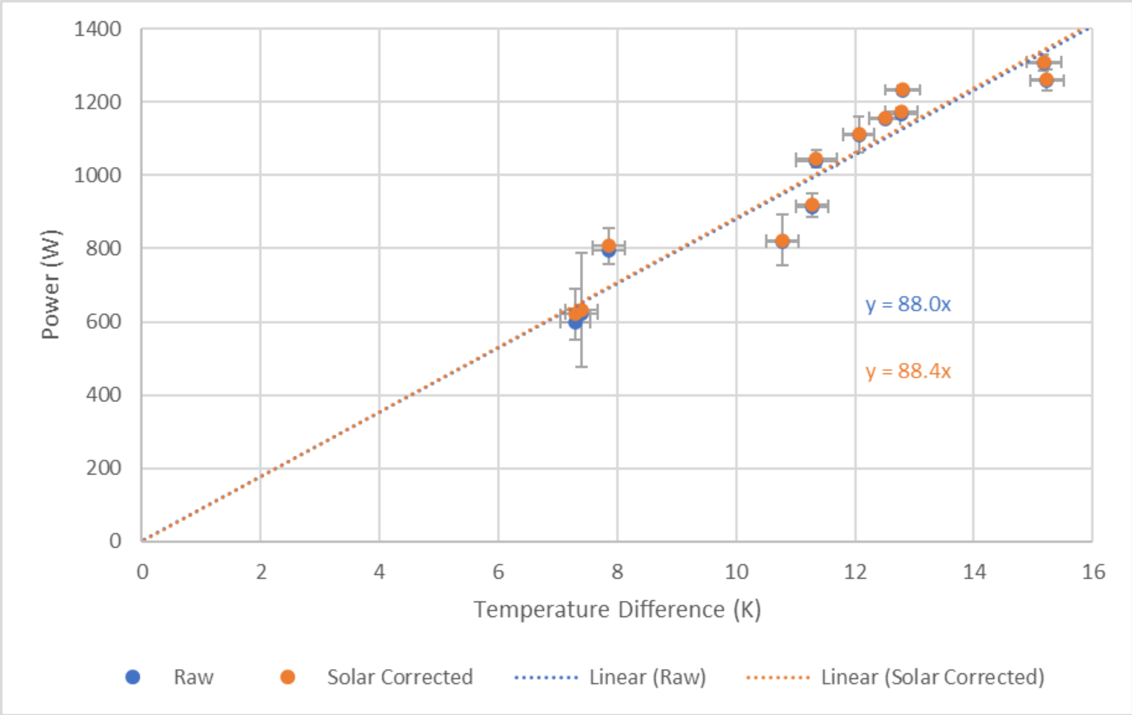


*Figure 4.21c The raw and solar corrected powers plotted against temperature difference for a twelve-day period, discounting the later peaks in internal temperature*

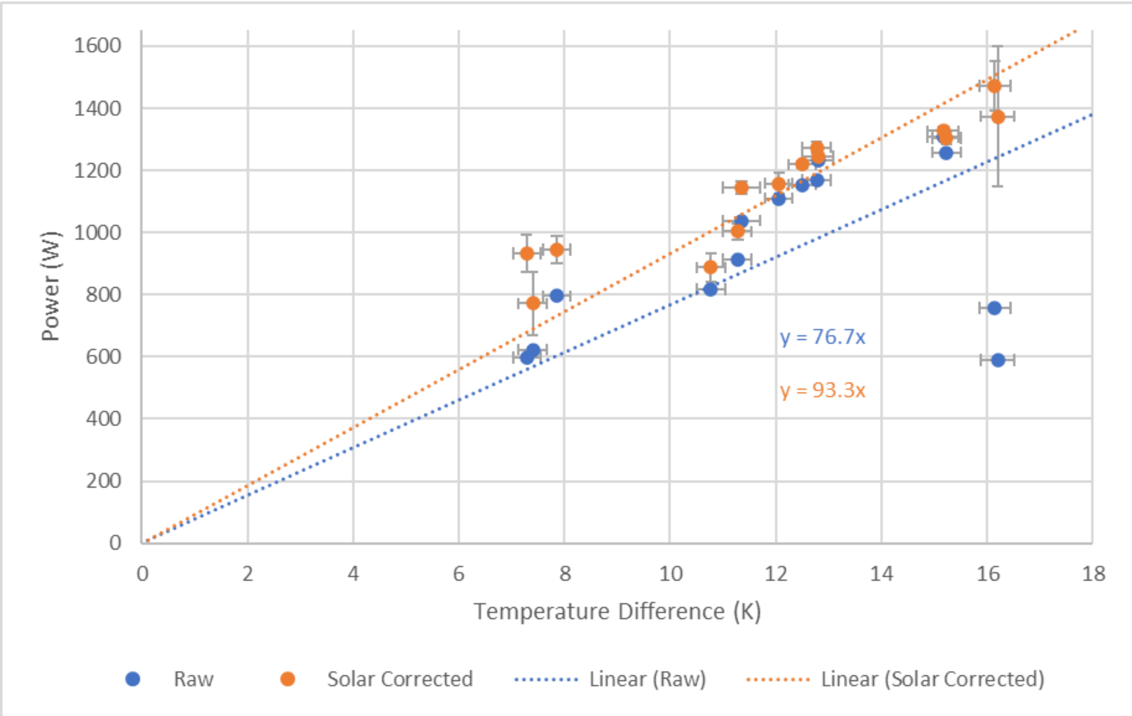


*Figure 4.21d The raw and solar corrected powers plotted against temperature difference for the full two-week period, with a set constant internal temperature of 21°C*

### 4.2.2 Comparison of the Simulated HTC to the As-Built, Design and Model Target HTCs

*Table 4.4* displays the HTCs calculated from the four different analyses discussed above compared to the calculated as-built and design/target HTCs of the Zed House, along with their respective absolute uncertainties.

*Table 4.4 The HTCs calculated from the four simulated co-heating analyses compared to the Zed House as-built and design/target HTCs*

| *Type* | *Period* | *HTC ($W \cdot K^{-1}$)* |
|---|---|---|
| Simulation | 2 Weeks | 93.6 ± 5.3 |
| | 12 Days | 88.4 ± 2.9 |
| | 1 Week | 88.1 ± 6.1 |
| | 2 Weeks (Int. T = Const. 21°C) | 93.3 ± 5.1 |
| As-Built | 2 Weeks | 137.2 ± 12.2 |
| Design | N/A | 105.5 |
| DesignBuilder Model Target | N/A | 92.8 ± 0.08 |

It is clear that the HTCs derived from the co-heating simulation were all significantly lower (up to 49.1 $W \cdot K^{-1}$, or 35.8%, lower at most) than the measured as-built HTC of 137.2 ± 12.2 $W \cdot K^{-1}$. However, this is to be expected, given that the DesignBuilder model was built using the Zed House design U-values, measured air change rate ($ac \cdot h^{-1}$) and excluding the thermal bridging heat loss (21.1005 $W \cdot K^{-1}$). As such, the simulated HTCs should be compared to the 'DesignBuilder model target'. This was calculated by summing the design fabric and measured ventilation heat losses (113.8 ± 0.08 $W \cdot K^{-1}$) and then deducting the non-repeating (linear) thermal bridging heat loss, resulting in a model target of 92.8 ± 0.08 $W \cdot K^{-1}$. Comparison to the HTCs derived from the co-heating simulation showed good agreement with the model target, in particular the HTCs determined over both two-week periods. These particular two HTCs were very similar, consequently, any concerns the peaks in internal temperature may have caused, regarding how the model handled solar radiation, were disregarded. It was decided that the simulated HTC derived from the full two-week period, and inclusive of the peaks in temperature due to overheating (93.6 ± 5.3 $W \cdot K^{-1}$), would be used as the DesignBuilder baseline, especially given that overheating is something that can be observed in co-heating tests. This value was 43.6 $W \cdot K^{-1}$ (31.8 %) lower than the measured as-built HTC.

## 4.3 Results from the Alternative Method Simulations

### 4.3.1 Initial Findings

Initial analysis of the data sets revealed that the five-day and forty-eight-hour testing periods provided extremely varied results, often with high levels of uncertainty. An example of this is demonstrated in *Figure 4.22,* which displays all the HTC results for all the testing periods and aggregation intervals for the 2021 extreme day data set, compared to the simulated co-heating method baseline HTC of 93.6 ± 5.3 $W{\cdot}K^{-1}$. Given that the five-day and forty-eight-hour periods provided such varied results, with the most extreme of these possibly caused by overheating of the dwelling, these testing periods were disregarded for the remainder of the analysis. In addition, for the purposes of multiple linear regression, it was decided that a two-week testing period would provide a greater spread of results on which to carry out the analysis, therefore the two-week testing period was used for the remainder of the analysis.

Furthermore, up to this moment, the 06:00-06:00, midday-midday and 18:00-18:00 aggregation intervals had been considered as a point of interest, in the same way similar intervals were used in the NHBC Report (Hulme & Doran, 2015). However, after plotting the data, such as is shown in *Figure 4.22*, these intervals were disregarded as they produced irregular results and also occurred after sunrise (during UK summertime) and thus may have resulted in skewed results due to the dwelling absorbing more solar radiation before it had re-emitted the solar radiation it had absorbed the day before. Therefore, only the midnight-midnight and dawn-dawn aggregation intervals were considered for the analysis of the other data sets.

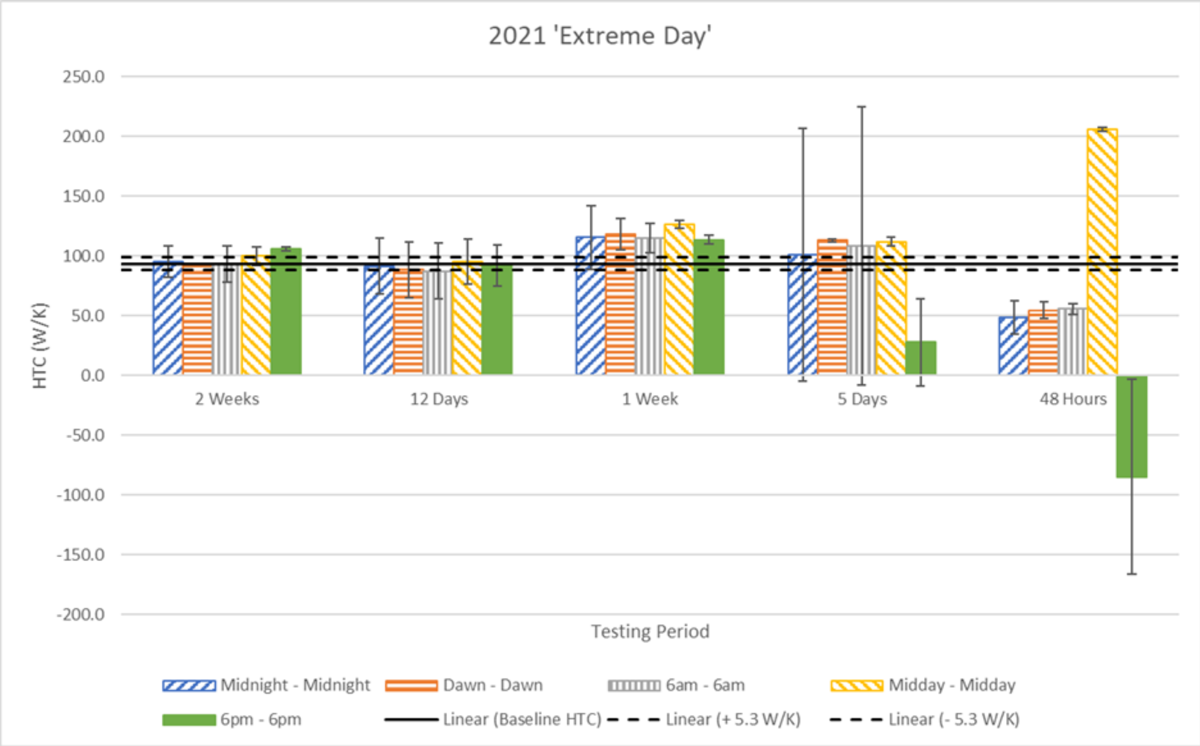


*Figure 4.22 Comparison of all the HTC results from the various testing periods and aggregation intervals for the 2021 extreme day data set*

### 4.3.2 Selecting the Most Appropriate HTC

In order to decide which HTC from the simulated alternative method would be the most appropriate to compare to the simulated baseline HTC of 93.6 ± 5.3 $W{\cdot}K^{-1}$, particular protocols had to be considered.

Firstly, for the co-heating method it is important that the majority of the heat flow through the dwelling during testing is from the internal environment towards the external environment. This is achieved by having a sufficient temperature difference such as 10 K. For similar reasons, except in reverse, it would have been preferable to achieve a 10 K temperature difference whilst performing the alternative method. However, given that the minimum internal temperature that could reasonably be achieved inside the dwelling was 16°C, the 10 K temperature difference was much harder to achieve and maintain with UK summertime temperatures. This was not ideal, however, in the interest of determining whether the method could possibly be applied in the UK during summertime months, analysis was still carried out, with any data sets that provided a negative temperature difference being disregarded as cooling was not occurring during these periods, such as the example shown in *Figure 4.23,* which comes from the 2019 average data set. As expected, it was found that all the average data sets were unusable as they all provided negative temperature differences, due to the fairly low UK summertime average temperatures. Overall, 67% of the total data sets were disregarded for due to this stipulation.

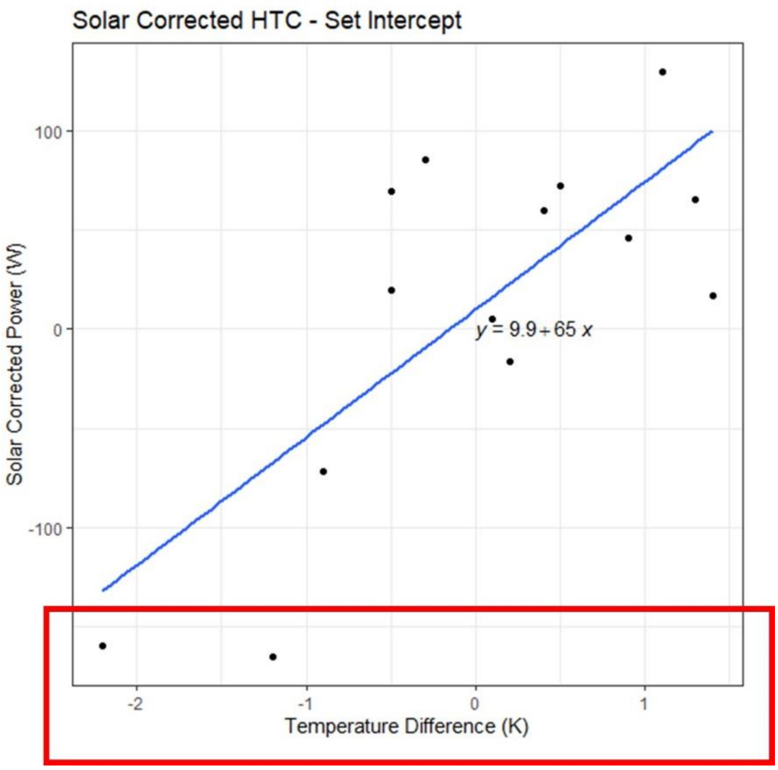


*Figure 4.23 An example of a negative temperature difference taken from the 2019 average data set*

Secondly, the statistical results from carrying out the multiple linear regressions on the remaining data sets were examined. Any data sets that provided a p-value greater than 0.05 were ignored as this indicated that the results were statistically invalid, shown in *Table 4.5*.

*Table 4.5 The temperature and solar coefficient t- and p-values for the remaining data sets*

| | | | *t-value* | *p-value* |
|---|---|---|---|---|
| Midnight-Midnight | 2021 Extreme Average | Temp. Coeff. | 6.413 | 0.000 |
| | | Solar Coeff. | 9.498 | 0.000 |
| | 2020 Extreme[5] | Temp. Coeff. | 4.687 | 0.001 |
| | | Solar Coeff. | 9.597 | 0.000 |
| | 2018 Extreme Day | Temp. Coeff. | 2.309 | 0.040 |
| | | Solar Coeff. | 8.538 | 0.000 |
| | 2018 Extreme Average | Temp. Coeff. | 0.876 | 0.398 |
| | | Solar Coeff. | 8.501 | 0.000 |
| Dawn-Dawn | 2021 Extreme Average | Temp. Coeff. | 7.465 | 0.000 |
| | | Solar Coeff. | 11.661 | 0.000 |
| | 2020 Extreme | Temp. Coeff. | 5.812 | 0.000 |
| | | Solar Coeff. | 11.042 | 0.000 |
| | 2018 Extreme Day | Temp. Coeff. | 2.43 | 0.032 |
| | | Solar Coeff. | 9.008 | 0.000 |
| | 2018 Extreme Average | Temp. Coeff. | 1.113 | 0.288 |
| | | Solar Coeff. | 9.427 | 0.000 |

In addition, any data sets that did not have a sufficient spread of temperature difference data (i.e., a spread less than 5 K), or were skewed, were also ignored, see *Table 4.6*. A good spread in data is necessary for regression analysis because it is important to have representative data that shows how the dependent variable changes with the independent variable(s). A data set that is small and/or skewed does not provide representative information of how one variable varies with the other. None of the remaining data sets presented skewness, with the highest level of skewness being 0.5. Despite having almost completely symmetric skewness, as displayed in *Table 4.6*, the spread in temperature difference data for the 2018 extreme day data set was small and may not have provided representative data for the regression analysis, therefore this data set was disregarded.

[5] The 2020 extreme day and extreme average periods were identical (5$^{th}$-18$^{th}$ August 2020) and therefore, for conciseness, were described as '2020 extreme'.

*Table 4.6 The spread, standard deviation and skewness in temperature difference data for the remaining data sets*

| | | ΔT | | |
|---|---|---|---|---|
| | | *Spread (°C)* | *Std. Dev* | *Skewness* |
| Midnight-Midnight | 2021 Extreme Average | 6.2 | 2.1 | 0.2 |
| | 2020 Extreme | 6.8 | 2.2 | 0.4 |
| | 2018 Extreme Day | 2.9 | 1.1 | -0.2 |
| Dawn-Dawn | 2021 Extreme Average | 6.1 | 2.1 | 0.2 |
| | 2020 Extreme | 6.6 | 2.1 | 0.5 |
| | 2018 Extreme Day | 3.3 | 1.0 | -0.1 |

Next, any collinearity between the independent variables in the remaining data sets was taken into account. If the independent variables (temperature difference and solar irradiance in this case) were correlated, the precision on the estimated coefficients from the multiple linear regression would be much lower. Inputting the 'VIF()' function into R Studio for the remaining data sets provided their corresponding Variance Inflation Factor (VIF), a value that measures how much correlation there is between the independent variables in the regression model. If the VIF has a value of 1 then the independent variables are not correlated. VIFs between 1 and 5 show moderate correlation but not serious enough to require further attention. A VIF over 5 shows that the independent variables are more highly correlated, and a VIF greater than 10 shows that there is severe collinearity (Glen, 2015). The data set with the greatest VIF over 5 was disregarded as demonstrated in *Table 4.7*.

*Table 4.7 The VIF values, signifying any collinearity, for the remaining data sets*

| | | *VIF (Collinearity)* |
|---|---|---|
| Midnight-Midnight | 2021 Extreme Average | 5.1 |
| | 2020 Extreme | 5.5 |
| Dawn-Dawn | 2021 Extreme Average | 4.8 |
| | 2020 Extreme | 5.3 |

After following these protocols and filtering the data sets accordingly, one data set remained (2021 extreme average), with both midnight-midnight and dawn-dawn aggregation interval results, shown in *Table 4.8*. Despite having a slightly higher percentage uncertainty it was decided that the result from the dawn-dawn aggregation interval should be used, as by this time of the day the dwelling would have had sufficient time to re-emit any solar radiation it had absorbed during the previous day. When analysing the data from a co-heating test, often a midnight-midnight aggregation interval would be used, since co-heating tests are performed during the ‘heating season’ when days are much shorter and there would be sufficient time between dusk and midnight for the dwelling to re-emit any absorbed solar radiation. In the summertime, days are much longer meaning the length of time between dusk and midnight is shorter and, therefore, would possibly not give the dwelling enough time to re-emit absorbed solar radiation. The dawn-dawn aggregation interval, on the other hand, would provide additional time for this to occur.

The final HTC value that best fitted the particular protocols considered was therefore 96.8 ± 12.7 $W{\cdot}K^{-1}$. This value came from the 2021 extreme average data set which occurred from 13$^{th}$ July up to, and including, 26$^{th}$ July 2021. The corresponding plot of raw and solar-corrected powers against internal-external temperature difference is displayed in *Figure 4.24*.

*Table 4.8 The midnight-midnight and dawn-dawn HTCs for the 2021 extreme average data set, along with their percentage uncertainties, solar coefficients (solar apertures ($m^2$)) and deviation from the baseline HTC 93.6 ± 5.3 $W{\cdot}K^{-1}$*

| | *HTC ($W{\cdot}K^{-1}$)* | *Solar Coefficient* | *Deviation from Baseline (%)* |
|---|---|---|---|
| Midnight-Midnight | 100.2 ± 11.9 | 2.1449 | 7.0 |
| Dawn-Dawn | 96.8 ± 12.7 | 2.2008 | 3.4 |

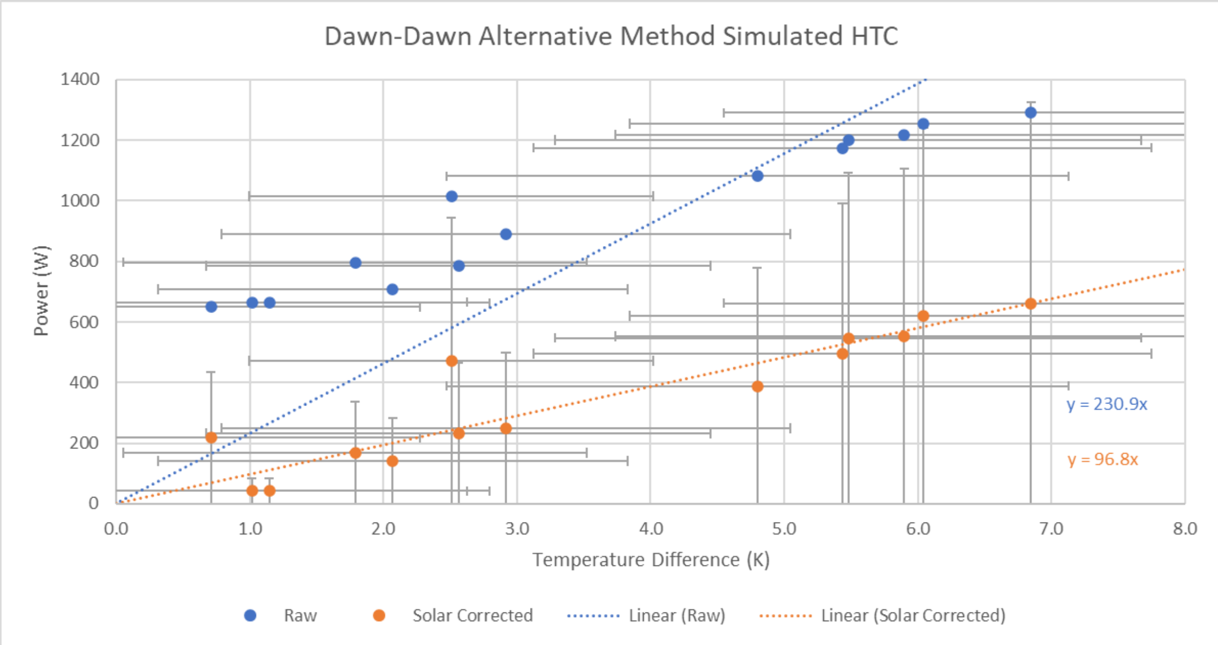


*Figure 4.24 A graph of the raw power and solar corrected power plotted against temperature difference for the dawn-dawn aggregation period from the 2021 extreme average data set, with the corresponding regression lines forced through the origin*

### 4.3.3 Comparison of the Simulated Alternative Method HTC to the Simulated Baseline, Model Target and As-Built HTCs

*Table 4.9* compares the simulated alternative method HTC with the simulated baseline co-heating method and design HTCs. When uncertainty is taken into account, the HTC from the alternative method simulation falls within the upper and lower boundaries of the baseline, as well as showing quite close agreement with the Zed House model target HTC. The simulated alternative method HTC does fall short of the as-built HTC, however, this is not a reasonable comparison to make, given that the model was not built using only measured values.

*Table 4.9 The Zed House simulated alternative method HTC compared to the Zed House simulated baseline, model target and as-built HTCs*

| *Simulated Alternative Method HTC (W·K$^{-1}$)* | *Simulated Baseline Co-heating HTC (W·K$^{-1}$)* | *DesignBuilder Model Target HTC (W·K$^{-1}$)* | *As-Built HTC (W·K$^{-1}$)* |
|---|---|---|---|
| 96.8 ± 12.7 | 93.6 ± 5.3 | 92.8 ± 0.08 | 137.2 ± 12.2 |

### 4.3.4 Simulating the Alternative Method in a Different Climate

Following the protocols that should be considered when analysing the data sets from the alternative method revealed that many data sets were unusable due to having negative temperature differences. This came about as a result of UK summertime temperatures not being able to achieve suitable temperature differences when the minimum reasonable internal temperature that could be achieved was 16°C.

As such, the possibility of changing the climate to one that might be more applicable (i.e., one that would be able to achieve larger temperature differences) around the Zed House was explored. (Law & Wong, 2020) have previously shown that the co-heating method is not always effective in Australia, more so in more northern territories and cities. A few of the cities they investigated were Darwin, Brisbane and Perth and of these three cities, Darwin was found to produce poor HTC results throughout the whole year, whilst Brisbane and Perth showed some better, though inaccurate or unreliable, results as well as poor results. Since these cities provided a mix of results for the co-heating test, it was contemplated whether the alternative method may perform better in these cities and their respective climates.

DesignBuilder has pre-loaded 'default' weather files for many cities and areas around the world which comes from the EnergyPlus hourly weather database. This database is predominantly comprised of real weather data which has been gathered, often with data coming from months from more than one year, to create representative weather data files for each location (DesignBuilder Software Ltd, 2022). Unfortunately, it had not been possible to use these for the UK summertime simulations as the closest data file location to Salford, or indeed Manchester, was Aughton - approximately 26 miles away. However, it was possible to use DesignBuilder weather files for Darwin, Brisbane and Perth. Since this was a short additional investigation to see if the alternative method may perform better in a different climate, only one two-week period for each city was simulated over: 23$^{rd}$ December 2021-6$^{th}$ January 2022. Since summer in Australia occurs approximately at the same time as the UK winter, it made sense to use the same time period that had been used for the baseline co-heating test, resulting in the simulation using the same dwelling model, method and time period, but a different climate.

*Table 4.10* displays the results of the three Australia-based alternative method simulations, which used dawn-dawn aggregation intervals in order to try and minimise the impact of solar radiation on the dwelling. Darwin and Brisbane both had very high HTCs, whereas Perth had a much lower HTC in comparison. Darwin had the smallest spread in temperature difference data but had the largest average temperature difference. Meanwhile, Brisbane had a slightly larger spread in temperature difference data but a smaller average, whilst Perth had the largest spread out of the three and the smallest average. It is also worth noting that, despite having the smallest absolute uncertainty, Brisbane’s temperature difference data was moderately skewed, which would likely be a contributing factor to the high HTC.

*Table 4.10 The HTCs along with the average solar irradiances and temperature differences, as well as the spreads, standard deviations and skewness of the temperature difference data, from the alternative method simulations carried out in the three Australian cities*

| | | | *ΔT* | | | |
|---|---|---|---|---|---|---|
| | *HTC ($W·K^{-1}$)* | *Average Solar ($W·m^{-2}$)* | *Average (°C)* | *Spread (°C)* | *Std. Dev.* | *Skewness* |
| Darwin | 163.7 ± 80.7 | 211.7 | 11.8 | 4.6 | 1.490228 | -0.19687 |
| Brisbane | 183.5 ± 16.0 | 283.8 | 8.2 | 5.1 | 1.408413 | -0.88509 |
| Perth | 81.8 ± 19.1 | 357.6 | 5.9 | 7.0 | 2.321855 | -0.41676 |

Further statistical analysis results from carrying out multiple linear regressions on the three data sets are presented in *Table 4.11*. Both Darwin and Brisbane have p-values greater than 0.05 showing that their results are not statistically valid. In addition, the independent variables for the Darwin and Brisbane data sets were severely collinear, and therefore their results should actually be disregarded. Of the three data sets, whilst the independent variables are still quite highly correlated and should be further investigated, the results for Perth are statistically valid.

*Table 4.11 The temperature and solar coefficient p-values, along with the VIFs for the HTCs from the alternative method simulation in each of the three cities*

| | *p-value* | | |
|---|---|---|---|
| | *Temp. Coeff.* | *Solar Coeff.* | *VIF (Collinearity)* |
| Darwin | 0.001 | 0.948 | 114.4109 |
| Brisbane | 0.000 | 0.855 | 34.81943 |
| Perth | 0.000 | 0.000 | 7.005 |

These results begin to show that even in a climate that is generally warmer than the UK summertime, the proposed alternative method still has difficulty performing well. In hotter, summer months, collinearity may be more likely, as hotter days could be associated with more sunny days, although this would have to be investigated properly. High levels of solar irradiance in the summer months, compared to winter months, clearly has some level of impact on the alternative method's performance, despite blinds and curtains in the dwelling being closed and a dawn-dawn aggregation interval being used to try and minimise the solar radiation impact.

## Chapter 5

# Implications

### Chapter Overview

This chapter explores the implications of the research and consists of the following sections:

- **5.1 The Alternative Method Overall**: considers the overall potential for the alternative method to work and fill the gap in current research.
- **5.2 Limitations Caused by External Elements**: discusses the similarities between the alternative method and the co-heating method through the limitations they experience caused by external elements.
- **5.3 Practical Barriers and Their Implications**: identifies the practical barriers that would impact the use of the alternative method in a real-world environment.

## 5.1 The Alternative Method Overall

At present, there are no recognised methodologies that are suited to determining the HTC of dwellings in warmer climates, particularly by way of cooling. Therefore, the initial proposal of an alternative method presented in this thesis looks to begin to fill this gap. Despite the alternative method being carried out through DesignBuilder simulations, the DesignBuilder model was backed by as-built and design data: design U-values (due to a lack of representative in-situ U-values), measured as-built air permeability and real weather data uploaded into weather files. Testing of the alternative method on the Zed House in a simulated environment showed that the principle of cooling a dwelling (or a reverse co-heating test) has the potential to determine the HTC of that dwelling when modelled. Though the simulated co-heating and alternative method HTCs both fell short of the as-built HTC, this difference can be accounted for due to the DesignBuilder model using design values as well as measured ones. Given how close to the simulated co-heating HTC the alternative method HTC is, it is likely that, if the simulations were run on the same model built entirely using as-built measurements, they would fall much closer to the as-built HTC of the Zed House.

## 5.2 Limitations Caused by External Elements

The alternative method is similar to the co-heating method, except that cooling techniques are employed as opposed to heating techniques. As such, the alternative method faces the same limitations when it comes to the external elements. For example, ‘when’ the method is performed’ is limited to when it is possible to maintain a sufficient temperature difference. With the alternative method in its current form, the method does not seem to work particularly well in the UK summertime climate, and presumably would not work in countries with similar climates. This is due to the fact that, with the limitation of most common cooling systems being unable to reach temperatures below 16°C, being able to achieve internal temperatures that are consistently below the external temperatures throughout the test is difficult, demonstrated in section 4.3.2 where 67% of the total data sets were disregarded for this reason. In addition, the alternative method is also subject to the risk of collinearity. High levels of solar irradiance during the hotter summer months seemed to have some level of impact on the alternative method's performance, even though blinds and curtains on the Zed House model were kept drawn during testing. In summer months, sunnier weather is perhaps associated with hotter weather, potentially introducing a greater risk of collinearity, though this would have to be investigated properly. This risk of collinearity has the potential to be a much larger issue in areas that achieve higher temperatures and levels of solar radiation and as such, it is likely that a different way of analysing the data, accounting for this problem, would need to be undertaken. In order to minimise the impact of solar radiation on the dwelling, use of an appropriate aggregation interval is required (dawn-dawn in the case of the alternative method) so that any solar radiation stored in the building fabric has had sufficient time to be released before the following day. Moreover, testing over a two-week period would allow for a larger data set for analysis, as well as a mix of weather conditions. However, as with the co-heating method, this presents issues around having to remove the occupants from the dwelling or, if the dwelling is an unoccupied, newly built dwelling, for example, keeping that dwelling off the market.

## 5.3 Practical Barriers and Their Implications

Whilst not the main focus of the research presented in this thesis, some, though not thorough, investigation into cooling systems was also conducted, due to the need to establish a cooling system for the alternative method simulations. Despite not being an exhaustive study, this investigation also identified some practical barriers that may need to be considered before performing the alternative method in the field.

The alternative method requires the use of a cooling system. Cooling systems, such as the split system used for the alternative method simulations - which used the compression refrigeration cycle - have COPs greater than 1, i.e., energy in does not equal energy out, explained in section 2.6.3. Electric resistance heaters used for the co-heating method, on the other hand, have COPs equal to 1, making use of a cooling system for the alternative method much more complex. As mentioned previously in section 3.8.3, the cooling loads from the simulation were calculated using the EnergyPlus “Ideal Loads” system, which likely had a built-in error, and therefore may have resulted in an oversimplification in the cooling outputs. In reality, there would be both internal and external inefficiencies of the cooling system through fans, motors, etc. In addition, assuming the COP of the cooling system would also lead to inaccuracies because COPs can vary depending on the external conditions. Heat meters are often used to measure the energy of the liquid flowing through a system, such as air source heat pumps. However heat meters could also be used for monitoring cooling systems (Bell Flow Systems, 2022). As such, when the alternative method is applied in a real test environment, use of a heat meter could potentially aid in accounting for these issues.

Furthermore, the split system used for the alternative method simulations was not portable, unlike the electric heaters that are used for the co-heating method. However, for two reasons, it would seem that portable cooling systems would be unsuitable for the application of the alternative method.

Firstly, industrial portable cooling systems were considered at the very beginning of this research, when collating initial thoughts and ideas. As it transpired, costs of these systems varied from £500 up to £2000 from retailers, depending on factors such as cooling capacity (electriQ, 2022; Orion Air Conditioning and Refrigeration Ltd, 2022a, 2022b; pumpsdirect2u Ltd, 2022), whilst a company specialising in HVAC systems quoted just over £50000 to have a cooling system, that could cool the whole dwelling to approximately 10.0°C (± 1.0°C), specially designed and commissioned. These options were deemed impractical, cost-wise, for testing an initial proposal of an alternative method.

Secondly, during the alternative method, as with the co-heating method, all windows and vents in the dwelling need to be shut or sealed. Portable cooling systems generally have ducts which would need access to the outside environment - via an open window, for example - and therefore would breach the requirements of having the dwelling sealed. Although portable non-ducted systems are available, these would not fit the preference of a split system unit outlined in section 2.6.3.2.

Consequently, the alternative method may be better suited to dwellings with in-built cooling systems. According to (IEA, 2018), the use of air conditioning systems are becoming increasingly common in hotter regions around the world. Therefore, it may be possible that an ‘integrated’ or ‘on-board’ adaptation of the alternative method, similar to those presented in section 2.4.2.4, could be performed in dwellings in warmer climates which have built-in cooling systems. In Australia, there were approximately 9.8 million households in 2021 according to the Australian Institute Of Health and Welfare (Australian Institute of Health and Welfare, 2022). The IEA predicted that, during that year, there would be two air conditioning units per household on average (IEA, 2020). That equates to just under 20 million air conditioning units in Australia for households alone.

In the cases of the ‘on-board’ monitoring research presented by Allinson et al. and Senave et al., which were performed in cooler climates on occupied dwellings, any internal gains, such as use of lights, were added to the heating input to the dwelling for the regression analysis (Allinson et al., 2022; Senave et al., 2019). For the alternative method performed in warmer climates, internal gains would need to be removed from the cooling system’s output. Therefore, a way of separating the internal gains (such as lighting) and the cooling input from the smart meter data would be required for an ‘on-board’ adaptation of the alternative method. Sub-metering of the cooling system and other loads, alongside, ideally, use of a heat meter - due to uncertainty in the COP as well as determining additional heat gains from the system - would potentially allow for this disaggregation.

# Chapter 6

# Conclusions and Recommendations

## Chapter Overview

This chapter concludes the thesis, bringing together all the key information and findings from the research. The following sections form the basis of this chapter:

- **6.1 What the Research Has Achieved**: highlights what was carried out and the key findings of the research.
- **6.2 Limitations**: summarises the key limitations of the alternative method.
- **6.3 Further Research**: considers further research that could be carried out to address the limitations and continue the development of the alternative method.
- **6.4 Summary**: provides a final overall evaluation of the alternative method.

## 6.1 What the Research Has Achieved

Baseline as-built measurements of the Zed House, including its HTC through performing a co-heating test, were determined. The measured HTC of the Zed House was found to be 137.2 ± 12.2 $W{\cdot}K^{-1}$. Additionally, IR imaging revealed multiple failures across the airtightness barrier, with inadequate sealing of the cold roof space and external partition walls being the largest areas for concern, allowing for unwanted air movement and infiltration.

A model of the Zed House was then built in DesignBuilder, a modelling software which uses EnergyPlus to perform simulations. The Zed House model was built using its design U-values and as-built air change rate. Due to a lack of required information, thermal bridging heat loss could not be input to the model. Using measured external data from the as-built co-heating test and the same (or as close to) settings and equipment, another baseline co-heating test was then simulated on the Zed House model.

Occasional peaks in the internal temperature were revealed which were most likely due to overheating caused by solar gains. The HTC of the Zed House model was 93.6 ± 5.3 $W{\cdot}K^{-1}$ which was in good agreement with the calculated Zed House model target HTC (92.8 ± 0.08 $W{\cdot}K^{-1}$). Though the HTC of the model fell short of the as-built HTC, this was attributed to the fact that the model was built using a combination of design and measured values. It is possible that, if the model were built using only measured values, the HTCs would be much closer.

Following the baseline testing, an initial proposal of an alternative method was laid out. An investigation into air conditioning systems revealed that a split system would be best for the purposes of trialling the alternative method through simulations in DesignBuilder. Other factors such as weather conditions, testing periods and aggregation intervals were also considered and later investigated during the simulations and analysis.

Model data was input into DesignBuilder, with the internal temperature set to 16°C due to air conditioning system limitations. Fifteen sets of weather data covering three (extreme day, extreme average and average) temperature periods over five years, from 2017 to 2021, were compiled and used to create the weather files applied in the DesignBuilder simulations. The proposed alternative method simulation was then run in DesignBuilder using each of the weather files.

By considering particular protocols, such as spread in data, statistical validity and collinearity, the most appropriate HTC from the resulting data sets was selected. This HTC had a value of $96.8 \pm 12.7$ $W{\cdot}K^{-1}$, and came from the 2021 extreme average data set, using the dawn-dawn aggregation interval in order to minimise the impact of solar radiation on the dwelling. This value also had quite close agreement with the Zed House model target HTC.

Additional analysis was then carried out by simulating the alternative method on the Zed House model in three Australian climates: Darwin, Brisbane and Perth. Perth provided the only statistically valid HTC, although it still had a moderate level of collinearity, with a value of $81.8 \pm 19.1$ $W{\cdot}K^{-1}$. This value is very different to the HTC obtained using UK summertime weather data, which demonstrates the possible need for a different method of analysis when contending with higher levels of collinearity as seen with the Australian data.

## 6.2 Limitations

### 6.2.1 Research Limitations

#### 6.2.1.1 Experiment-Driven Limitations

Time constraints between the Zed House becoming unoccupied and the co-heating test being performed over the university's Christmas shutdown period, meant that a blower door test could not be undertaken on the dwelling prior to the co-heating test being set up. Only one week was available between the occupants vacating the dwelling and the two-week Christmas shutdown period, and this time was used to set up the Zed House and allow the temperatures in the house to become homogenous and ensure there was no temperature stratification. As a result of this, it was deemed that there was not enough time to perform a blower door test on the dwelling during this week, and so the blower door test was performed once the co-heating test was complete. Additionally, some of the thermal images taken during the blower door test may appear to be out of focus. Unfortunately, these were the best available from that test, despite trying to get the best image quality possible when taking the thermal images.

The equipment used during the co-heating test to collect external weather conditions was set up towards the end of the week prior to the Christmas shutdown. As such, data for that full week was not collected and, after a discussion, it was deemed more suitable to collect all the weather data for that week from Time and Date AS. Furthermore, solar radiation was measured horizontally as this was the only source available. Failure of the anemometer also meant that wind speed on site was not measured.

Whilst in situ U-value measurements were taken, these were limited due to the time constraints prior to the Christmas shutdown period as well as limited availability of heat flux plates as a result of other tests being run by the facility at the same time. The measurements that were taken were ultimately not deemed representative of the whole house, so that when it came to creating the Zed House model in DesignBuilder, the decision was made to use the design U-values from the Zed House SAP document instead. Additionally, some of the optical and thermal images indicating the locations of the HFPs were taken after the removal of the HFPs.

Further to this, the model construction details, presented in section 3.6.2, were completed as fully as they could be with the use of the details provided on the Zed House SAP documents. It is likely that these are not a completely exact representation of the as-built construction, however the model had to be built using the resources and information available at the time, whilst also applying a limited level of DesignBuilder experience.

Finally, as explained in section 3.8.3, when using an air conditioning unit, the unit itself will likely produce heat. When running the alternative method simulations, DesignBuilder showed that all electricity was converted to cooling loads, with no heating loads generated in the results. As such, it was concluded that the idealised EnergyPlus “Ideal Loads” system and the simple HVAC system used to simulate the alternative method in DesignBuilder, must have already accounted for this additional heat generation and factored it in to its calculation of the heating and cooling loads.

#### 6.2.1.2 Resource-Driven Limitations

Weather data for the simulations run in DesignBuilder were compiled from Time and Date AS. The decision to use this as the source for the weather data was made because the closest DesignBuilder weather file to Salford was Aughton which is approximately 26 miles. It was therefore determined, due to this distance, that the Aughton weather file would not be representative of weather conditions in Salford, and thus was discounted. CIBSE weather files were also considered, however weather data from here was not freely available, and due to budgetary constraints, also had to be discounted. Meanwhile, the Met Office did not provide sufficient historical data to be able to produce suitable weather files. After looking into various sources that could provide weather data, it was found the Time and Date AS would be the most suitable, as data from this source was freely available, and provided historical data that could date back to at least the previous five years. Unfortunately, Time and Date AS did have the drawback of not providing regular wind or any solar irradiance data. However, a standard wind speed of 4 $m \cdot s^{-1}$, determined from ISO 2017a, was used in place of this and NASA POWER 2021 was able to provide horizontal solar irradiance data. It is likely that, in reality, wind speed would vary during the different seasons, and so the standard windspeed of 4 m·s-1 used for the co-heating simulations, may not be as applicable for the alternative simulations. However, ISO 2017a did not specify the time of year this value represented, and so it was used for the alternative simulation as well.

A further resource-based limitation arose from the design U-values for the windows and French doors provided by the Zed House SAP document. Whilst it is accepted that, in reality, the U-values for the windows and French doors would vary depending on their size, the SAP document specified that the design U-value for all the Zed House windows and doors was 1.2 $W \cdot m^{-2} \cdot K^{-1}$, therefore, when inputting the design U-values into DesignBuilder, only this value could be used.

### 6.2.2 Limitations of the Alternative Method

Carrying out the research revealed that the UK summertime climate may not be ideal for performing the alternative method, as it was difficult to achieve and maintain suitable temperature differences with a sufficient spread across them. Furthermore, high levels of solar irradiance and collinearity seemed to have a more significant impact on the results from the alternative method, despite the use of blinds and curtains in the test dwelling and a dawn-dawn aggregation interval to minimise the effects of solar radiation.

The alternative method simulations also made use of a split system air conditioning unit. In reality, these systems would have internal and external inefficiencies as well as inaccuracies in their COP, which were not accounted for in the simulations due to the EnergyPlus “Ideal Loads” system. Additionally, it was identified that, despite the use of portable heaters for the co-heating method, portable cooling systems would be unsuitable for the alternative method in a real-world environment. This was due to costs and breaching the requirements of a sealed dwelling for testing.

## 6.3 Further Research

Moving forward, the research should move from theoretical, simulated testing to practical testing with more thorough examination of equipment, dwellings and climates.

The equipment used for the co-heating method is well documented, and it is known that the energy input to the heaters to carry out the method is the same as the energy output, as electric resistance heaters have a COP of 1. Since refrigeration cycles, specifically compression refrigeration cycles, have COPs greater than one - meaning the energy input does not equal the energy output - a way of measuring the energy output from the cooling system would need to be found. One possible avenue of investigation could look into the use of heat meters for this. Furthermore, as with the co-heating method, fans may be required to allow for better mixing of the air and homogeneous air flow, however this would also have to be explored.

More dwellings in warmer climates have built-in split system air conditioning units. Section 5.3 identified that using portable cooling systems would be unsuitable for the alternative method. It may therefore be sensible to trial an ‘integrated’ or ‘on-board’ adaptation of the alternative method in somewhere like Australia, similar to the methods presented and used by Allinson et al., Farmer et al. and Senave et al.

(Allinson et al., 2022; Farmer et al., 2016; Senave et al., 2019). For data analysis, a way of separating the internal gains and the cooling system's output to the dwelling from the smart meter data would also need to be identified, such as the possibility of sub-metering.

Since the research presented in this thesis focused on a high-performance dwelling, further research could also look at the performance of the alternative method on a more traditional dwelling: first by perhaps following a theoretical and simulated approach, and then by carrying out the alternative method in a practical, as-built environment.

Finally, trialling the method in other hot climates and weather conditions could begin to provide a more rounded understanding of the way the alternative method performs and how, for example, excessive solar radiation impacts the way the method is able to perform. This could initially be done in a climatic chamber, so that individual elements could be controlled and varied as well as easily repeated, before testing in a real environment.

## 6.4 Summary

As outlined in the introduction and literature review, there is a global issue surrounding the performance gap of dwellings, with average performance gaps in countries around the world ranging from 11% up to 74% (Fitton, 2021). This means that the as-built performance of a large number of dwellings across the globe do not reflect their modelled performance, leading to an increase in energy consumption. Measuring the performance gap can help towards solving this issue, however current methods, such as the co-heating method, are not appropriate in hotter climates, and thus there is large gap in research methodology regarding seasonality. This thesis highlights that a refrigeration-based method could go some way towards closing this gap of seasonality, meaning that further steps can then be taken towards solving the performance gap issue in these cooling dominated climates, where overheating may be as much of a problem as heat loss in heating dominated climates. In the long run, however, finding a method that is either quick and cheap to run or that requires minimal disturbance to occupants (such as on-board monitoring) would be preferable when determining performance gap.

Looking back at the research questions originally presented in section 1.3, the research has begun to at least take steps towards answering these questions. Overall, the alternative method presented in this thesis opens new doors to being able to measure performance gap in warmer climates. Currently, there is no recognised, suitable method that can be applied in warmer climates around the world to determine a dwelling's HTC, therefore it is likely that, in these climates, there are still dwellings that are underperforming. The initial proposal of the alternative method has been tested in a simulated environment and has shown that it has the potential to work, whilst also highlighting particular areas that need additional focus and research, such as weather conditions and the potential for 'on-board' testing. When running the simulation with Australian weather data, it was found that the HTC obtained for Perth was quite different to that obtained for the UK, suggesting that an alternative method of analysis may be necessary when using data that is subject to higher levels of collinearity. The findings from this research are simply the early stages of development for the alternative method; however, as the co-heating method has proven, continued testing and refining could result in a method which has the potential to fill the current gap of seasonality.

# Appendix A

*Figures A.1 and A.2* display the average daily internal temperatures (*A.1*) and solar irradiances (*A.2*) compared to the power inputs, with the axis zoomed in in the case of the internal temperatures for a clearer comparison. It is evident in both figures that when the internal temperature and/or solar irradiance increase, power input increases. The only noticeable anomalies come from the final two recordings of solar irradiance, where solar irradiance was high but power input did not decrease. This is because, despite evidently being very sunny, these two days were very cold with average external temperatures of 4.9°C and 4.8°C, respectively.

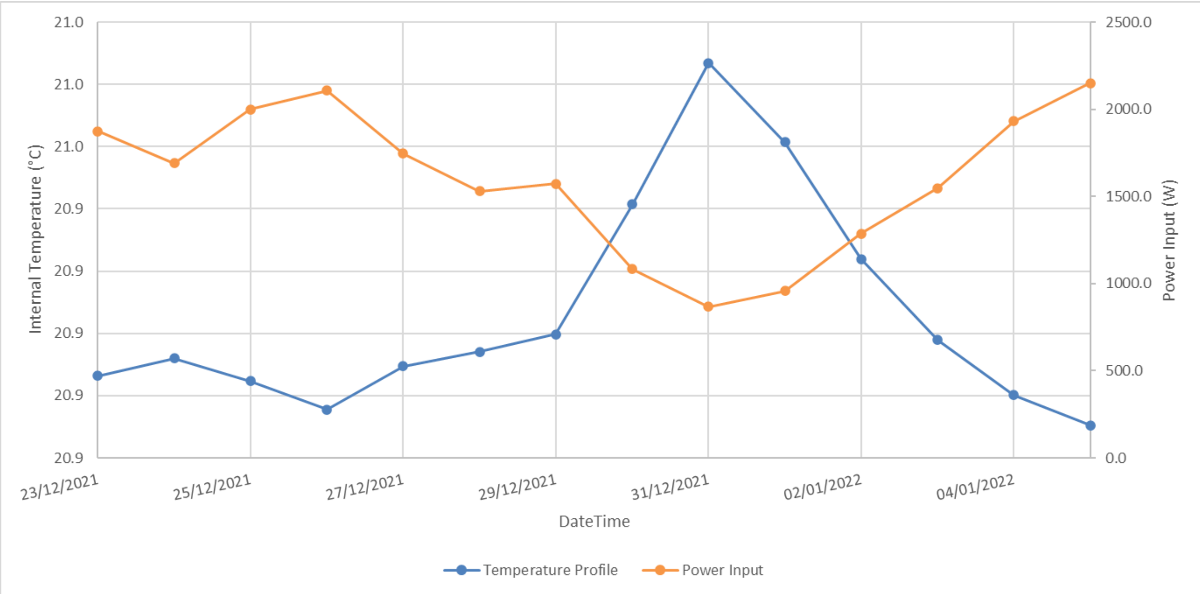


*Figure A.1 The average daily internal temperatures and power inputs to the Zed House during the co-heating test performed between 23rd December 2021 00:00 and 6th January 2022 00:00*

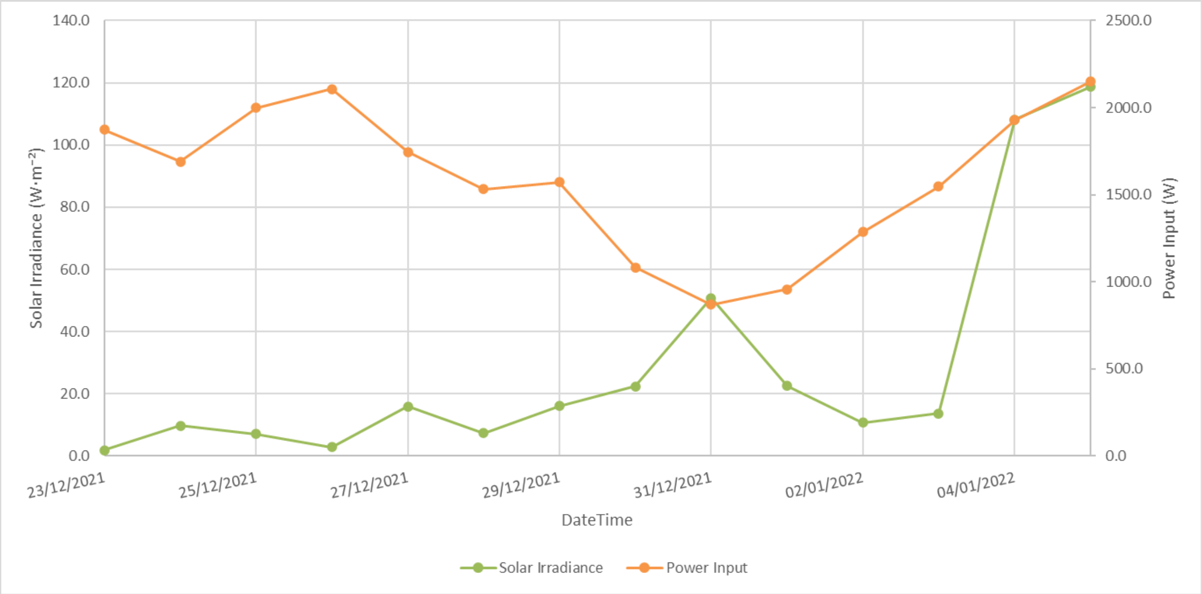


*Figure A.2 The average daily solar irradiances and power inputs to the Zed House during the co-heating test performed between 23rd December 2021 00:00 and 6th January 2022 00:00*

# Appendix B

The heat flux measurements for all five locations measured within the Zed House are shown in *Figure B.1*. It is evident that the location of HFP 5, which was placed on a section of the study ceiling deemed as 'non-representative', is an area of significant heat transfer. *Figure B.2* provides the same heat flux data with HFP 5 removed, so that the heat flux through the other four areas can be distinguished more clearly. In comparison to the 'non-representative' area, the 'representative' area on the study ceiling has a significantly lower and more stable heat flux. As expected, the 'non-representative' area of the bedroom 3 wall is also an area of higher levels of heat transfer compared to the 'representative' area of the bedroom 3 wall, although both do show the same heat flux patterns. The measured location on the kitchen floor shows a broadly steady heat flux throughout the measurement period.

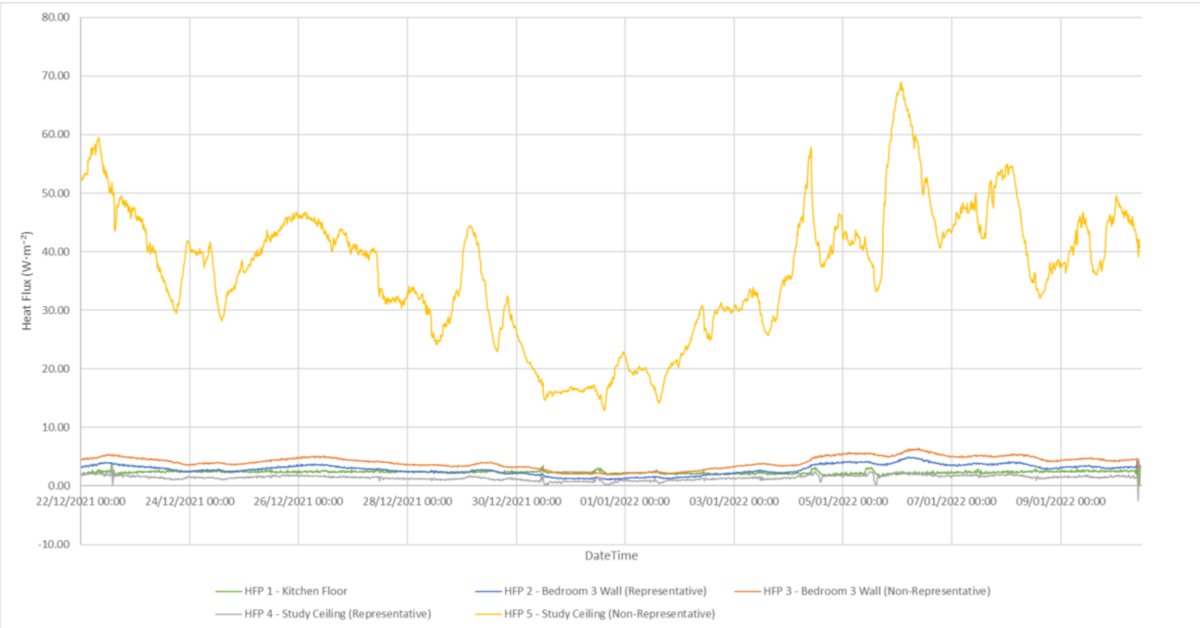


*Figure B.1 The heat flux measurements at the five locations within the Zed House*

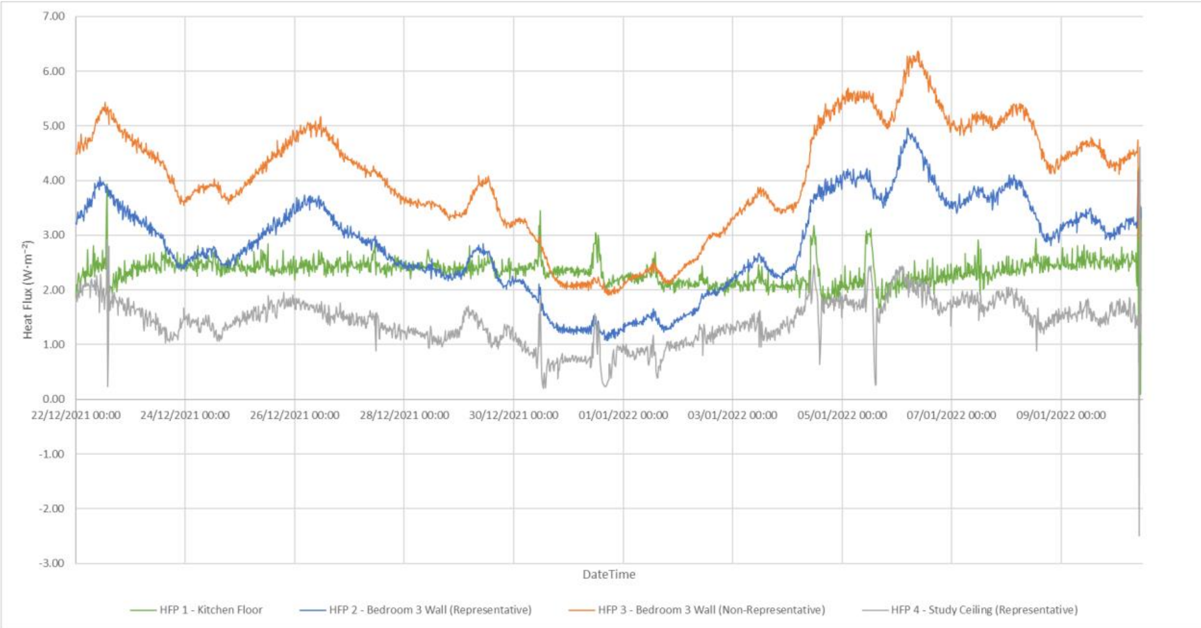


*Figure B.2 The heat flux measurements at four locations in the Zed House (excluding HFP 5 - Study Ceiling (Non-Representative)*

# Appendix C

This appendix provides the original details and outputs from the blower door test performed on the Zed House on 13th January 2022. *Figures C.1 and C.2* show the calculated results from the test, including the air change rate at 50 Pa. The graphs displayed in *Figure C.3 and C.4* are automatically generated by the Retrotec software once the tests are complete and display the building pressure and the flow vs. induced pressure for the depressurisation and pressurisation tests.

## Summary

| retrotec FanTestic | version: **5.9.40** | licensed to: **Salford University** |
|---|---|---|
| Test date: **2022-01-13** | By: **GH EC** | |
| Customer: | | |
| Building Lot Number: | | |
| Building address: | | |

| **Building and Test Information** | |
|---|---|
| Test file name: | **ATTMA 2022-01-13 1734 Z-House BU Corrections** |
| Building volume [m³]: | **282.2** |
| Envelope Area [{m²]: | **283.6** |
| Floor Area [{m²]: | **58** |
| Building Height (from ground to top) [m]: | |

| **Results** | |
|---|---|
| Air flow at 50 Pa, $Q_{50}$ [m³/h] | **1630** |
| Air changes, $n_{50}$ | **5.81** |
| Equivalent leakage area at 50 Pa [cm²] | **817.5** |
| Permeability at 50 Pa [m³/h/m²] | **5.782** |

*Figure C.1 The blower door test summary*

## Combined Test Data (Average Values)

| | Results | Uncertainty |
|---|---|---|
| Air flow at 50 Pa, $Q_{50}$ [m³/h] | 1630 | +/-0.3% |
| Air changes, $n_{50}$ | 5.81 | +/-0.3% |
| Equivalent leakage area at 50 Pa [cm²] | 817.5 | +/-0.3% |
| Permeability at 50 Pa [m³/h/m²] | 5.782 | +/-0.3% |

*Figure C.2 The average combined test data from the depressurisation and pressurisation tests*

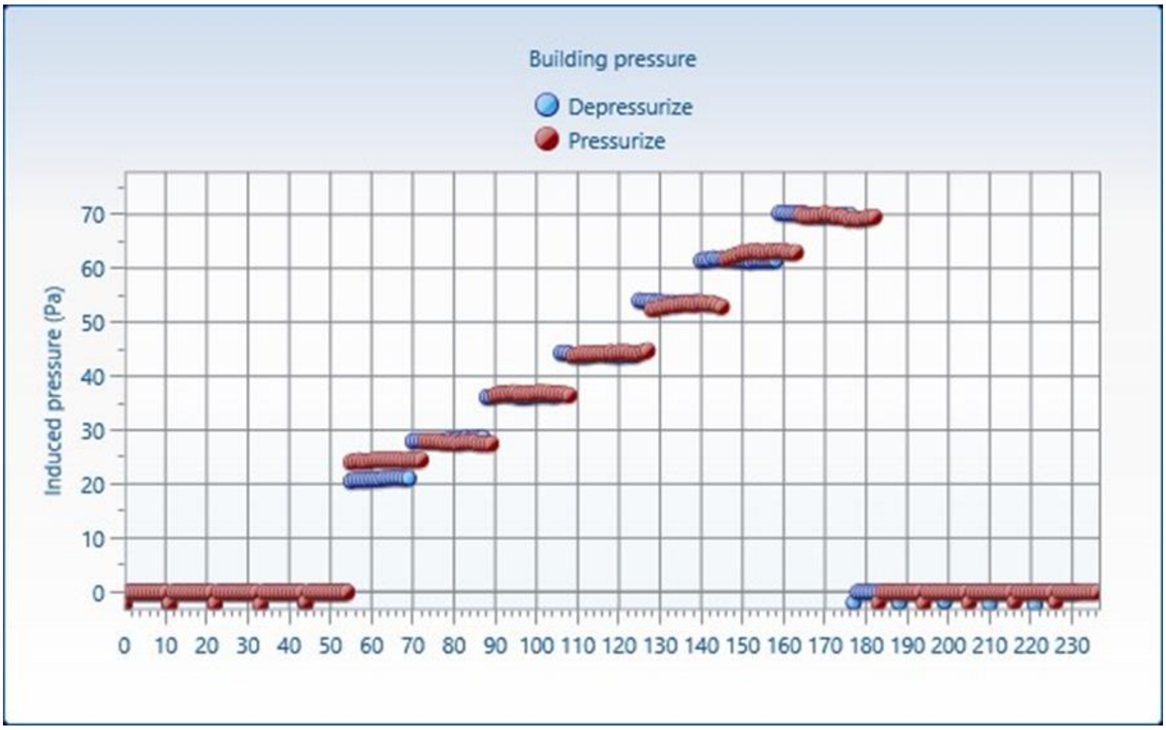


*Figure C.3 The generated graph of building pressure during the depressurisation and pressurisation tests*

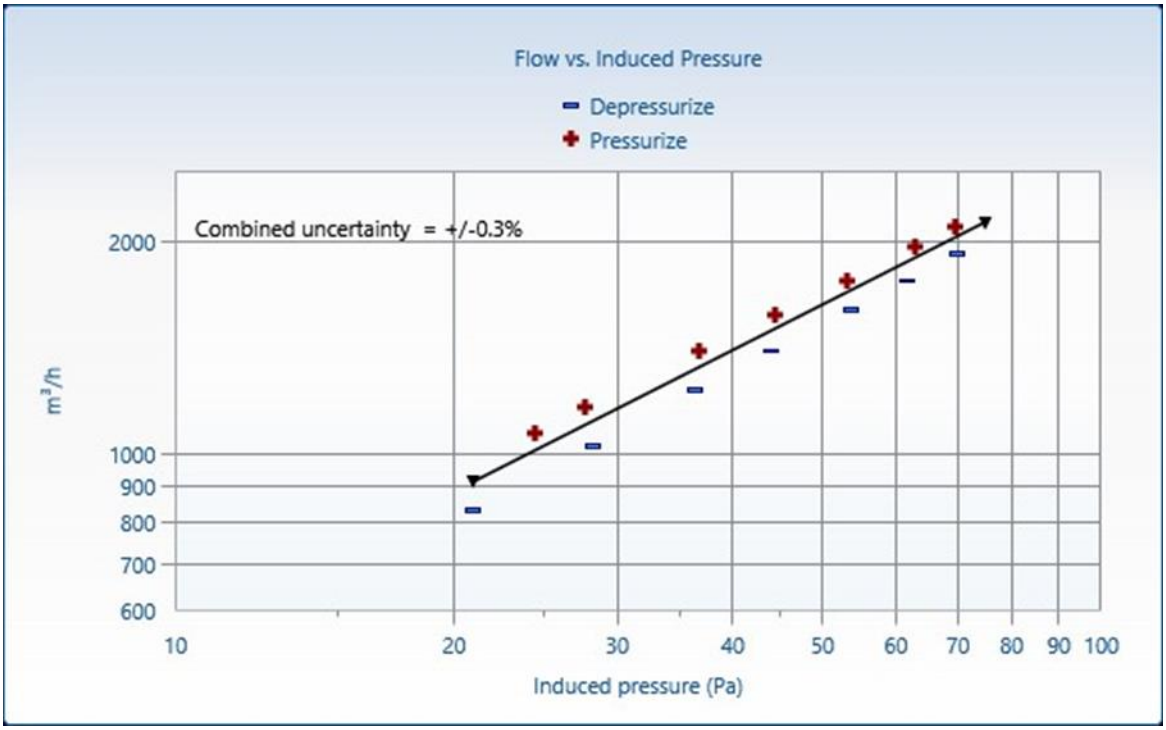


*Figure C.4 The generate graph of flow vs. induced pressuring during the depressurisation and depressurisation tests*

# References

Air Con Direct. (2020). *Air Con Direct—Air Conditioner Buying Guide—Which Air Conditioner is right for you?* Air Con Direct. https://www.aircondirect.co.uk/content/air-con-buying-guide

Allinson, D., Roberts, B., Lomas, K., Loveday, D., Gorse, C., Thomas, F., Miles-Shenton, D., Johnston, D., Glew, D., Rakhshan, K., Fylan, F., Farmer, D., Elwell, C., Crawley, J., Hollick, F., Wingfield, J., Roberts, G., & Reevell, L. (2022). *Technical Evaluation of SMETER Technologies (TEST) project*. https://doi.org/10.13140/RG.2.2.23975.62886

Alzetto, F., Farmer, D., Fitton, R., Hughes, T., & Swan, W. (2018). Comparison of whole house heat loss test methods under controlled conditions in six distinct retrofit scenarios. *Energy and Buildings*, *168*, 35–41. https://doi.org/10.1016/j.enbuild.2018.03.024

Alzetto, F., Pandraud, G., Fitton, R., Heusler, I., & Sinnesbichler, H. (2018). QUB: A fast dynamic method for in-situ measurement of the whole building heat loss. *Energy and Buildings*, *174*, 124–133. https://doi.org/10.1016/j.enbuild.2018.06.002

American Home, Water & Air. (2020, May 22). *How Many Degrees Can An Air Conditioner Cool? | American Home Water & Air*. https://americanhomewater.com/how-many-degrees-can-an-air-conditioner-cool/

ASHRAE. (2004). *EnergyPlus Testing with ANSI/ASHRAE Standard 140-2001 (BESTEST)*. https://simulationresearch.lbl.gov/dirpubs/epl_bestest_ash.pdf

ASTM. (2010). *ASTM Standard E779-87 StandardTest Method for Determining Air Leakage Rate by Fan Pressurization. ASTMA Book of Standards*.

ATTMA. (2021). *ATTMA Technical Standard L1 (TSL1)—Measuring Air Permeability in the Envelopes of Simple Buildings Fan Pressurisation Method—Issue 4.0*. https://www.bcta.group/attma/download/attma-technical-standard-l1-tsl1-measuring-air-permeability-in-the-envelopes-of-simple-buildings-fan-pressurisation-method-issue-4-0/

Australian Institute of Health and Welfare. (2022, August 2). *Home ownership and housing tenure*. Australian Institute of Health and Welfare.

https://www.aihw.gov.au/reports/australias-welfare/home-ownership-and-housing-tenure

Barratt Developments PLC. (2022). *Zed House, Manchester*. Barratt Developments PLC. https://www.barrattdevelopments.co.uk/showcase/zed-house

Bauwens, G., Ritosa, K., & Roels, S. (2021). *EBC Annex71 ST3 Physical parameter identification*. KU Leuven. https://dynastee.info/wp-content/uploads/2021/09/EBC_Annex71-ST3_Physical-parameter-identification.pdf

Bauwens, G., & Roels, S. (2014). Co-heating test: A state-of-the-art. *Energy and Buildings*. https://doi.org/10.1016/j.enbuild.2014.04.039

Bell Flow Systems. (2022). *Heat Flow Meter Guide*. Bell Flow Systems. https://www.bellflowsystems.co.uk/heat-meter-guide.html

Bevans, R. (2020, February 20). *An introduction to multiple linear regression*. Scribbr. https://www.scribbr.com/statistics/multiple-linear-regression/

Bouchié, R., Alzetto, F., Brun, A., Boisson, P., & Thebault, S. (2014). *Short methodologies for in-situ assessment of the intrinsic thermal performance of the building envelope*.

Bouchié, R., Alzetto, F., Brun, A., Weeks, C., Preece, M., Ahmad, M., & Sisinni, M. (2015). *Methodologies for the assessment of intrinsic energy performance of buildings' envelop*. https://www.researchgate.net/publication/299369611_Methodologies_for_the_assessment_of_intrinsic_energy_performance_of_buildings'_envelop

Box, T. (1880). *A Practical Treatise on Heat, as Applied to the Useful Arts for the use of Engineers, Architects etc.* (3rd ed.). E. & F. N. Spon.

BRE. (2009). *Appendix S: Reduced Data SAP for existing dwellings*. Building Research Establishment. https://www.bregroup.com/sap/standard-assessment-procedure-sap-2009/reduced-data-sap-from-1-april-2012/

BRE. (2012). *Appendix S: Reduced Data SAP for existing dwellings*. Building Research Establishment. https://www.bregroup.com/sap/standard-assessment-procedure-sap-2012/

BRE. (2014). *The Government's Standard Assessment Procedure for Energy Rating of Dwellings 2012 edition*. Building Research Establishment. https://www.bregroup.com/sap/standard-assessment-procedure-sap-2012/

BRE. (2019, March 8). *The Passivhaus Standard | BRE Group*. BRE Group. https://bregroup.com/a-z/the-passivhaus-standard/

BSI. (1999). *BSI (1999) BS EN ISO 13187:1999 Thermal performance of buildings—Qualitative detection of thermal irregularities in building envelopes—Infrared method*. British Standard Institution. https://bsol-bsigroup-com.salford.idm.oclc.org/Bibliographic/BibliographicInfoData/000000000001569434

BSI. (2014). *BSI (2014) BS ISO 9869-1:2014 Thermal insulation—Building elements—In-situ measurement of thermal resistance and thermal transmittance Part 1: Heat flow meter method*. British Standard Institution. https:/bsol-bsigroup-com.salford.idm.oclc.org/

BSI. (2015a). *BS EN ISO 6781-3:2015 Performance of buildings. Detection of heat, air and moisture irregularities in buildings by infrared methods. Qualifications of equipment operators, data analysisists and report writers*. British Standard Institution. https://bsol-bsigroup-com.salford.idm.oclc.org/Bibliographic/BibliographicInfoData/000000000030259341

BSI. (2015b). *BSI (2015) BS EN ISO 9972:2015 Thermal performance of buildings—Determination of air permeability of buildings—Fan pressurisation method*. British Standard Institution. https://bsol-bsigroup-com.salford.idm.oclc.org/Bibliographic/BibliographicInfoData/000000000030242976

BSI. (2017a). *BSI (2017) BS EN ISO 6946: 2017 Building components and building elements. Thermal resistance and thermal transmittance. Calculation methods*. British Standard Institution. https://bsol-bsigroup-com.salford.idm.oclc.org/Bibliographic/BibliographicInfoData/000000000030313347

BSI. (2017b). *BSI (2017) BS EN ISO 10211:2017 Thermal bridges in building construction. Heat flows and surface temperatures. Detailed calculations*. British Standard Institution. https://bsol-bsigroup-com.salford.idm.oclc.org/

BSI. (2017c). *BSI (2017) BS EN ISO 12831-1:2017 Energy performance of buildings. Method for calculation of the design heat load. Space heating load, Module M3-3*. British Standard Institution. https://bsol-bsigroup-com.salford.idm.oclc.org/

BSI. (2017d). *BSI (2017) BS EN ISO 13789:2017 Thermal performance of buildings. Transmission and ventilation heat transfer coefficients. Calculation method.* British Standard Institution. https://bsol-bsigroup-com.salford.idm.oclc.org/

BSI. (2017e). *BSI (2017) BS EN ISO 15193-1:2017+A1:2021 Energy performance of buildings. Energy requirements for lighting. Specifications, Module M9*. British Standard Institution. https://bsol-bsigroup-com.salford.idm.oclc.org/

BSI. (2017f). *BSI (2017) BS EN ISO 52016-1:2017 Energy performance of buildings. Energy needs for heating and cooling, internal temperatures and sensible and latent heat loads. Calculation procedures*. British Standard Institution. https://bsol-bsigroup-com.salford.idm.oclc.org/

BSI. (2018). *BSI (2018) BS EN ISO 7345:2018 Thermal performance of buildings and building components—Physical quantities and definitions*. British Standard Institution. https://bsol-bsigroup-com.salford.idm.oclc.org/Bibliographic/BibliographicInfoData/000000000030294397

BTS. (2018). *Low Pressure Pulse Test Field Trial Report*. Build Test Solutions. https://buildtestsolutions.com/air-leakage-testing/pulse/

BTS. (2021a). *Heat3D – Infrared U-value Measurement – Build Test Solutions*. Build Test Solutions. https://buildtestsolutions.com/u-value-measurement/heat3d/

BTS. (2021b). *Pulse Brochure*. https://buildtestsolutions.com/air-leakage-testing/pulse/

Butler, D., & Dengel, A. (2013). *Review of co-heating test methodologies: Primary research.* NHBC Foundation. https://www.nhbcfoundation.org

Campbell Scientific. (2020). *CMP3 Pyranometer Product Manual*. Campbell Scientific. https://s.campbellsci.com/documents/au/manuals/cmp3.pdf

Camuffo, D. (2014). Chapter 2A - Theoretical Grounds for Humidity. In D. Camuffo (Ed.), *Microclimate for Cultural Heritage (Second Edition)* (pp. 49–76). Elsevier. https://doi.org/10.1016/B978-0-444-63296-8.00002-0

Carrié, F. R., & Leprince, V. (2016). Uncertainties in building pressurisation tests due to steady wind. *Energy and Buildings*, *116*, 656–665. https://doi.org/10.1016/j.enbuild.2016.01.029

Carver, D. (2022, January 27). *What were the outcomes of COP26?* UK Parliament. https://commonslibrary.parliament.uk/what-were-the-outcomes-of-cop26/

Chadderton, D. V. (2013). *Building Services Engineering* (Sixth). Routledge.

CIBSE. (2006). *Tests for software accreditation and verification.* Chartered Inst. of Building Services Engineers. https://www-ihsti-com.salford.idm.oclc.org/CIS/search?f=All&t=cibse+tm33&sqm=AllTerms

CIBSE. (2015, July). *CTT8 CIBSE Top Tips 8: Temperature in Indoor Workplaces (Thermal Comfort) | CIBSE*. https://www.cibse.org/knowledge-research/knowledge-portal/ctt8-cibse-top-tips-8-temperature-in-indoor-workplaces-thermal-comfort

Custom Weather. (2022). *Forecast Products*. Custom Weather. https://customweather.com/products/forecast-products/

Delmotte, C., & Laverge, J. (2001). Interlaboratory tests for the determination of repeatability and reproducibility of buildings airtightness measurements. *Proceedings of the 32nd AIVC Conference*, 183–187. Scopus.

DesignBuilder Software Ltd. (2022). *DesignBuilder Help—Welcome to DesignBuilder v5*. DesignBuilder Help - Welcome to DesignBuilder V5. http://designbuilder.co.uk/helpv5.5/

Doran, S. (2001). *Field investigations of the thermal performance of construction elements as built*. https://doi.org/10.13140/RG.2.1.3397.9042

Dunklee. (2021, October 16). *What Outside Temperature Is Too Cold for Air Conditioner?* -. Dunklee Cooling & Heating. https://dunckleeinc.com/what-outside-temperature-is-too-cold-for-air-conditioner/, https://dunckleeinc.com/what-outside-temperature-is-too-cold-for-air-conditioner/

electriQ. (2022). *AirFlex 14000 BTU 4kW Portable Air Conditioner with Heat Pump for rooms up to 38 sqm*. Electriq. https://www.electriq.co.uk/p/airflex15

Energy House Laboratories. (2021). *Energy House* **|** *Energy House 2.0* **|** *University of Salford*. Energy House 2.0. https://energyhouse2.salford.ac.uk/energy-house-labs/energy-house/

Everett, R. (1985). Rapid Thermal Calibration of Houses. In *Open University: Milton Keynes, UK.* (Report ERG 055; Issue ERG 055). Open University. http://www.open.ac.uk/people/rce4

Farmer, D., Gorse, C., Swan, W., Fitton, R., Brooke-Peat, M., Miles-Shenton, D., & Johnston, D. (2017). Measuring thermal performance in steady-state conditions at each stage of a full fabric retrofit to a solid wall dwelling. *Energy and Buildings*, *156*, 404–414. https://doi.org/10.1016/j.enbuild.2017.09.086

Farmer, D., Johnston, D., & Miles-Shenton, D. (2016). Obtaining the heat loss coefficient of a dwelling using its heating system (integrated coheating). *Energy and Buildings*, *117*, 1–10. https://doi.org/10.1016/j.enbuild.2016.02.013

Feeley, S. (2018). *BRE Test Report Pulse vs Blower Door comparison airtightness chamber testing—Build Test Solutions Ltd* (No. P112784-1001 Issue 2). Building Research Establishment. https://buildtestsolutions.com/air-leakage-testing/pulse/

Fitton, R. (2021). *EBC Annex 71 ST1-4 Challenges and general framework*. KU Leuven. https://dynastee.info/wp-content/uploads/2021/09/EBC_Annex-71-ST1-4_Challenges-and-general-framework.pdf

FlyCarpet Inc. (2015). *Online Interactive Psychrometric Chart*. Flycarpet.Net. http://www.flycarpet.net/en/psyonline

Francisco, P. W., Palmiter, L., & Davis, B. (1998). Modeling the thermal distribution efficiency of ducts: Comparisons to measured results. *Energy and Buildings*, *28*(3), 287–297. https://doi.org/10.1016/S0378-7788(98)00028-0

Glen, S. (2015, September 22). Variance Inflation Factor. *Statistics How To*. https://www.statisticshowto.com/variance-inflation-factor/

Gupta, R., & Gregg, M. (2015). Do Deep Low Carbon Retrofits Actually Work? *Energy Procedia*, *78*, 919–924. https://doi.org/10.1016/j.egypro.2015.11.019

Hens, H., Janssens, A., Depraetere, W., Carmeliet, J., & Lecompte, J. (2007). Brick Cavity Walls: A Performance Analysis Based on Measurements and Simulations. *Journal of Building Physics*, *31*(2), 95–124. https://doi.org/10.1177/1744259107082685

Holden, D. J., & Randall, N. (2019). *Verification Report Low Pressure PULSE Air Test Process*. Building Research Establishment. https://buildtestsolutions.com/air-leakage-testing/pulse/

Housez, P. P., Pont, U., & Mahdavi, A. (2014). A comparison of projected and actual energy performance of buildings after thermal retrofit measures. *Journal of Building Physics*, *38*(2), 138–155. https://doi.org/10.1177/1744259114532611

Hsu, Y.-S., Zheng, X., Cooper, E., Gillott, M., & Wood, C. J. (2021). Evaluation of the indoor pressure distribution during building airtightness tests using the pulse and blower door methods. *Building and Environment*, *195*, 107742. https://doi.org/10.1016/j.buildenv.2021.107742

Hulme, J., & Doran, S. (2015). *In-situ measurements of wall U-values in English housing*. Building Research Establishment. https://www.gov.uk/government/publications/in-situ-measurements-of-wall-u-values-in-english-housing

Hummelshøj, R. M., Piers, I., & Žaltkauskiene, J. (2016). *ECO-Life—Sustatainable Zero Carbon ECO-Town Developments Improving Quality of Life across EU* [Final publishable summary report]. COWI. https://www.ecolife-project.eu/

IEA. (2018, May). *The Future of Cooling – Analysis*. IEA. https://www.iea.org/reports/the-future-of-cooling

IEA. (2020, December 13). *Is cooling the future of heating? – Analysis*. IEA. https://www.iea.org/commentaries/is-cooling-the-future-of-heating

IEA. (2021). *Global Energy Review 2021 – Analysis*. International Energy Agency. https://www.iea.org/reports/global-energy-review-2021

Jack, R., Loveday, D., Allinson, D., & Lomas, K. (2018). First evidence for the reliability of building co-heating tests. *Building Research & Information*, *46*(4), 383–401. https://doi.org/10.1080/09613218.2017.1299523

JCGM. (2008). *JCGM 100:2008 GUM 1995 with minor corrections. Evaluation of measurement data—Guide to the expression of uncertainty in measurement*. JCGM. https://www.bipm.org/en/committees/jc/jcgm/publications

Ji, Y., Fitton, R., Swan, W., & Webster, P. (2014). Assessing overheating of the UK existing dwellings – A case study of replica Victorian end terrace house. *Building and Environment*, *77*, 1–11. https://doi.org/10.1016/j.buildenv.2014.03.012

Johnston, D., Farmer, D., Brooke-Peat, M., & Miles-Shenton, D. (2016). Bridging the domestic building fabric performance gap. *Building Research & Information*, *44*(2), 147–159. https://doi.org/10.1080/09613218.2014.979093

Johnston, D., Miles-Shenton, D., & Farmer, D. (2015). Quantifying the domestic building fabric 'performance gap'. *Building Services Engineering Research and Technology*, *36*(5), 614–627. https://doi.org/10.1177/0143624415570344

Johnston, D., Miles-Shenton, D., Farmer, D., & Wingfield, J. (2013). Whole house heat loss test method (Coheating). *Leeds Metropolitan University: Leeds, UK*.

Johnston, D., & Siddall, M. (2016). The Building Fabric Thermal Performance of Passivhaus Dwellings—Does It Do What It Says on the Tin? *Sustainability*, *8*(1), Article 1. https://doi.org/10.3390/su8010097

Kipp & Zonen. (2013, July 2). *What is the Difference between Horizontal and Tilted Global Solar Irradiance? - Kipp & Zonen*. KippZonen.Com. https://www.kippzonen.com/News/408/The-Difference-between-Horizontal-and-Tilted-Global-Solar-Irradiance#.Y85bP3bP1PY

Kirimtat, A., & Krejcar, O. (2018). A review of infrared thermography for the investigation of building envelopes: Advances and prospects. *Energy and Buildings*, *176*, 390–406. https://doi.org/10.1016/j.enbuild.2018.07.052

Kronvall, J. (1978). Testing of houses for air leakage using a pressure method. *ASHRAE Transactions*, *84*(1), 72–79.

Law, A., & Wong, J. P. C. (2020). Application of the Co-heating test in Australian climates. *Energy and Buildings*, *224*, 110153. https://doi.org/10.1016/j.enbuild.2020.110153

Li, F. G. N., Smith, A. Z. P., Biddulph, P., Hamilton, I. G., Lowe, R., Mavrogianni, A., Oikonomou, E., Raslan, R., Stamp, S., Stone, A., Summerfield, A. J., Veitch, D., Gori, V., & Oreszczyn, T. (2015). Solid-wall U-values: Heat flux measurements compared with standard assumptions. *Building Research & Information*, *43*(2), 238–252. https://doi.org/10.1080/09613218.2014.967977

Mangematin, E., Pandraud, G., & Roux, D. (2012). Quick measurements of energy efficiency of buildings. *Comptes Rendus Physique*, *13*(4), 383–390. https://doi.org/10.1016/j.crhy.2012.04.001

Marshall, A., Fitton, R., Swan, W., Farmer, D., Johnston, D., Benjaber, M., & Ji, Y. (2017). Domestic building fabric performance: Closing the gap between the in situ measured and modelled performance. *Energy and Buildings*, *150*, 307–317. https://doi.org/10.1016/j.enbuild.2017.06.028

McMullan, R. (2012). *Environmental Science in Building* (Seventh). Palgrave Macmillan.

Meulemans, J., Alzetto, F., Farmer, D., & Gorse, C. (2017). QUB/e: A Novel Transient Experimental Method for in situ Measurements of the Thermal Performance of Building Fabrics. *Building Information Modelling, Building Performance, Design and Smart Construction*, 115–127. https://doi.org/10.1007/978-3-319-50346-2_9

NASA. (2022). *POWER | Data Access Viewer*. POWER | Data Access Viewer. https://power.larc.nasa.gov/data-access-viewer/

NASA POWER. (2021, July 22). *NASA POWER | Docs | Methodology | Solar Assessment—NASA POWER | Docs*. NASA POWER. https://power.larc.nasa.gov/docs/methodology/energy-fluxes/solar-validation/

National Statistics. (2020). *Energy Consumption in the UK (ECUK) 1970—2019*. https://www.gov.uk/government/statistics/energy-consumption-in-the-uk-2020

National Statistics. (2021). *Energy Consumption in the UK (ECUK) 1970—2020*. https://www.gov.uk/government/statistics/energy-consumption-in-the-uk-2021

National Statistics. (2022a). *Energy Consumption in the UK (ECUK) 1970—2021*. https://www.gov.uk/government/statistics/energy-consumption-in-the-uk-2022

National Statistics. (2022b). *Provisional UK greenhouse gas emissions national statistics 2021*. https://www.gov.uk/government/statistics/provisional-uk-greenhouse-gas-emissions-national-statistics-2021

National Statistics. (2022c). *2021 UK greenhouse gas emissions, provisional figures*. https://assets.publishing.service.gov.uk/government/uploads/system/uploads/attachment_data/file/1064923/2021-provisional-emissions-statistics-report.pdf

NCRAS. (2021). *National Climate Resilience and Adaptation Strategy 2021-2025*. NCRAS, Department of Agriculture, Water and the Environment, Canberra, February. CC BY 4.0. http://awe.gov.au/publications

OpenEI. (2009). *Climate Zone 5C | Open Energy Information*. OpenEI. https://openei.org/wiki/Climate_Zone_5C

Orion Air Conditioning and Refrigeration Ltd. (2022a). *Ebac 10970GB-GB BKool-12 Industrial Portable Air Conditioning 3.5Kw/12000Btu 240V~50Hz*. OrionAirSales: Commercial Products Sales. https://www.orionairsales.co.uk/ebac-10970gb-gb-bkool-12-industrial-portable-air-conditioning-35kw12000btu-240v50hz-14204-p.asp

Orion Air Conditioning and Refrigeration Ltd. (2022b). *Fral SC14 Portable Air Conditioning 4.1Kw/14000Btu Heating and Cooling A++ 240V~50Hz*. OrionAirSales: Commercial Products Sales. https://www.orionairsales.co.uk/fral-sc14-portable-air-conditioning-41kw14000btu-heating-and-cooling-a-240v50hz-3991-p.asp

Passivhaus Trust. (2018, September 28). *UK Passivhaus reaches 1000*. Passivhaus Trust. https://www.passivhaustrust.org.uk/news/detail/?nId=787

Persily, A. K., & Linteris, G. T. (1983). A comparison of measured and predicted infiltration rates. *ASHRAE Trans.; (United States)*, *89*, Article CONF-830640-. https://www.osti.gov/biblio/6499412

Press Office. (2022, July 28). *Record high temperatures verified*. Met Office. https://www.metoffice.gov.uk/about-us/press-office/news/weather-and-climate/2022/record-high-temperatures-verified

pumpsdirect2u Ltd. (2022). *PAC15 Portable Split Air Conditioning Unit (4.5KW) 230v FIXED LINE 3 MTR*. http://www.pumpsdirect2u.com/air-con-ventilation-6/pac-portable-air-conditioning-split-system-345/pac15-portable-split-conditioning-unit-230v-6265.htm

Razak, A. M. Y. (2007). 14—Power augmentation. In A. M. Y. Razak (Ed.), *Industrial Gas Turbines* (pp. 376–408). Woodhead Publishing. https://doi.org/10.1533/9781845693404.2.376

Reynders, G., Erfani, A., & Saelens, D. (2021). *EBC Annex71 ST2 Building behaviour identification*. KU Leuven. https://dynastee.info/wp-content/uploads/2021/09/EBC_Annex71-ST2_Building-behaviour-identification.pdf

Rye, C., & Scott, C. (2012). *The SPAB research report 1. U-value report*. https://www.spab.org.uk/advice/research/findings

Senave, M., Roels, S., Verbeke, S., Lambie, E., & Saelens, D. (2019). Sensitivity of Characterizing the Heat Loss Coefficient through On-Board Monitoring: A Case Study Analysis. *Energies*, *12*, 3322. https://doi.org/10.3390/en12173322

Sonderegger, R. C., Condon, P. E., & Modera, M. P. (1980). *In-situ measurements of residential energy performance using electric co-heating*. https://www.osti.gov/biblio/5492967

Sonderegger, R. C., & Modera, M. P. (1979). *Electric co-heating: A method for evaluating seasonal heating efficiencies and heat loss rates in dwellings*. https://escholarship.org/uc/item/0ff5q27p

Stamp, S. F. (2015). *Assessing uncertainty in co-heating tests: Calibrating a whole building steady state heat loss measurement method* [University College London]. https://discovery.ucl.ac.uk

Subbarao, K. (1988). *PSTAR—Primary and Secondary Terms Analysis and Renormalization: A Unified Approach to Building and Energy Simulations and Short-Term Testing; A Summary* [Summary Report]. Solar Energy Research Institute. https://www.nrel.gov/docs/legosti/old/3347.pdf

Swan, W., Fitton, R., Smith, L., Abbott, C., & Smith, L. (2017). Adoption of sustainable retrofit in UK social housing 2010-2015. *International Journal of Building Pathology and Adaptation*, *35*(5), 456–469. https://doi.org/10.1108/IJBPA-04-2017-0019

The National Archives. (2008). *Climate Change Act 2008*. Statute Law Database. https://www.legislation.gov.uk/ukpga/2008/27/contents

The National Archives. (2011). *The Carbon Plan—Reducing greenhouse gas emissions*. https://www.gov.uk/government/publications/the-carbon-plan-reducing-greenhouse-gas-emissions--2

The National Archives. (2016). *Conservation of fuel and power. Approved Document L1a*. https://www.gov.uk/government/publications/conservation-of-fuel-and-power-approved-document-l

The National Archives. (2019). *2019 UK Greenhouse Gas Emissions*. https://www.gov.uk/government/statistics/final-uk-greenhouse-gas-emissions-national-statistics-1990-to-2019

The National Archives. (2021). *Net Zero Strategy: Build Back Greener*. https://www.gov.uk/government/publications/net-zero-strategy

The National Archives. (2023). *Conservation of fuel and power: Approved Document L1a*. https://www.gov.uk/government/publications/conservation-of-fuel-and-power-approved-document-l

Time and Date AS. (2022a). *Past Weather in Salford, England, United Kingdom—Yesterday or Further Back*. Timeanddate. https://www.timeanddate.com/weather/uk/salford/historic

Time and Date AS. (2022b). *Sunrise and sunset times in Salford*. Timeanddate. https://www.timeanddate.com/sun/uk/salford

Time and Date AS. (2022c). *Sunrise and sunset times in Salford, December 2021*. Timeanddate. https://www.timeanddate.com/sun/uk/salford?month=12&year=2021

Time and Date AS. (2022d). *Sunrise and sunset times in Salford, January 2022*. Timeanddate. https://www.timeanddate.com/sun/uk/salford?month=1&year=2022

UNEP. (2021). *2021 Global Status Report for Buildings and Construction: Towards a Zero-emission, Efficient and Resilient Buildings and Construction Sector*. United Nations Environment Programme. https://www.unep.org/resources/report/2021-global-status-report-buildings-and-construction

United Nations. (2015). *The Paris Agreement*. https://www.un.org/en/climatechange/paris-agreement

United Nations. (2021a). *COP26 Explained*. https://ukcop26.org/cop26-goals/

United Nations. (2021b). *The Glasgow Climate Pact*. UN Climate Change Conference (COP26) at the SEC – Glasgow 2021. https://ukcop26.org/the-glasgow-climate-pact/

University of Pennsylvania. (2017). *Averaging, Errors and Uncertainty—Lab Manual, Undergraduate Labs, Department of Physics & Astronomy*. University of Pennsylvania. https://www.physics.upenn.edu/sites/default/files/Managing%20Errors%20and%20Uncertainty.pdf

University of Salford. (2014). *University of Salford Energy House* [Photograph].

USGPO. (2021, April 22). *FACT SHEET: President Biden Sets 2030 Greenhouse Gas Pollution Reduction Target Aimed at Creating Good-Paying Union Jobs and Securing U.S. Leadership on Clean Energy Technologies*. The White House. https://www.whitehouse.gov/briefing-room/statements-releases/2021/04/22/fact-sheet-president-biden-sets-2030-greenhouse-gas-pollution-reduction-target-aimed-at-creating-good-paying-union-jobs-and-securing-u-s-leadership-on-clean-energy-technologies/

Watson, K. (2021, November 30). *Maximum & Minimum Workplace Temperature | Office & Warehouse Law*. Safe Workers. https://www.safeworkers.co.uk/equipment-environment/safe-working-temperatures/

Zero Carbon Hub. (2014). *Performance Gap | Zero Carbon Hub*. https://www.zerocarbonhub.org/current-projects/performance-gap

Zero Carbon Hub. (2016, March 30). *ZERO CARBON HUB TO CLOSE* | *Zero Carbon Hub*. Zero Carbon Hub. https://www.zerocarbonhub.org/news/zero-carbon-hub-close

Zheng, K., & Smith, L. (2020). *Pulse test in very air tight Passivhause standard buildings*. Build Test Solutions. https://buildtestsolutions.com/air-leakage-testing/pulse/